

For Reference

---

NOT TO BE TAKEN FROM THIS ROOM



For Reference

NOT TO BE TAKEN FROM THIS ROOM

Ex LIBRIS  
UNIVERSITATIS  
ALBERTAENSIS













THE UNIVERSITY OF ALBERTA

SECONDARY DISTENSION SIMILAR TENSILE EFFECTS

IN THE

THERMALITY OF A2O DIOXIDE

TO MY PARENTS



SARIL KADAM AL-SAYED

A THESIS

SUBMITTED TO THE FACULTY OF GRADUATE STUDIES  
IN PARTIAL FULFILLMENT OF THE REQUIREMENTS FOR THE  
DEGREE OF DOCTOR OF PHILOSOPHY

DEPARTMENT OF CHEMISTRY

EDMONTON, ALBERTA

FALL 1969

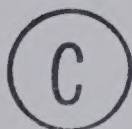




THE UNIVERSITY OF ALBERTA

SECONDARY DEUTERIUM KINETIC ISOTOPE EFFECTS  
IN THE  
THERMOLYSIS OF AZO COMPOUNDS

B Y



BASIL HASHIM AL-SADER

A THESIS

SUBMITTED TO THE FACULTY OF GRADUATE STUDIES  
IN PARTIAL FULFILMENT OF THE REQUIREMENTS FOR THE  
DEGREE OF DOCTOR OF PHILOSOPHY

DEPARTMENT OF CHEMISTRY

EDMONTON, ALBERTA

FALL 1969





THE UNIVERSITY OF ALBERTA  
FACULTY OF GRADUATE STUDIES

The undersigned certify that they have read and recommend to the Faculty of Graduate Studies for acceptance, a thesis entitled SECONDARY DEUTERIUM KINETIC ISOTOPE EFFECTS IN THE THERMOLYSIS OF AZO COMPOUNDS submitted by Basil Hashim Al-Sader, in partial fulfilment of the requirements for the degree of Doctor of Philosophy.





## A C K N O W L E D G M E N T S

The author would like to express his deep gratitude to Dr. Robert J. Crawford, who conceived this research problem, and who gave invaluable guidance and counselling during the progress of this work. The author would also like to give special thanks to Dr. D. M. Cameron for his help with the kinetic apparatus, and Dr. A. Mishra for his many helpful discussions.

The author would like to thank Mr. R. Swindlehurst and his staff in the spectroscopy laboratory, Dr. A. Hogg and Mr. T. Budd for their help with the mass spectrometry, the technical staff of the Department of Chemistry, and Mrs. Pearl Williams for her time and effort spent in typing this thesis.

Finally, the author is particularly grateful to the Department of Chemistry and the University of Alberta for the financial support.

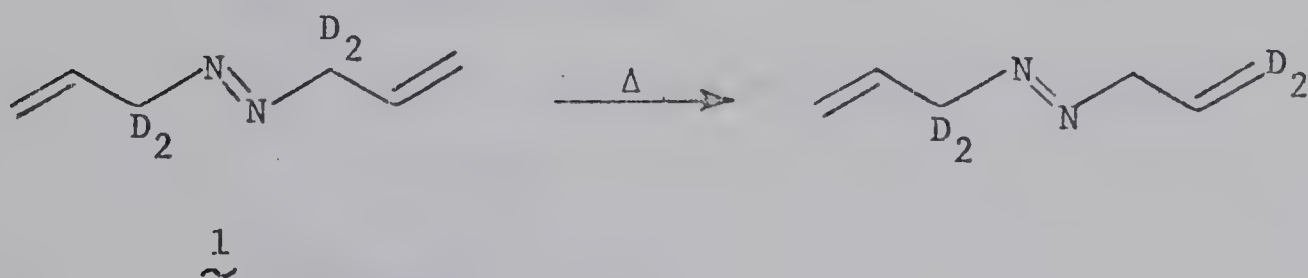




## A B S T R A C T

Four deuterated 1-pyrazolines were synthesized and the magnitude of their secondary kinetic isotope effects were measured. The  $\alpha$ -effect implies that both carbon-nitrogen bonds are breaking in the rate of determining transition state. Product studies imply that while deuterium substitution at the  $\beta$ -position of 1-pyrazoline slows down the rate of cyclization of the trimethylene produced, substitution at the  $\alpha$ -positions does not change the rate of cyclization.

A study of azo-bis-3-propene thermolysis leads to the conclusions that (a) allyl radicals are produced (b) that the allyl radicals are not capable of hydrogen abstraction (c) that both carbon-nitrogen bonds are breaking in the rate-determining transition state and (d) that a good Polanyi plot may be obtained for azo alkane thermolysis studies. Nuclear magnetic resonance analysis of the azo compound (1) recovered after 40% reaction indicated that a small amount of deuterium scrambling to the  $\gamma$ -position had occurred.



This was rationalized in terms of the addition of allyl radicals to the nitrogen-nitrogen double bond. This prevented the precise determination of secondary deuterium kinetic isotope effects in the azo-bis-3-propene system.





## TABLE OF CONTENTS

	Page
ACKNOWLEDGMENTS	iii
ABSTRACT	iv
LIST OF TABLES	viii
LIST OF FIGURES	x
CHAPTER I	
<u>1-PYRAZOLINES</u>	
<u>Historical</u>	1
(A) Thermal isomerization of cyclopropane	1
(B) Thermolysis of 1-pyrazolines	3
(C) Theoretical treatment of trimethylene	16
(D) Secondary deuterium kinetic isotope effects	19
<u>Problem</u>	42
<u>Results</u>	44
(A) Synthesis of deuterated 1-pyrazolines	44
(B) Kinetic studies	51
(C) Product analysis and isotopic labeling studies	58
<u>Discussion</u>	63
<u>Experimental</u>	76
(A) Preparations	76
(a) Pyrazolidine	76
(b) 1-Pyrazoline	77



	Page
(c) Deuterated 1-pyrazolines	77
(B) Deuterium analysis	81
(C) Kinetic measurements	81
(D) Product analysis	83
CHAPTER II <u>AZO-BIS-3-PROPENE</u>	86
<u>Introduction</u>	86
(A) Gas phase thermolysis of azoalkanes	86
(B) Polanyi relations	92
<u>Proposal</u>	95
<u>Results</u>	100
(A) Synthesis of azo-bis-3-propenes	100
(B) Kinetic studies	107
(C) Control runs	115
(D) Product analysis and deuterium labeling studies	116
<u>Discussion</u>	119
<u>Conclusion</u>	135
<u>Experimental</u>	136
(A) Preparations	136
(a) N,N'-Diallylhydrazine	137
(b) Azo-bis-3-propene	137
(c) 3-Propenyl-azo-3'-propene-3',3'-d <sub>2</sub>	139
(d) Azo-bis-3-propene-3,3-d <sub>2</sub>	141





(B) Kinetic Measurements	142
(C) Control Experiments	143
(D) Product Analysis	143
VITA	155





## LIST OF TABLES

		Page
TABLE I	Kinetic parameters of 1-pyrazoline and methyl substituted 1-pyrazoline thermolysis	5
TABLE II	Effect of deuterium substitution in <u>3</u> at 241.75°C	8
TABLE III	Butene product proportions from pyrolysis of <u>2</u> and methylcyclopropane	16
TABLE IV	Solvolytic $\alpha$ -deuterium isotope effects	25
TABLE V	Solvolytic $\beta$ -deuterium isotope effects	28
TABLE VI	Radical $\alpha$ -deuterium isotope effects	33
TABLE VII	Radical $\beta$ -deuterium isotope effects	38
TABLE VIII	Inverse $\alpha$ -deuterium isotope effects	40
TABLE IX	The thermolysis of 1-pyrazoline ( <u>1</u> ) and the least square calculation for the rate constant	55
TABLE X	Rate constants and secondary kinetic isotope effects for $\alpha$ -deuterated 1-pyrazolines at 229.40 $\pm$ 0.05°	56
TABLE XI	Rate constants and secondary kinetic isotope effects for $\beta$ -deuterated 1-pyrazolines	57
TABLE XII	Cyclopropane and propylene yields on thermolysis of pyrazolines at 241°	60



		Page
TABLE XIII	The predicted and the observed $\alpha$ -deuterium isotope effects in the thermolysis of $\alpha$ -deuterated-1-pyrazolines <u>34</u> and <u>35</u> at 229.5°C	65
TABLE XIV	Relative retention data for the thermolysis products of 1-pyrazoline <u>1</u>	85
TABLE XV	Kinetic parameters in the thermal decomposition of some azo compounds	89
TABLE XVI	The predicted $\alpha$ -deuterium isotope effects in the thermolysis of $\alpha$ -deuterated azo-bis-3-propenes <u>55</u> and <u>56</u> at 150°C	98
TABLE XVII	Rate constants and activation parameters for the thermolysis of azo-bis-3-propene ( <u>54</u> )	110
TABLE XVIII	Least squares calculation of the activation parameters for the thermolysis of azo-bis-3-propene ( <u>54</u> )	111
TABLE XIX	Rate constants and secondary kinetic isotope effects for $\alpha$ -deuterated azo-bis-3-propene	114
TABLE XX	Rates of thermolysis of azo-bis-3-propene ( <u>54</u> ) at different pressures and 158.812°C	114
TABLE XXI	Corrected isotope effects for <u>55</u> and <u>56</u>	129
TABLE XXII	Activation energies of some azo alkanes and bond dissociation energies of the corresponding R-H bonds	134
TABLE XXIII	Relative retention data for the thermolysis products of azo-bis-3-propene ( <u>54</u> )	145





## LIST OF FIGURES

Figure		Page
1	Infrared spectrum of 1-pyrazoline	47
2	NMR spectrum of 1-pyrazoline	47
3	NMR spectrum of 1-pyrazoline-4- $\underline{d}_1$	49
4	NMR spectrum of 1-pyrazoline-4,4- $\underline{d}_2$	49
5	NMR spectrum of 1-pyrazoline-3,3- $\underline{d}_2$	50
6	NMR spectrum of 1-pyrazoline-3,3,5,5- $\underline{d}_4$	50
7	Plot of $\log (E_\infty - E_t)$ vs. $t$ for the thermolysis of 1-pyrazoline at $229.40 \pm 0.05^\circ$	54
8	Plot of standard free energy vs. reaction coordinate	71
9	Schematic diagram of the apparatus used for the kinetic studies	82
10	Schematic diagram of the bulb crusher	84
11	Polanyi plots of $E_a$ vs. $D(R-H)$ for reactions $X + RH = XH + R$	94
12	NMR spectrum of diethyl-N,N'-diallylbis-carbamate ( <u>57</u> )	103
13	Infrared spectrum of azo-bis-3-propene ( <u>54</u> )	103
14	NMR spectrum of azo-bis-3-propene ( <u>54</u> )	104
15	NMR spectrum of 3-propenyl-azo-3'-propene-3',3'- $\underline{d}_2$ ( <u>55</u> )	104
16	NMR spectrum of azo-bis-3-propene-3,3- $\underline{d}_2$ ( <u>56</u> )	104





Figure		Page
17	Plot of $\log (E_{\infty} - E_t)$ vs. $t$ for the thermolysis of azo-bis-3-propene at $152.69^{\circ}$	109
18	NMR spectrum of 1,5-hexadiene	118
19	NMR spectrum of products from thermolysis of 3-propenyl-azo-3'-propene-3',3'- $\underline{d}_2$ (55)	118
20	NMR spectrum of products from thermolysis of azo-bis-3-propene-3,3- $\underline{d}_2$	118
21	Plot of $E_a$ vs. reaction coordinate	131
22	Polanyi plot for the thermolysis of azo compounds	133
23	NMR spectrum of N-allyl-N,N'-dicarboethoxyhydrazine (62)	140



## CHAPTER I

## H I S T O R I C A L

(A) Thermal Isomerization of Cyclopropane

The mechanism of the gas phase thermal isomerization of cyclopropane to propylene has been investigated by several workers.

Chambers and Kistiakowsky (1) carried out the first thorough kinetic studies on the thermal isomerization of cyclopropane to propylene. They found that the isomerization is homogeneous, unimolecular and proceed with an activation energy of 65.0 kcal mole<sup>-1</sup> and frequency factor of  $10^{15.17}$  at high pressure. Two mechanisms were suggested by these authors. The first operated through a ring opening to give a trimethylene diradical, which was then subjected to a hydrogen shift to give propylene or rotation to cyclopropane. The second mechanism involved a ring opening concerted with hydrogen migration to produce propylene. Neither was preferred to the other by the authors.

Since then a large variety of diagnostic experiments have been applied in an attempt to distinguish between these two mechanisms.

The very elegant work of Rabinovitch and co-workers (2a) on the geometrical isomerization of trans-cyclopropane-d<sub>2</sub>, indicated that the trans compound underwent geometrical isomerization to the cis isomer approximately 12 times faster than its structural isomerization to propylene-d<sub>2</sub>. Thus, they concluded that both





geometrical and structural isomerization may be occurring from the same intermediate.

Further evidence for the intermediacy of the trimethylene diradical in the thermal isomerization of cyclopropane was provided by the works of Rabinovitch (2b,c,d) and Benson (3).

Rabinovitch and co-workers (2) proposed that the two electrons on the terminal methylene groups of the intermediate are not free of their mutual influence, and considered it as an "expanded-ring intermediate". This could be the reason why several attempts to trap such an intermediate by scavengers such as oxygen (2b), nitric oxide (4) or ethylene (5) have been unsuccessful.

Benson (3) calculated, from the data of the thermal isomerization of cis-cyclopropane- $d_2$  (2b) and the thermochemistry of these molecules, a life-time of  $10^{-10.5}$  second for the trimethylene diradical\* at 444°C which is at least 100 times less than the collision time at one atmosphere pressure.

Additional information has been inferred on the nature of the isomerization of cyclopropane, from the addition of methylene to olefins, wherein the trimethylene diradical has been suggested as an intermediate.

---

\* Benson's calculations were based on the trimethylene diradical being a true diradical (pair of spectroscopic doublets). This should not be confused with Hoffman's trimethylene species to be discussed later (page 16).



Rabinovitch (6) assumed that singlet methylene adds to the olefinic double bond in a three-centered mechanism to form a "hot" cyclopropane ring, and that all of the propylene, except that which is formed by insertion, arises from subsequent ring opening of the "hot" cyclopropane.

Benson(7) however, believes that "a short-lived diradical must be formed as the initial step, in the addition of both the singlet and triplet methylene to an olefin". He illustrated his point by calculation, based on the intermediacy of the trimethylene diradical, of the propylene to cyclopropane ratio. Considering the following scheme:



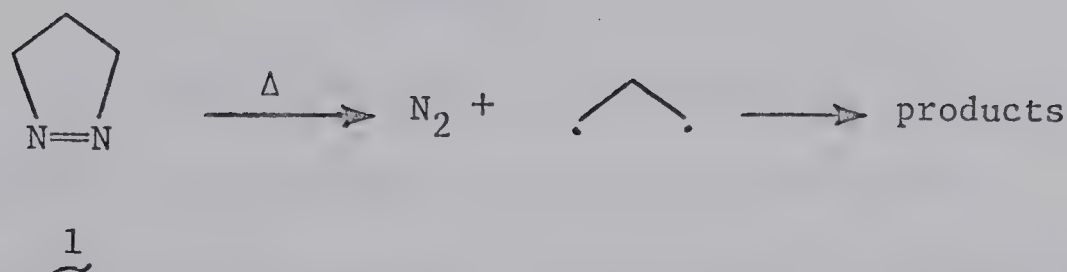
Benson calculated,  $k_{-1} = 10^{11.6} \text{ sec}^{-1}$  and  $k_2 = 10^{10.6} \text{ sec}^{-1}$ . Therefore, he predicted (3a) that about 90% cyclopropane and 10% propylene would be formed from such an intermediate, which is in good agreement with the experimental results (8).

#### (B) Thermolysis of 1-pyrazolines

The mechanism of the gas phase thermolysis of 1-pyrazoline (1) has been suggested by Crawford and co-workers (9-12) to proceed through a trimethylene intermediate.







Crawford and Mishra (12) during their kinetic studies on the thermolysis of 1 and its methylated derivatives Table I, observed the following:

- (1) A progressive decrease in activation energy on going from 1 to 3,3,5,5-tetramethyl-1-pyrazoline (9).
- (2) Methyl substitution on C<sub>3</sub> or C<sub>5</sub> of 1 brings about a 1.2±0.2 kcal per mole per methyl group reduction in the activation energy of the thermolysis process.
- (3) cis-3,5-Dimethyl-1-pyrazoline (6) and trans-3,5-dimethyl-1-pyrazoline (7) displayed activation parameters similar to that of 3,3-dimethyl-1-pyrazoline (5).

On the basis of these observations, they concluded that both carbon-nitrogen bonds are being cleaved in the rate-determining step.

Further evidence for the simultaneous two-bond cleavage mechanism has been obtained by Cameron (13) in the thermolysis of 3-vinyl-1-pyrazoline (11). He observed that the introduction of a vinyl group into the 3 position of the 1-pyrazoline ring brings about a 10.2±0.8 kcal mole<sup>-1</sup> decrease in the activation energy. This decrease, when compared with the 12.6±0.8 kcal mole<sup>-1</sup> suggested



TABLE I

Kinetic parameters of 1-pyrazoline  
and methyl substituted 1-pyrazoline thermolysis

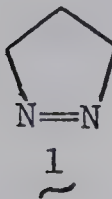
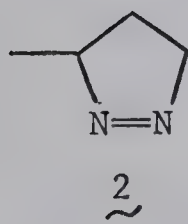
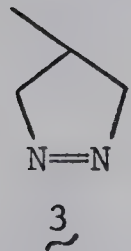
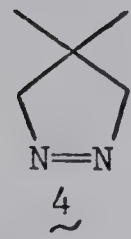
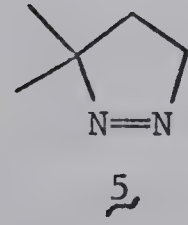
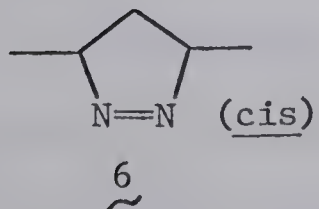
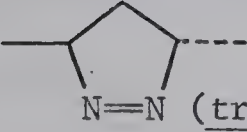
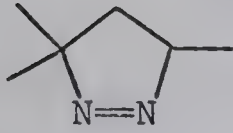
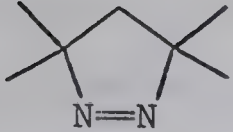
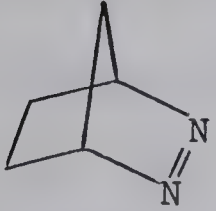
Compound	Ea (kcal)	Log A	$\Delta S_{250^\circ}^\ddagger$ (e.u.)
 1	42.4±0.3	15.93±0.13	11.2±0.6
 2	41.0±0.3	15.7±0.15	10.1±0.7
 3	42.2±0.2	15.85±0.05	10.8±0.3
 4	42.8±0.2	14.10±0.07	2.9±0.3
 5	40.0±0.2	15.85±0.3	10.8±0.2
 6	40.3±0.3	15.54±0.11	9.4±0.5





TABLE I

(cont'd)

Compound	Ea (kcal)	Log A	$\Delta S_{250^\circ}^\ddagger$ (e.u.)
 7	40.2±0.3	15.67±0.11	10.0±0.5
 8	39.0±0.4	15.42±0.21	8.9±0.9
 9	37.7±0.4	14.49±0.12	4.6±0.8
 10	36.9±0.2	14.74±0.10	5.8±0.5

as the delocalization energy of the allyl radical (14), implies that, complete electron delocalization is nearly attained in the rate-determining transition state (i.e.  $C_3-N_2$  is almost completely broken in the transition state). A secondary  $\alpha$ -deuterium kinetic isotope effect of  $1.21 \pm 0.03$  at  $134-135^\circ\text{C}$  was observed when the rate of thermolysis of 11 was compared to that of 3-vinyl-1-pyrazoline-5,5-



$\underline{d}_2$  (12). This value, which is in agreement with those observed by Seltzer (15) in the thermolysis of azoalkanes, led to the conclusion that a cleavage of  $C_5-N$  bond is also taking place in the rate-determining step.\*

Additional evidence for the simultaneous two-bond cleavage mechanism has been provided by Ali's kinetic studies (16) on the thermolysis of cis- and trans-3,4-dimethyl-1-pyrazoline-5,5- $\underline{d}_2$  (13 and 14, respectively).

Mishra's kinetic and product studies (12) on the thermolysis of 4-methyl-1-pyrazoline-4- $\underline{d}_1$  (15), Table II, provided strong evidence that nitrogen elimination occurs in the rate-determining step of the thermolysis reaction to yield a hydrocarbon intermediate. When the rate constant of thermolysis of 4-methyl-1-pyrazoline (3) was compared to that of 15 a relatively small kinetic isotope effect was observed, which implies that the C-H bond is not significantly changed in its nature in the rate-determining step ( $k_1$ ). But a large mechanistic isotope effect was observed in the product-determining step ( $k_2$ ). This observed isotope effect implies that cyclopropane and olefin came from the same intermediate formed after the rate-determining step of the thermolysis process (Scheme I).

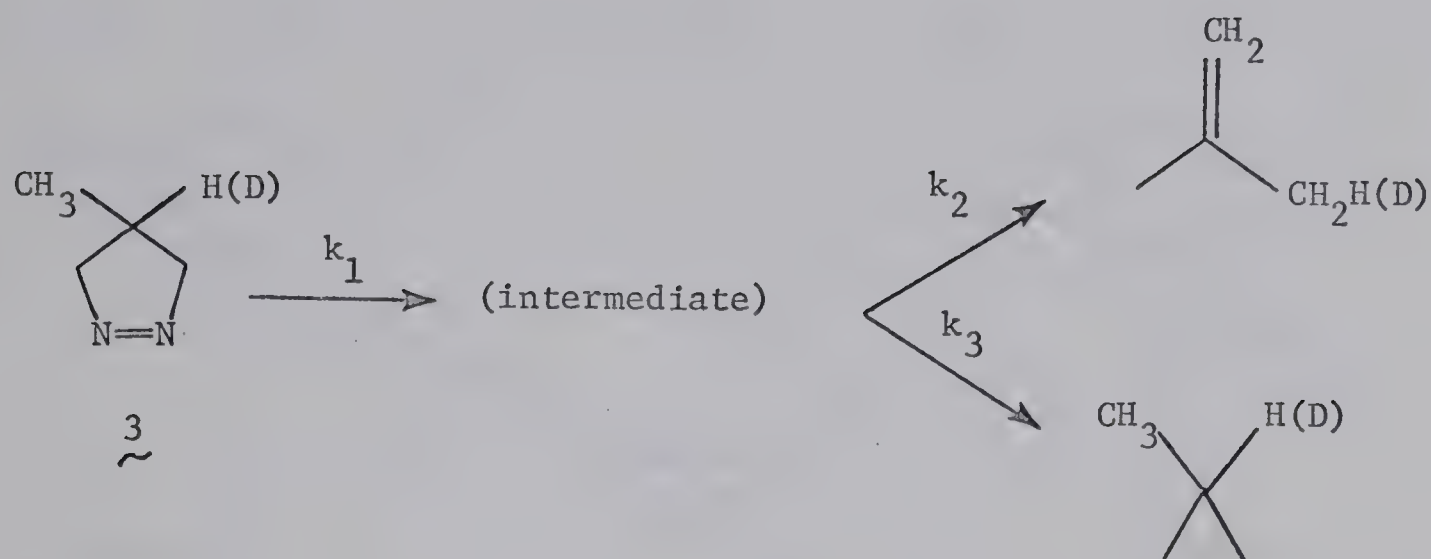
Further stereochemical evidence has been provided by

---

\* (The authors feel that the  $C_3-N$  bond rupture is in advance of the  $C_5-N$  bond, but that both bonds are undergoing valence change in the rate-determining transition state).







$$k_{2\text{H}}/k_{3\text{H}} = 47.7/52.3 \quad \text{and} \quad k_{2\text{D}}/k_{3\text{D}} = 34.0/66.0;$$

$$\text{then } k_{3\text{D}}k_{2\text{H}}/k_{3\text{H}}k_{2\text{D}} = 1.80 \pm 0.8, \quad k_{1\text{H}}/k_{1\text{D}} = 1.07 \pm 0.03$$

Scheme I

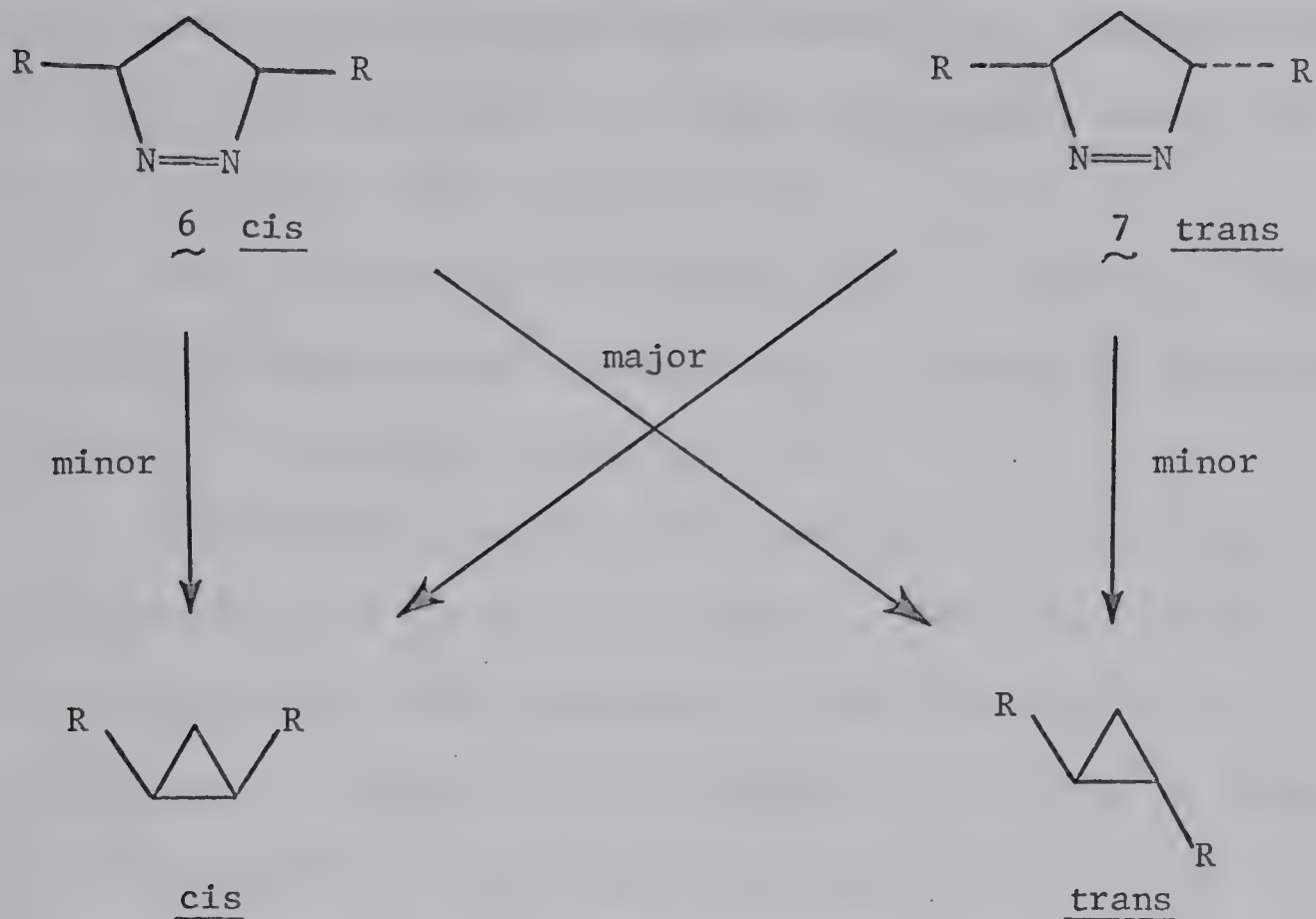
TABLE II

Effect of deuterium substitution in 3 at 241.75°C

Compound	$10^4 k \text{ (sec}^{-1}\text{)}$	% cyclopropane	% 2-methylpropene
<u>3</u>	$64.1 \pm 0.6$	$52.3 \pm 0.3$	$47.7 \pm 0.3$
<u>15</u>	$59.5 \pm 0.6$	$66.0 \pm 0.3$	$34.0 \pm 0.4$

Mishra (9) on the intermediacy of trimethylene species. When 6 or 7 was thermolyzed, each gave 1,2-dimethyl cyclopropane, but mainly of opposite geometry (Scheme II).





Scheme II

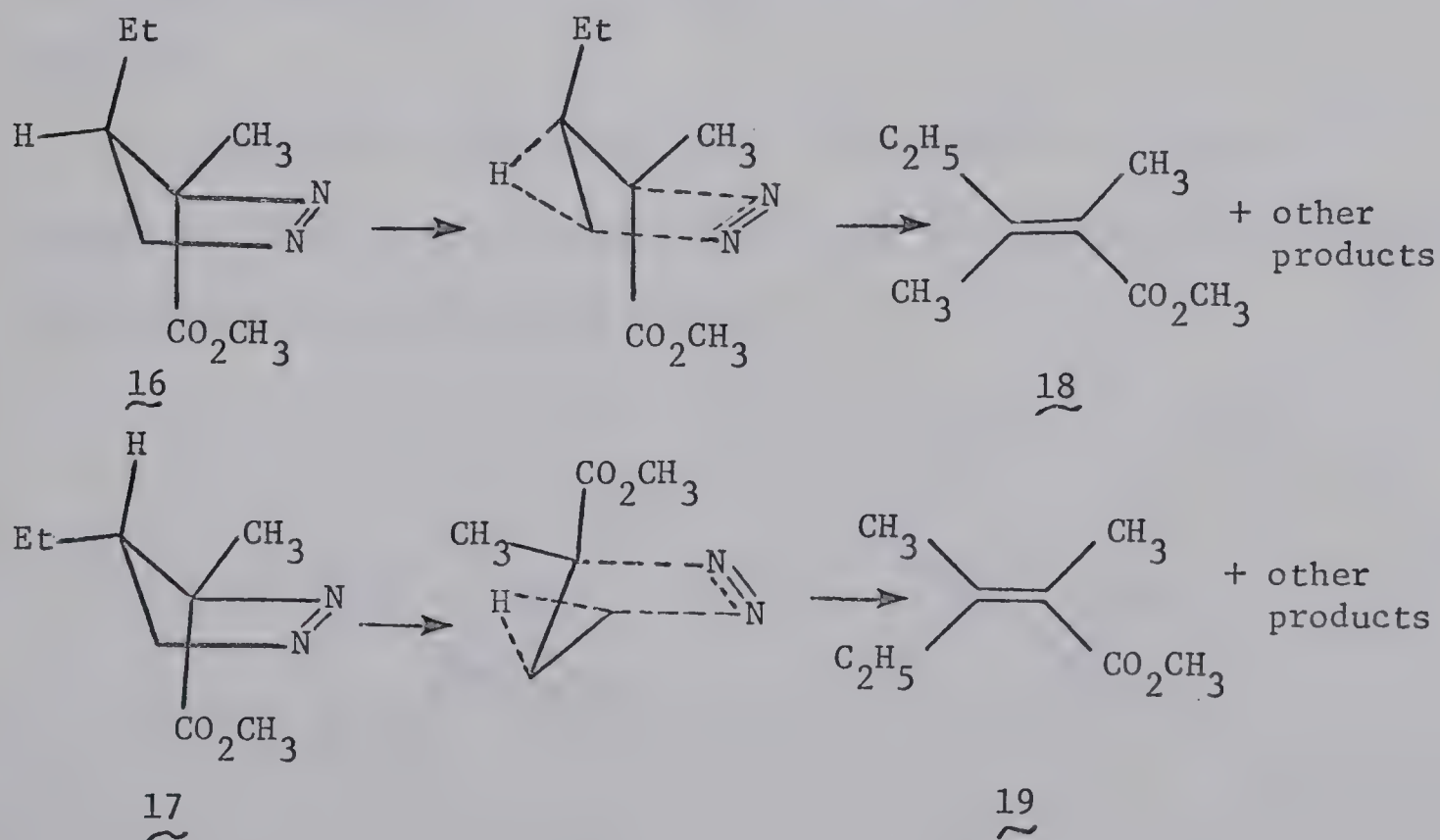
A heterolytic one-bond cleavage mechanism to give a dipolar intermediate was excluded on the basis that such a mechanism cannot explain the decrease in activation energy upon alkyl substitution on C<sub>3</sub> and C<sub>5</sub> of 1, e.g., compare 3,3,5-trimethyl-1-pyrazoline (8) with 5 Table I. For the homolytic one-bond cleavage mechanism the thermolysis of 5 would be expected to have the same activation energy as that of 9 and differ only by a statistical factor of 2 in the pre-exponential rate factor for 9. The observed enthalpies and entropies of activation are not consistent with such an interpretation (12). The difference in activation parameters is, however, consistent with a process wherein both bonds are undergoing



cleavage in the rate-determining step. Furthermore, the one-bond cleavage mechanism would suggest that the activation parameters for 3-methyl-1-pyrazoline (2), 6, and 7 should be similar, but as may be seen from Table I, this is not the case.

That the elimination of nitrogen is the rate-determining step of the thermolysis was confirmed when an attempt to interconvert 6 and 7, by a control run, was unsuccessful.

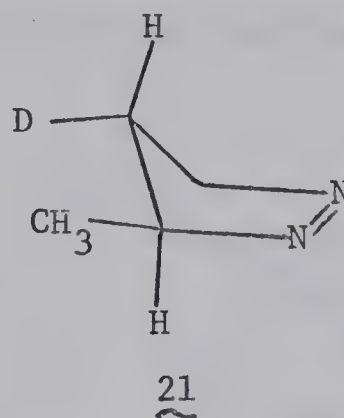
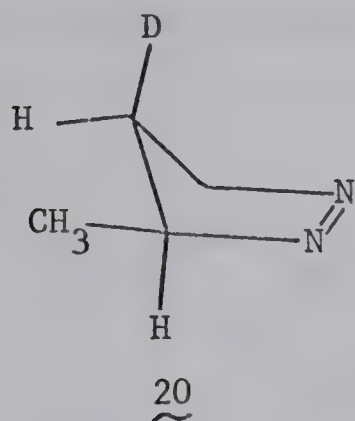
McGreer and co-workers (17) have studied the mechanism of the thermolysis of 16 and 17 in solution. They observed that olefin formation is highly stereospecific and that only one of the substituted 2-pentenoic acid derivatives, 18 and 19, is formed from the thermolysis of 16 and 17 respectively. On the basis of the above observation they suggested a mechanism of hydrogen migration concerted with nitrogen elimination in the olefin forming process.





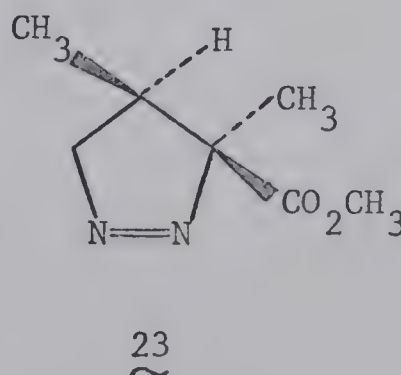
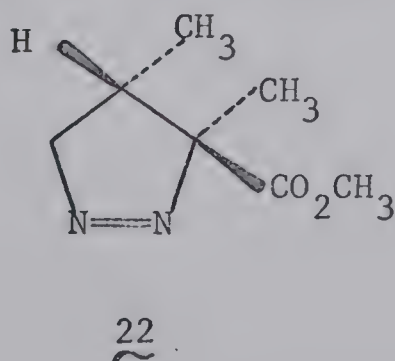


The possibility that the above mechanism is operating in the gas phase thermolysis of 1-pyrazolines was excluded by Erickson's (18) results of the thermolysis of cis- and trans-4-deuterio-3-methyl-1-pyrazolines (20 and 21). From the nuclear magnetic resonance



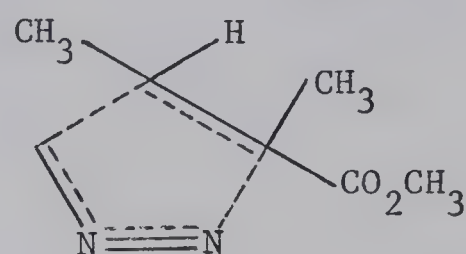
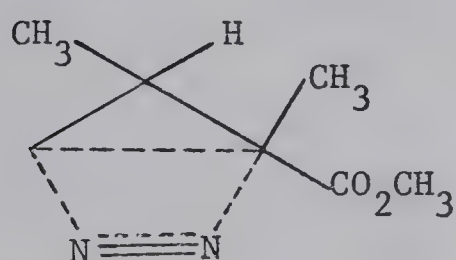
integration ratios of the olefinic products of the deuterium labeling, it was found that these ratios are independent of the initial stereochemistry of the reactants 20 and 21. Furthermore, these product ratios demonstrate that both hydrogen and deuterium migrate in the same proportions from both 20 and 21 as predicted by Mishra's mechanism.

Van Auken and Rinehart (19) have carried out both the thermal and photolytic decomposition of cis- and trans-3,4-dimethyl-3-carbomethoxy-1-pyrazolines (22 and 23).



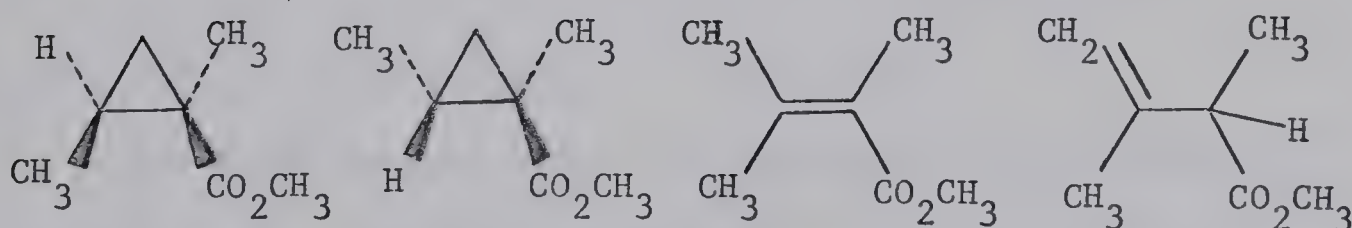


From the photolytic decomposition of 22 and 23 the authors observed that cyclopropane formation was highly stereoselective, and besides the normal products encountered in thermolysis, some starting olefins were formed, presumably through reversal of the normal 1,3-addition. On the basis of these observations, they suggested concerted molecular transition states, 24, for the photolysis.



24

In the case of the thermal decomposition, the following product distributions were observed:

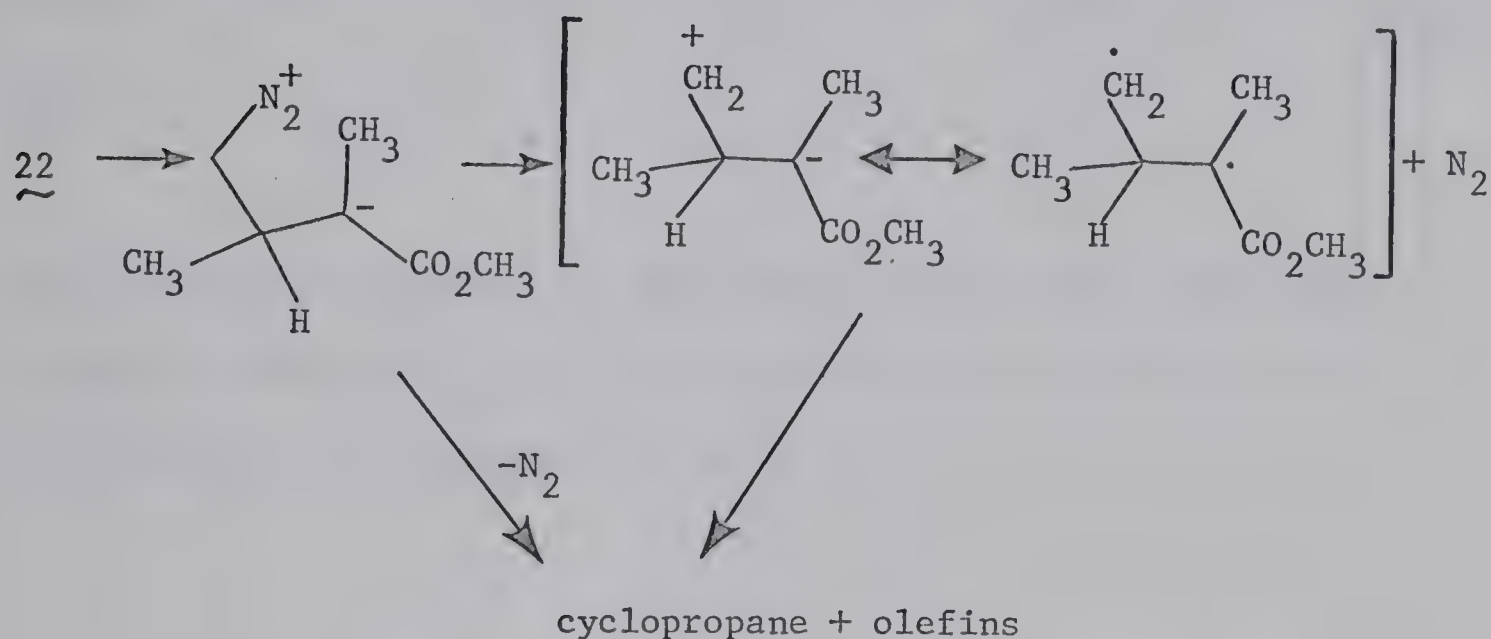


<u>22</u>	12.3%	17.6%	65.8%	4.3%
<u>23</u>	34.5%	28.3%	32.8%	4.4%





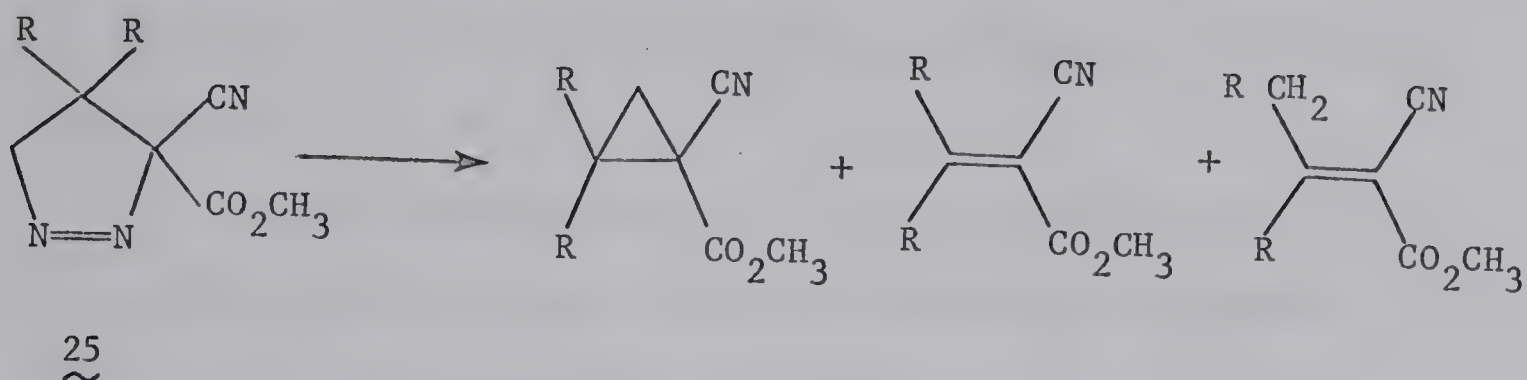
Thus, they proposed a heterolytic one-bond cleavage mechanism with the subsequent formation of a dipolar intermediate as follows:



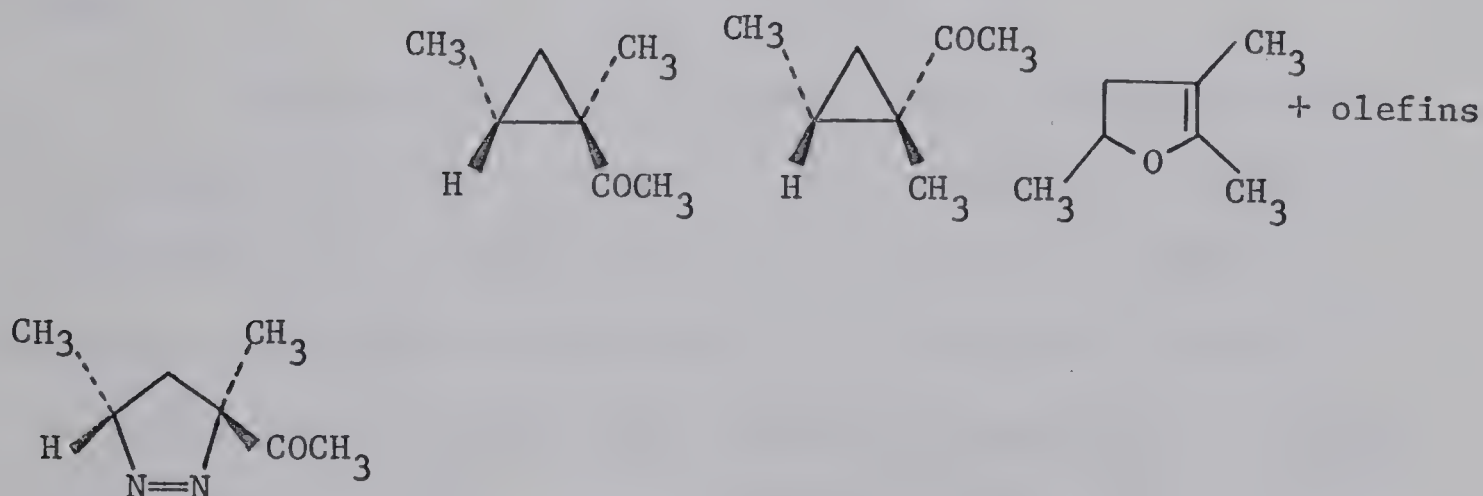
As a consequence of dipolar intermediate formation, one should expect, in specific cases, an alkyl migration from  $C_4$  to  $C_5$ , and that the delocalization of the developing negative charge on  $C_3$  onto a suitable carbonyl group will lead to dihydrofuran formation through ring-closure on the oxygen atom.

The above possibilities have been realized by McGreer and co-workers (20) and Hamelin and Carrié (21) through their experimental investigations. When McGreer and co-workers carried out the thermal decomposition of 3-cyano-3-carbomethoxy-4,4-dialkyl-1-pyrazoline (25), they observed olefinic products resulting from alkyl migration. Thus, they concluded that alkyl migration is concerted with nitrogen elimination. The authors also observed





the dihydrofuran formation in the thermolysis of cis-3,5-dimethyl-3-acetyl-1-pyrazoline (26). No dihydrofuran has been observed in the thermolysis of the trans isomer 27.



<u>26</u> <u>cis</u>	16%	24%	23%	37%
<u>27</u> <u>trans</u>	61%	17%	0%	22%

These results indicate that the cis isomer 26 gave rise to an intermediate or transition state which had a suitable geometry for cyclization at the oxygen atom.



A similar conclusion has been reached by Hamlin and Carrié (21) from their studies on the thermolysis of 3-cyano-3-carboethoxy-1-pyrazolines.

All the above studies were carried out in solution on compounds containing strongly electron withdrawing substituents, thus an ionic mechanism is highly probable.

Crawford and co-workers have carried out their studies in the gas phase. It is very likely that a different mechanism is operating and the trimethylene species is formed. The same conclusion has been reached by McGreer and co-workers (20c) when they carried out the thermolysis of the foregoing compounds in the gas phase.



The assumption made by Crawford about the generation of an intermediate which is similar to that produced by cyclopropane isomerization was further confirmed by comparing the yield of propylene (11.57%) relative to that of cyclopropane (88.43%) on the thermolysis of 1 with that predicted by Benson (3a) on cyclopropane isomerization. Comparison of the olefin products formed by the thermolysis of 3-methyl-1-pyrazoline (2) with those produced from methylcyclopropane thermolysis lend credence to the suggestion that both reactions proceeded through a common intermediate (Table III) (12).





TABLE III

Butene product proportions from  
pyrolysis of 2 and methylcyclopropane

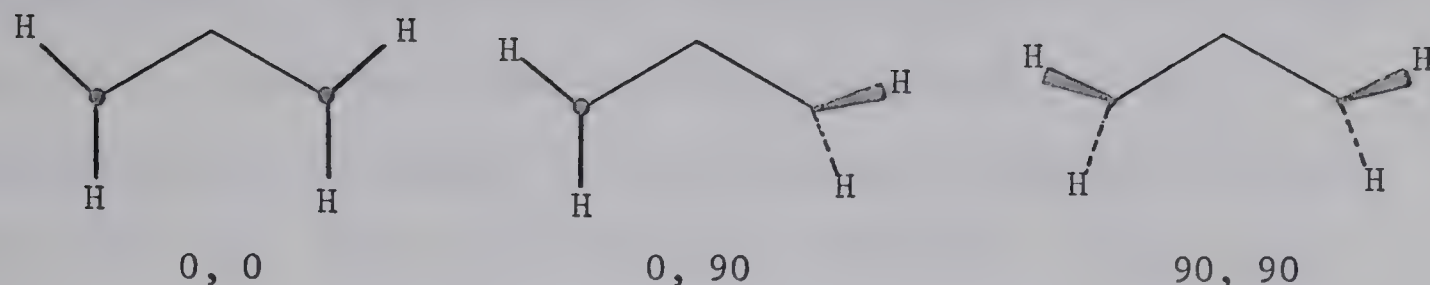
Reactant	Temp., °C	1-Butene	<u>cis</u> -2-Butene	<u>trans</u> -2-Butene	Other
<u>2</u>	250	1.0	0.53±0.05	0.35±0.05	 25.0
Methylcyclo- propane	469	1.0	0.63	0.28	 0.23

(C) Theoretical Treatment of Trimethylene

Theoretical calculations have recently been carried out by Hoffmann (22) on the trimethylene species using the extended Hückel molecular orbital method. The number of degrees of freedom in the general  $\text{CH}_2\text{CH}_2\text{CH}_2$  potential surface was reduced to the three most important degrees of freedom of the molecule; the central CCC angle and the rotations of the terminal methylene groups out of the plane defined by the three carbon atoms. The total energy of the system was investigated with respect to the variation of these three degrees of freedom.

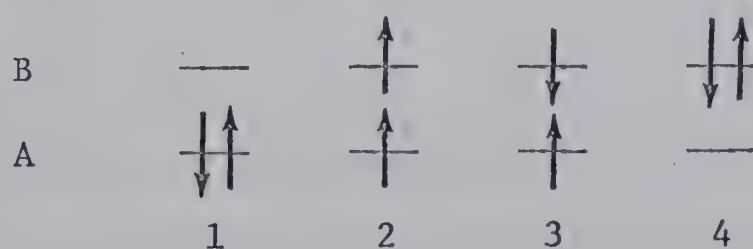
Three geometries are recognized for the trimethylene species.





From the examination of the ground configuration potential energy surface, the 90,90 geometry was found to be the most stable point on it at small CCC angle, and this will become a cyclopropane when the geometrical restraints are further relaxed. But the 0,0 configuration (i.e., terminal methylene coplanar with the three carbon-chain) displayed an energy minimum on the potential energy surface with a CCC angle of approximately  $125^\circ$ . The 0,90 geometry was predicted to be always higher in energy than the other two, but also apparently has a subsidiary energy minimum, at a central angle of  $110^\circ$ .

Two energy levels, close in energy, were considered during his calculations on the trimethylene, which led to four possible states arising from the placement of the two electrons in the molecular orbitals.







On the basis of electron interaction, it is very likely that the triplet state 2, arising from an "excited" electronic configuration, will be the true ground state for the trimethylene, but this possibility was not examined since the extended Hückel calculations do not take into account the electron interaction. State 1 was concluded to be the ground electronic configuration for the trimethylene, with a high barrier to internal rotation. While the first excited configuration, states 2 and 3, were concluded to be "floppy" entities with no barrier to internal rotation, Hoffmann further indicated that these two states, 2 and 3, showed a very broad valley for all three configurations on the potential surface. Thus, the most stable configuration of the trimethylene species was assigned as state 1 with 0,0 structure and a CCC bond angle of  $125^\circ$ .

The antisymmetric (A) level for the singlet trimethylene was found to be lower than the symmetric (S) by approximately 0.55 e.v.



This was attributed to a hyperconjugative interaction between the central methylene and the termini, which destabilized the (S) level leaving the (A) level unaffected. Thus the predicted preferred



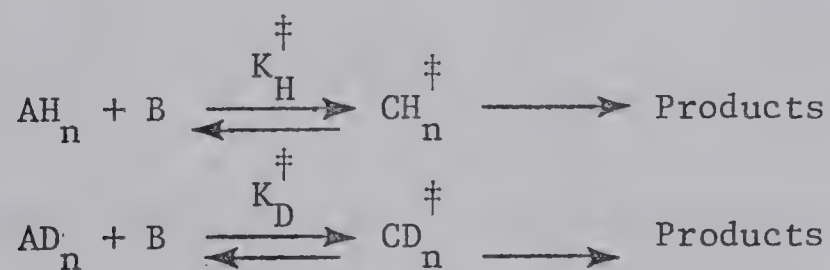
motion for the two terminal methylene groups to close to cyclopropane is conrotatory, and this is in good agreement with those observed by Crawford and Mishra (9) in the thermolysis of cis- and trans-3,5-dimethyl-1-pyrazoline (6 and 7) (see Scheme II, page 9).

(D) Secondary Deuterium Kinetic Isotope Effects (23)

(a) Derivation of Bigeleisen Equation

The Bigeleisen (24) derivation of rate constants for competitive reactions of isotopic molecules is carried out within the framework of the transition state theory, in which a quasi-equilibrium is established between the reactants and the transition state.

In the case of secondary deuterium isotope effects, the following equations may be written:



$K^\ddagger$  is essentially, but not exactly, an equilibrium constant between the activated complex and the reactants; it differs primarily in that there is one degree of freedom less in the transition state than in the ground state.

The transition state theory leads to the following expression for the reaction rate constant  $k$ .



$$k = \frac{k' T}{h} \kappa K^{\ddagger} \quad (1)$$

Where  $k'$  and  $h$  are Boltzmann and Plank's constants respectively,  $T$  the absolute temperature,  $\kappa$  is the transmission coefficient and  $K^{\ddagger}$  as defined above. Consequently the ratio of the rate constants for the two isotopic reactions can be expressed as

$$\frac{k_H}{k_D} = \frac{\kappa_H}{\kappa_D} \frac{K_H^{\ddagger}}{K_D^{\ddagger}} \quad (2)$$

$K^{\ddagger}$  can be expressed in terms of the partition functions of the reactants and of the activated complex. Thus equation 2 becomes

$$\frac{k_H}{k_D} = \frac{\kappa_H}{\kappa_D} \frac{Q_{CHn}^{\circ \ddagger}}{Q_{CDn}^{\circ \ddagger}} \frac{Q_{ADn}^{\circ}}{Q_{AHn}^{\circ}} \quad (3)$$

Where the  $Q$ 's are the complete set of partition functions for the reaction, and  $Q^{\ddagger}$ 's are those of the transition state, less that degree of freedom which corresponds to that along the reaction coordinate.

The initial assumption is made that  $\kappa_H = \kappa_D$ . On the basis of Born-Oppenheimer approximation of the possible separability of electronic and nuclear motion,  $Q^{\circ}$  may be regarded as

$$Q^{\circ} = Q_{\text{elect.}} \times Q_{\text{trans.}} \times Q_{\text{rot.}} \times Q_{\text{vib.}}$$





The isotope effects on electronic energies, to a high approximation, are accepted to be negligible. This means that the potential energy surfaces for isotopic molecules are the same to a very high degree of approximation. Thus, each partition function can be regarded as

$$Q^{\circ} = Q_{\text{trans.}} \times Q_{\text{rot.}} \times Q_{\text{vib.}} \times \text{constant}$$

Then the isotope effect can be calculated in terms of the ratio of the isotopic partition functions for nuclear motion.

The following three fundamental approximations are made in order to calculate isotope effects in terms of the ratios of the isotopic partition functions:

- (a) Rotational-vibrational interactions are neglected.
- (b) Rotational partition functions are assumed classical at room temperature.
- (c) The anharmonicity of the vibrational partition functions are neglected.

Then after substituting for each term, the isotope effect at temperature T, is

$$\frac{k_1}{k_2} = \frac{\left[ \frac{I_{A_2} I_{B_2} I_{C_2}}{I_{A_1} I_{B_1} I_{C_1}} \right]^{\frac{1}{2}} \left( \frac{M_2}{M_1} \right)^{\frac{3}{2}} \prod_j \frac{3N-6}{[1-\exp(-u_{1j})]} \frac{\exp[\sum(u_{1j}-u_{2j})/2]}{\prod_i \frac{3N-7}{[1-\exp(-u_{1i}^{\dagger})]} \frac{\exp[\sum(u_{1i}^{\dagger}-u_{2i}^{\dagger})/2]}}{\left[ \frac{I_{A_2}^{\dagger} I_{B_2}^{\dagger} I_{C_2}^{\dagger}}{I_{A_1}^{\dagger} I_{B_1}^{\dagger} I_{C_1}^{\dagger}} \right]^{\frac{1}{2}} \left( \frac{M_2^{\dagger}}{M_1^{\dagger}} \right)^{\frac{3}{2}} \prod_i \frac{3N-7}{[1-\exp(-u_{1i}^{\dagger})]} \frac{\exp[\sum(u_{1i}^{\dagger}-u_{2i}^{\dagger})/2]}{\prod_i \frac{3N-7}{[1-\exp(-u_{2i}^{\dagger})]}} \quad (4)$$



where 1 and 2 refer to light and heavy isotopic species, respectively; ‡ refers to the transition state;  $I_b$  are principal moments of inertia and  $M$ 's are molecular masses;  $u = h\nu/k'T$  where  $\nu$  is a normal vibrational frequency, and  $k'$  and  $h$  are as defined earlier.

The difficulties in calculating the ratios of the moments of inertia can be avoided by making use of the Teller-Redlich product rule, which allows us to express the isotope effects as a function of vibrational frequency alone. The ratios of the molecular masses can be replaced by the ratios of the individual atomic masses (some of which will disappear by cancellation). This is the basis of Bigeleisen's treatment of calculating the kinetic isotope effect.\* Using equation 4 and replacing the indices 1 and 2 by H and D respectively, and rearranging it, we obtain equation 5.

---

\*

(Thus the isotope effect can be calculated from a knowledge of the complete vibrational frequencies of all molecular species, part of which may be known and part estimated).





$$\frac{k_H}{k_D} = \frac{\frac{v_H^\ddagger}{v_D^\ddagger} \prod_{i=1}^{3N^\ddagger-7} \frac{u_i^\ddagger(H) [1-\exp\{-u_i^\ddagger(D)\}] \exp\{-1/2u_i^\ddagger(H)\}}{u_i^\ddagger(D) [1-\exp\{-u_i^\ddagger(H)\}] \exp\{-1/2u_i^\ddagger(D)\}}}{\prod_{j=1}^{3N-6} \frac{u_j(H) [1-\exp\{-u_j(D)\}] \exp\{-1/2u_j(H)\}}{u_j(D) [1-\exp\{-u_j(H)\}] \exp\{-1/2u_j(D)\}}} \quad (5)$$

$v^\ddagger$  refers to the zero or imaginary frequency of the transition state, or frequency of decomposition. Equation 5 is referred to as the complete Biegeleisen expression. Tunneling through the potential barrier is neglected, and the symmetry numbers are omitted.

In order to enable them to calculate the kinetic isotope effects, Wolfsberg and Stern (25) have developed a computer program, using the program written by Schachtschneider (26). The input data consist of molecular geometries, atomic masses and force constants for the initial and transition states. Wolfsberg's program, thus, calculates isotopic effects between two states from the frequencies generated by the Schachtschneider program. Therefore, the kinetic isotope effect can be calculated from the knowledge of force constants and geometry of the reactants and the transition states. Normally the force constants far from the reaction center are generally assumed not to change in going from the reactant to the transition state. Only those centers close to the reaction site are included in the calculations. In case of the transition state the force constants are evaluated by altering reactant state



force constants in such a way as to fit the experimentally observed isotope effects.

(b) Examples of Secondary Deuterium Isotope Effects on Ionic Reactions

(i) Effects of the First Kind

The secondary  $\alpha$ -deuterium isotope effects on the rates of numerous solvolytic reactions, approaching  $SN_1$  in character, have been measured independently by Mislow (27), Streitwieser (28), Johnson (29), Lewis (30), Saunders (31), Borcic (32), and Shiner (33) and their co-workers, Table IV. It has been attributed to the change in bond hybridization from  $sp^3$  to  $sp^2$  on going from the ground state to the transition state (carbonium ion). Streitwieser (28) described as the most important factor, in the  $\alpha$ -deuterium effect, the lower frequency of the "out-of-plane" bending vibration of the  $sp^2$  hybridized C-H bond in the carbonium ion compared to that of the corresponding vibration of the  $sp^3$  hybridized C-H bond in the ground state.

Bartell(34) has ascribed the  $\alpha$ -deuterium isotope effect to a non-bonding interaction(steric effect) between the  $\alpha$ -hydrogen atom with the adjacent groups or atoms within the molecule, which is greater in the tetrahedral bonding than in the planar-trigonal bonding. Bartell's argument is that, since the amplitudes of vibration of hydrogen atoms are greater than the amplitudes of the heavier deuterium atoms by a readily predictable amount than non-bonded repulsions, averaged over the atomic vibrations, are greater for hydrogen atoms than deuterium atoms. Moreover, there are more, and



T A B L E I V

Solvolytic  $\alpha$ -deuterium isotope effects

Compound	Solvent	T°C	$k_H/k_D$	$\Delta\Delta G^\ddagger/n$ (cal)	Reference
Benzyl-1-d <sub>1</sub> tosylate	CH <sub>3</sub> COOH	50	1.12	73±22	27
Benzyl-1,1-d <sub>2</sub> tosylate	CH <sub>3</sub> COOH	50	1.25	71±8	27
Isopropyl-1-d <sub>1</sub> brosylate	CH <sub>3</sub> COOH	70	1.12	77±6	27
2,2-Diphenylethyl-1,1-d <sub>2</sub> tosylate	CH <sub>3</sub> COOH	75	1.21	66±8	31b
2(p-Methoxyphenyl)ethyl-1,1-d <sub>2</sub> tosylate	CH <sub>3</sub> COOH	75	1.18	57±2	31b
2,2-Diphenylethyl-1,1-d <sub>2</sub> tosylate	HCOOH	75	1.21	66±5	31b
2(p-Methoxyphenyl)ethyl-1,1-d <sub>2</sub> tosylate	HCOOH	50	1.20	58±10	31b
2-phenylethyl-1,1-d <sub>2</sub> tosylate	HCOOH	75	1.17	59±6	31a
Isopropyl-1-d <sub>1</sub> tosylate	CH <sub>3</sub> COOH	24.93	1.22±0.2	117±9	28b
Methyltolylcarbonyl-1-d <sub>1</sub> chloride	80% aq(CH <sub>3</sub> ) <sub>2</sub> CO	38	1.10	63±9	30
1-Methylheptyl-1-d <sub>1</sub> brosylate	CH <sub>3</sub> OH	70	1.10	64	29
1-Phenylethyl- $\alpha$ -d <sub>1</sub> chloride	50% H <sub>2</sub> O-CH <sub>3</sub> CH <sub>2</sub> OH	25	1.153±0.001	84	33
1-Phenylethyl- $\alpha$ -d <sub>1</sub> bromide	80% H <sub>2</sub> O-CH <sub>3</sub> CH <sub>2</sub> OH	25	1.122±0.001	68	33
Cyclopropylmethyl- $\alpha$ -d <sub>2</sub> tosylate	CH <sub>3</sub> CH <sub>2</sub> OH	20.0	1.42	102	32a
Cyclopropylmethyl- $\alpha$ -d <sub>2</sub> tosylate	CH <sub>3</sub> COOH	20.0	1.34	85	32a

cont'd





T A B L E I V

cont'd

Compound	Solvent	T°C	$k_D/k_D$	$\Delta\Delta G^\ddagger/n$ (cal)	Reference
Cyclopropylmethyl- $\alpha$ -d <sub>2</sub> benzenesulfonate	CH <sub>3</sub> CH <sub>2</sub> OH	20.0	1.42±0.05	107	32b
Cyclopropylmethyl- $\alpha$ -d <sub>2</sub> benzenesulfonate	CH <sub>3</sub> COOH	20.0	1.30±0.02	80	32b
Cyclopentyl-1-d <sub>1</sub> tosylate	CH <sub>3</sub> COOH	50	1.15±0.01	90	28a
Cyclohexyl-1-d <sub>1</sub> tosylate	CH <sub>3</sub> COOH	75	1.19±0.04	130	27
Cyclododecyl-1-d <sub>1</sub> tosylate	CH <sub>3</sub> COOH	25	1.17±0.02	93	27



stronger non-bonded repulsions in the crowded tetrahedral reactant ( $sp^3$ ) than in the planar carbonium ion transition state ( $sp^2$ ). Accordingly, the trigonal transition state is relieved of non-bonded repulsions to a greater extent when it contains hydrogen than when it contains deuterium.

(ii) Effects of the Second Kind

The  $\beta$ -deuterium isotope effects have been studied extensively in solvolytic reactions with a carbonium ion intermediate. The results of these studies are recorded in Table V. Lewis and co-workers (35) have interpreted the  $\beta$  effect in terms of a hyperconjugative  $\beta$ -CH bond weakening in the transition state, due to the stabilization of the developing positive charge, at the reaction center, by the  $\beta$ -CH bonds. A similar conclusion and interpretation was reached by Shiner and co-workers (33, 36). A contrary explanation was advanced, for the  $\beta$ -effect, by Bartell (34) who interpreted the effect in terms of steric interactions which will be reduced with the change of hybridization around the reaction site ( $sp^3$  to  $sp^2$ ). On the basis of his recent work, Brown (37) stresses the importance of steric effects as a dominant factor in the secondary isotope effects. But more recently, Karabatsos and co-workers (38) concluded, through their calculations, using Bartell's equations, that in ordinary systems with hyperconjugation possible, only a small fraction of the observed  $\beta$ -effect is due to the steric contribution. An alternative explanation has been proposed by Halevi [(23), pp.134-38], who interprets the



T A B L E V

Solvolytic  $\beta$ -deuterium isotope effects

Compound	Solvent	T°C	$k_H/k_D$	$\Delta\Delta G^\ddagger/n$ (cal)	Reference
2-Pentyl-1,1,1,3,3,3-d <sub>5</sub> chlorosulfite	Dioxane	61.5	1.47	58	35a
2-Pentyl-1,1,1,3,3,3-d <sub>5</sub> chlorosulfite	Dioxane	77.5	1.41	58	35a
2-Pentyl-1,1,1,3,3,3-d <sub>5</sub> bromide	HCOOH	98	1.39	56	35b
2-Pentyl-1,1,1,3,3,3-d <sub>5</sub> tosylate	80% CH <sub>3</sub> CH <sub>2</sub> CH <sub>3</sub>	58.2	1.40	51	35b
2-Pentyl-1,1,1,3,3,3-d <sub>5</sub> tosylate	CH <sub>3</sub> COOH	58.2	1.64	75	35b
2-Pentyl-1,1,1,3,3,3-d <sub>5</sub> tosylate	HCOOH	39.9	1.69	76	35b
t-Amylchloride-d <sub>8</sub>	80% CH <sub>3</sub> CH <sub>2</sub> CH <sub>2</sub> OH	25	2.35	64	36a
2-Chloro-2-methylbutane-3,3-d <sub>2</sub>	80% CH <sub>3</sub> CH <sub>2</sub> CH <sub>2</sub> OH	25	1.40	95*	36a
2-Chloro-2,3-dimethylbutane-3-d <sub>1</sub>	80% CH <sub>3</sub> CH <sub>2</sub> CH <sub>2</sub> OH	25	1.28	156*	36b
2-Chloro-2-methylbutane-1,1,1-d <sub>3</sub>	80% CH <sub>3</sub> CH <sub>2</sub> CH <sub>2</sub> OH	25	1.34	59	36d
2-Chloro-2,4-dimethylpentane-1,1,1-d <sub>3</sub>	80% CH <sub>3</sub> CH <sub>2</sub> CH <sub>2</sub> OH	25	1.34	66	36d

cont'd





T A B L E V

cont'd

Compound	Solvent	T°C	$k_H/k_D$	$\Delta G^\ddagger/n$ (cal)	Reference
2-Chloro-2,4-dimethylpentane-3,3-d <sub>2</sub>	80% CH <sub>3</sub> CH <sub>2</sub> OH	25	1.47	125	36d
2-Chloro-2-methylpentane-3,3-d <sub>2</sub>	80% CH <sub>3</sub> CH <sub>2</sub> OH	25	1.34	101	36d
t-Butyl-d <sub>9</sub> chloride	60% CH <sub>3</sub> CH <sub>2</sub> OH	25	1.103 <sup>†</sup>	57.9	36e
1-Phenylethyl-β-d <sub>3</sub> chloride	50% CH <sub>3</sub> CH <sub>2</sub> OH	25	1.224	39.88	33
1-Phenylethyl-β-d <sub>3</sub> bromide	80% CH <sub>3</sub> CH <sub>2</sub> OH	25	1.220	39.2	33
2-Propyl-1,1,1,3,3-d <sub>5</sub> tosylate	CH <sub>3</sub> COOH	24.99	2.121	74±5	28b
<u>trans</u> -Cyclopentyl-2-d <sub>1</sub> tosylate	CH <sub>3</sub> COOH	50	1.16	95	28a
<u>cis</u> -Cyclopentyl-2-d <sub>1</sub> tosylate	CH <sub>3</sub> COOH	50	1.22	127	28a
Cyclopentyl-2,2,5,5-d <sub>4</sub> tosylate	CH <sub>3</sub> COOH	50	2.06	116	28a

\* Possibly a primary effect in olefin formation.

† Per one deuterium atom.



deuterium isotope effects in terms of an inductive phenomenon.

As may be seen from the preceding discussion much controversy surrounds the interpretation of secondary deuterium isotope effects.

Wolfsberg and Stern (25) amalgamated the above arguments about the causes of secondary  $\alpha$ - and  $\beta$ -deuterium isotope effects in the form of a difference in force fields between the reactants and the transition state. They advanced the suggestion that secondary deuterium isotope effects on reaction rates arise from the decrease in force constants on going from the ground state to the transition state. The major contribution arises from the bending force constants as in the case of  $\alpha$ -effect, and the stretching and H-C-C and H-C-H bending force constants in case of  $\beta$ -effect. The magnitude of the effects depends upon the magnitude of these changes. A general decrease of these force constants on going to the transition state will lead to normal isotope effects, i.e.  $k_H > k_D$ , as in the case of  $sp^3$  to  $sp^2$  hybridization. However, an increase in the force constants will generally lead to inverse isotope effects, i.e.,  $k_H < k_D$ , as in the case of  $sp^2$  to  $sp^3$  hybridization.

Therefore, the study of secondary deuterium isotope effects provides a useful method to estimate the degree of force constant changes at the isotopic position between the reactant and the transition state, and consequently a powerful tool in determining the degree of bond cleavage that occurs in the transition state.

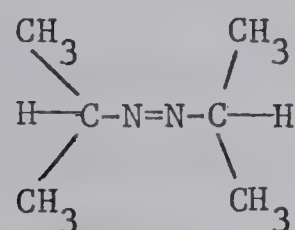


As mentioned, all the above studies on secondary deuterium isotope effects have been carried out on ionic reactions, but it has been argued that they should be similar for ionic and for radical reactions (39).

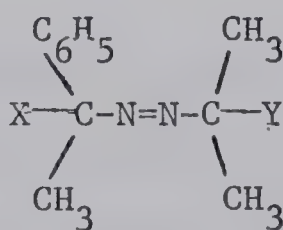
(c) Examples of Secondary Deuterium Isotope Effects on Radical Reactions

(i) Effects of the First Kind

Cohen and Wang (40) and Overberger and DiGiulio (41) have compared the activation energies and rates of thermolysis of azoisopropane (28),  $\alpha$ -phenylethylazoisopropane (29a) and azo-bis- $\alpha$ -phenylethane (30a). Since the activation energy decreased by



28



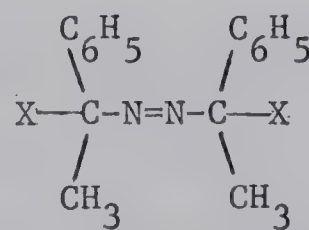
29

(a) X = Y = H

(b) X = D,

Y = H

(c) X = H, Y = D



30

(a) X = H

(b) X = D

about 4 kcal mole<sup>-1</sup> each time a phenyl group replaced a methyl group in this series and since the ratio of rates for compounds 30a, and 29a was greater than a statistical factor of 2 [at 120°C the rate constants for thermolysis of 29a and 30a respectively





are  $1.32 \times 10^{-5} \text{ sec}^{-1}$  and  $48.5 \times 10^{-5} \text{ sec}^{-1}$  (41)] these authors concluded that both carbon-nitrogen bonds break simultaneously in the rate-determining step.

This interpretation has been further substantiated by the magnitude of the secondary  $\alpha$ -deuterium kinetic isotope effect found by Seltzer (15a) for azo-bis- $\alpha$ -phenylethane- $\alpha, \alpha'$ - $\underline{d}_2$  (30b). The observed effect,  $k_H/k_D = 1.27$  Table VI, was approximately twice the usual effect for a transition from tetrahedral to trigonal at one carbon atom which is occurring in other "unimolecular" reactions (Table IV), indicating that the two C-N bonds are breaking simultaneously in the transition state of the rate-determining step.

Thermolysis of  $\alpha$ -phenylethylazoisopropane (29a) presented a somewhat different picture. In the case of  $\alpha$ -phenylethyl- $\alpha$ - $\underline{d}_1$ -azoisopropane (29b) (15b), Seltzer interpreted the isotope effect,  $k_H/k_D = 1.148$  Table VI, as demonstrating that the  $\alpha$ -phenylethyl-carbon-nitrogen bond is being stretched by an amount approximately equal to the stretch of each  $\alpha$ -phenylethyl-carbon-nitrogen bond in the thermolysis of 30a. In the case of  $\alpha$ -phenylethylazo-2-propane-2- $\underline{d}_1$  (29c) (15b) the isotope effect,  $k_H/k_D = 1.04$ , has been interpreted to present a much smaller stretching of the 2-propyl-carbon-nitrogen bond. Seltzer also concluded that in this system both C-N bonds stretch in the same step, but to unequal degrees by the time the molecule reaches the transition state of the rate-determining step.



T A B L E V I

Radical  $\alpha$ -deuterium isotope effects

Reaction	Solvent	T°C	$k_H/k_D$	$\Delta\Delta G^\ddagger/n$ (cal)	Reference
1. Thermolysis of $\begin{array}{c} \text{CH}_3 \quad \text{CH}_3 \\   \quad   \\ \text{C}_6\text{H}_5 - \text{C} - \text{N} = \text{N} - \text{C} - \text{C}_6\text{H}_5 \\   \quad   \\ \text{D} \quad \text{D} \end{array}$ <p style="text-align: center;"><u>30b</u></p>	Ethylbenzene	105	1.27	89	15a
2. Thermolysis of $\begin{array}{c} \text{CH}_3 \quad \text{CH}_3 \\   \quad   \\ \text{C}_6\text{H}_5 - \text{C} - \text{N} = \text{N} - \text{C} - \text{CH}_3 \\   \quad   \\ \text{D} \quad \text{H} \end{array}$ <p style="text-align: center;"><u>29b</u></p>	Diphenylether- benzoquinone solution	143.2	1.148	114	15b
3. Thermolysis of $\begin{array}{c} \text{CH}_3 \\   \\ \text{C}_6\text{H}_5 - \text{C} - \text{N} = \text{N} - \text{CH}_3 \\   \\ \text{D} \end{array}$ <p style="text-align: center;"><u>31b</u></p>	Diphenylether- benzoquinone solution	161.0	1.13	105	15c

cont'd



T A B L E V I

cont'd

Reaction	Solvent	T°C	$k_H/k_D$	$\Delta G^\ddagger/n$ (cal)	Reference
4. Thermolysis of $  \begin{array}{c}  \text{H} \quad \text{C}_6\text{H}_5 \quad \text{H} \\    \quad   \quad   \\  \text{C}_6\text{H}_5 - \text{C} - \text{C} - \text{N} = \text{N} - \text{C} - \text{C} - \text{C}_6\text{H}_5 \\    \quad   \quad   \quad   \\  \text{H} \quad \text{D} \quad \text{D} \quad \text{H}  \end{array}  $					
meso-	Ethylbenzene	106.47	1.221	75	40
dl-	Ethylbenzene	106.47	1.202	69	40
5. $\beta$ -scission of $  \begin{array}{c}  \text{CH}_3 \\    \\  \text{C}_6\text{H}_5 - \text{C} - \text{O} \cdot \\    \\  \text{CD}_3  \end{array}  $	Carbontetrachloride -cyclohexane	75	1.12	78	42
6. Thermolysis of $  \begin{array}{c}  \text{O} \\     \\  \text{t-BuO} - \text{O} - \text{C} - \text{CD}_2 - \text{C}_6\text{H}_5  \end{array}  $	Chlorobenzene	76.04	1.28-1.31*	98-107	43

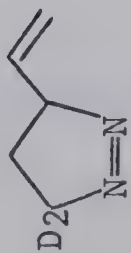
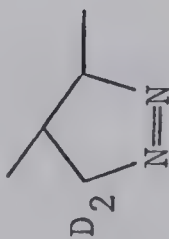
cont'd





T A B L E V I

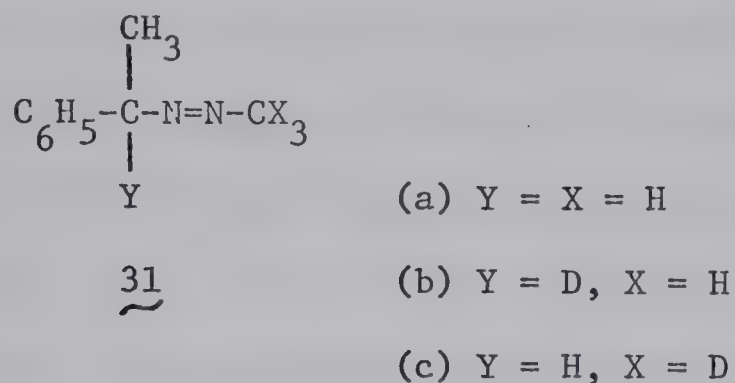
cont'd

Reaction	Solvent	T°C	$k_H/k_D$	$\Delta\Delta G^\ddagger/n$ (cal)	Reference
7. Thermolysis of $\begin{array}{c} \text{CH}_3 \\   \\ \text{t-BuO}-\text{O}-\text{C}-\text{C}-\text{C}_6\text{H}_5 \\    \quad   \\ \text{O} \quad \text{D} \end{array}$	Chlorobenzene	60.67	$1.14^\ddagger$	100	43
8. Thermolysis of 	Gas phase	134.5	1.21	77	13
9. Thermolysis of 					
<u>cis-</u> <u>trans-</u>	Gas phase Gas phase	220.9 220.9	1.19 1.21	86 93	16 16

\* 87%  $\alpha$ -D<sub>2</sub> $^\ddagger$  77%  $\alpha$ -D



In the case of the less symmetric azo compound  $\alpha$ -phenylethylazomethane (31a), thermolysis of  $\alpha$ -phenylethyl- $\alpha$ - $\underline{\text{d}}_1$ -azomethane



(31b) (15c) gave an isotope effect,  $k_{\text{H}}/k_{\text{D}}$ , of 1.13 (Table VI) and  $\alpha$ -phenylethylazomethane- $\alpha', \alpha', \alpha' - \underline{\text{d}}_3$  (31c) (15c) produced an isotope effect,  $k_{\text{H}}/k_{\text{D}}$ , of 0.97. These observations led Seltzer (15c) to the conclusion that 31 reacts via a two step mechanism. The rupture of  $\alpha$ -phenylethyl-C-N bond occurs in the rate-determining step, while the rupture of the methyl-C-N bond in the unstable methylazo radical occurs in a subsequent fast step. The inverse  $\alpha$ -effect for the thermolysis of 31a vs. 31c has been interpreted as a small amount of tightening of the azomethyl-C-N bond during the stretching of the benzylic-C-N bond. Thus, Seltzer and co-workers (15) have established that the substitution of hydrogen by deuterium on the nitrogen bearing carbon of an azoalkane increases  $\Delta\Delta G^\ddagger$  by 89 to 114 cal per deuterium (i.e., a 12 to 15% decrease in the rate per deuterium at 105°) when that carbon-nitrogen bond is breaking in the rate-determining transition state.

Secondary  $\alpha$ -deuterium isotope effects for other radical reactions are recorded in Table VI.



(ii) Effect of the Second Kind

Secondary  $\beta$ -deuterium isotope effects have been studied independently by Boozer (44) on the autooxidation of 2-phenylpropane-1-d, Seltzer (45) on the thermolysis of azo-bis- $\alpha$ -phenylethane- $\beta,\beta,\beta$ -d<sub>6</sub>, Rummel (46) on the thermolysis of azo-bis-isobutyronitrile-d<sub>12</sub>, Koenig (47) on the thermolysis of t-butyl perpivalate-d<sub>9</sub>, Crawford (12, 18) on the thermolysis of 4-methyl-1-pyrazoline-4-d (15) and cis- and trans-4-deuterio-3-methyl-1-pyrazolines (20 and 21, respectively), the results of such studies are reported in Table VII. The  $\beta$ -isotope effect has been interpreted in terms of hyperconjugative stabilization of the radical by the  $\beta$  C-H bonds in the transition state.

(d) Inverse Deuterium Isotope Effects

Several workers (48, 49, 50, 51, 52) have provided strong evidence that an inverse isotope effect ( $k_H < k_D$ ) is the rule in addition reactions to double bonds, Table VIII. It has been interpreted in terms of increase of bending trigonal CH bonds ( $sp^2$ ) into the tetrahedral configuration ( $sp^3$ ) in going from the ground state ( $sp^2$ ) to the transition state ( $sp^3$ ).

Szwarc and co-workers have studied the addition reaction of methyl radicals to styrene-1,2,2-d<sub>3</sub> (53) and styrene-2,2-d<sub>2</sub> (54) in isooctane at 50°C and 65°C respectively. Although in the expected direction, the magnitude of the isotope effects (Table VIII) were smaller than calculated (82%) on the assumption of a tetrahedral transition state. In view of this the authors





T A B L E V I I

Radical  $\beta$ -deuterium isotope effects

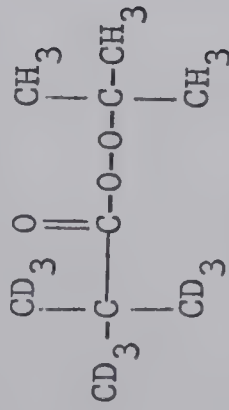
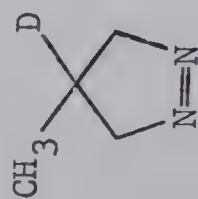
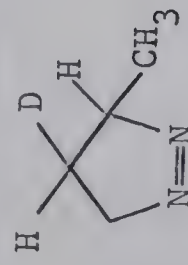
Reaction	Solvent	T°C	$k_H/k_D$	$\Delta G^\ddagger/n$ (cal)	Reference
1. Autooxidation of $\begin{array}{c} \text{CH}_3 \\   \\ \text{C}_6\text{H}_5-\text{C}-\text{H} + \text{RO}_2^\cdot \longrightarrow \text{C}_6\text{H}_5-\text{C}^\cdot + \text{RO}_2\text{H} \\   \qquad \qquad \qquad   \\ \text{CH}_2\text{D} \qquad \qquad \qquad \text{CH}_2\text{D} \end{array}$	Chlorobenzene	65	1.1	63.9	44
2. Thermolysis of $\begin{array}{c} \text{CD}_3 \quad \text{CD}_3 \\   \qquad   \\ \text{C}_6\text{H}_5-\text{C}-\text{N}=\text{N}-\text{C}-\text{C}_6\text{H}_5 \\   \qquad   \\ \text{H} \qquad \text{H} \end{array}$	Ethylbenzene	105	1.112	13	45
3. Thermolysis of $\begin{array}{c} \text{CD}_3 \quad \text{CD}_3 \\   \qquad   \\ \text{NC}-\text{C}-\text{N}=\text{N}-\text{C}-\text{CN} \\   \qquad   \\ \text{CD}_3 \quad \text{CD}_3 \end{array}$	Toluene	65-80	1.24-1.21	12-11	46

cont'd



T A B L E V I I

cont'd

Reaction	Solvent	T°C	$k_H/k_D$	$\Delta\Delta G^\ddagger/n$ (cal)	Reference
4. Thermolysis of 	Chlorobenzene	60-65	1.24	15.8	47
5. Thermolysis of 	Gas phase	241.75	1.07	34.5	12
6. Thermolysis of 	Gas phase	218	1.07	32.3	18
<div>cis- 20</div> <div>trans- 21</div>	Gas phase	218	1.05	23.3	18



T A B L E V I I I

Inverse  $\alpha$ -deuterium isotope effects

Reaction	T°C	$k_H/k_D$	Ref.
1. Addition of a variety of reagents to <u>trans</u> -stilbene- $\underline{d}_2$		0.88	48
2. KSCN catalyzed isomerization of maleic acid-2,3- $\underline{d}_2$	80	0.88	49
3. Polymerization of $C_6H_5CD=CH_2$	60	0.91	50
4. Polymerization of $C_6H_5CD=CH_2$	70	0.86	51
5. Polymerization of $C_6H_5CH=CD_2$	60	0.88	50
6. Polymerization of $C_6H_5CH=CD_2$	70	0.81	51
7. (2+2) Cycloaddition of diphenylketene with $\beta,\beta$ -dideuteriostyrene	65	0.91	52
8. $C_6H_5CD=CD_2 + CH_3$ radicals	50	0.90	53
9. $C_6H_5CH=CD_2 + CH_3$ radicals	65	0.89	54
10. $CD_3CH=CD_2 + H\cdot$	25	0.93	55





concluded that the configuration of the transition state deviated only slightly from that of the initial state (i.e. the CH bonds are only slightly bent).

Similar considerations might apply to the small rate-enhancement observed by Takahasi and co-workers (55) on the addition of preformed hydrogen atoms to propylene-d<sub>6</sub>, Table VIII.



## P R O B L E M

As stated in the historical section, the mechanism of 1-pyrazoline thermolysis has been suggested (12, 13) to involve the rupture of both carbon-nitrogen bonds simultaneously in the rate-determining step of the thermolytic reaction, and that a nitrogen free intermediate is formed. This interpretation arose as a result of a progressive decrease in activation energy on going from 1 to 9. The decrease per methyl group, approximately 1.2 kcal mole<sup>-1</sup>, was that expected by analogy with azoalkane thermolysis (12). The increase in rate and decrease in activation energy by methyl substitution have been attributed to the extra stabilization by the methyl group of the unpaired electrons in the transition state. However, 1.2 kcal mole<sup>-1</sup> per methyl group is comparable to steric or conformational factors encountered in cyclic compounds (e.g., 1,3-diaxial interactions), thus the increase in rate could arise from an increase in ground state energies.

The synthesis of 1-pyrazoline-3,3-d<sub>2</sub> (34) and 1-pyrazoline-3,3,5,5-d<sub>4</sub> (35) was undertaken in order to eliminate the possibility of any conformational complications, or serious changes in non-bonded interactions, that might be present in methyl-1-pyrazolines. We hoped to further elucidate the mechanism of 1-pyrazoline thermolysis by measuring the magnitude of the secondary  $\alpha$ -deuterium isotope effects in the thermolysis of 34 and 35 to see whether a step-wise mechanism or simultaneous two-bond cleavage



mechanism is operating in the rate-determining step (15).

It has also been indicated in the historical section, that Mishra (12) and Erickson (18) have provided strong kinetic evidence for the existence of a common intermediate, in 1-pyrazoline thermolysis, which leads to cyclopropane and olefin in subsequent processes. We desired further proof of this and so undertook to prepare 1-pyrazoline-4- $\underline{d}_1$  (32) and 1-pyrazoline-4,4- $\underline{d}_2$  (33) on the basis that propylene formation from 1 required a hydrogen shift whereas cyclopropane formation does not. Therefore, if hydrogen migration is concerted with nitrogen elimination then one would observe a primary kinetic isotope effect in the thermolysis of 32 and 33. Otherwise the effect of deuterium substitution on C-4 of 1-pyrazoline ring would be reflected in the product-determining step if the migration of hydrogen occurs after the rate-determining step.

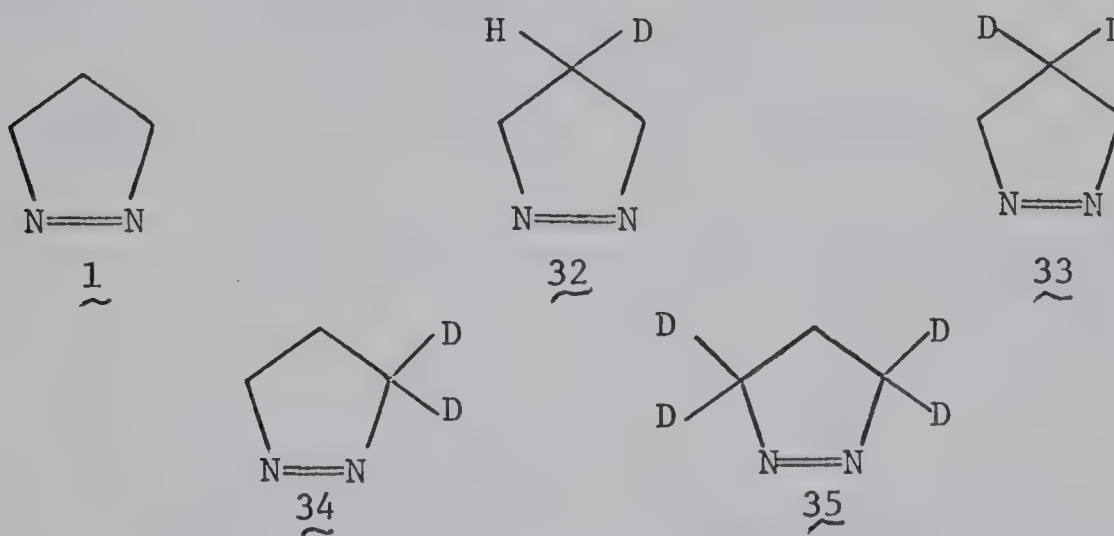




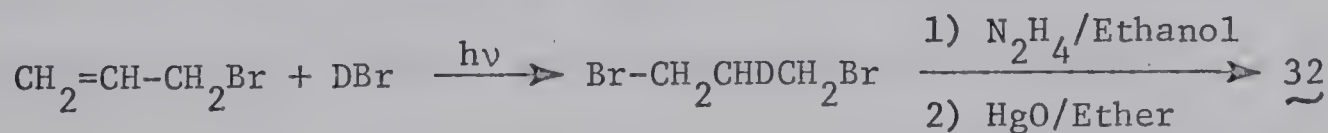
## R E S U L T S

(A) The Synthesis of Deuterated 1-Pyrazolines

Four deuterated 1-pyrazolines 32, 33, 34 and 35 were synthesized from the mercuric oxide oxidation of the corresponding pyrazolidines which in turn were prepared from the reaction of deuterated 1,3-dibromopropanes with anhydrous hydrazine.



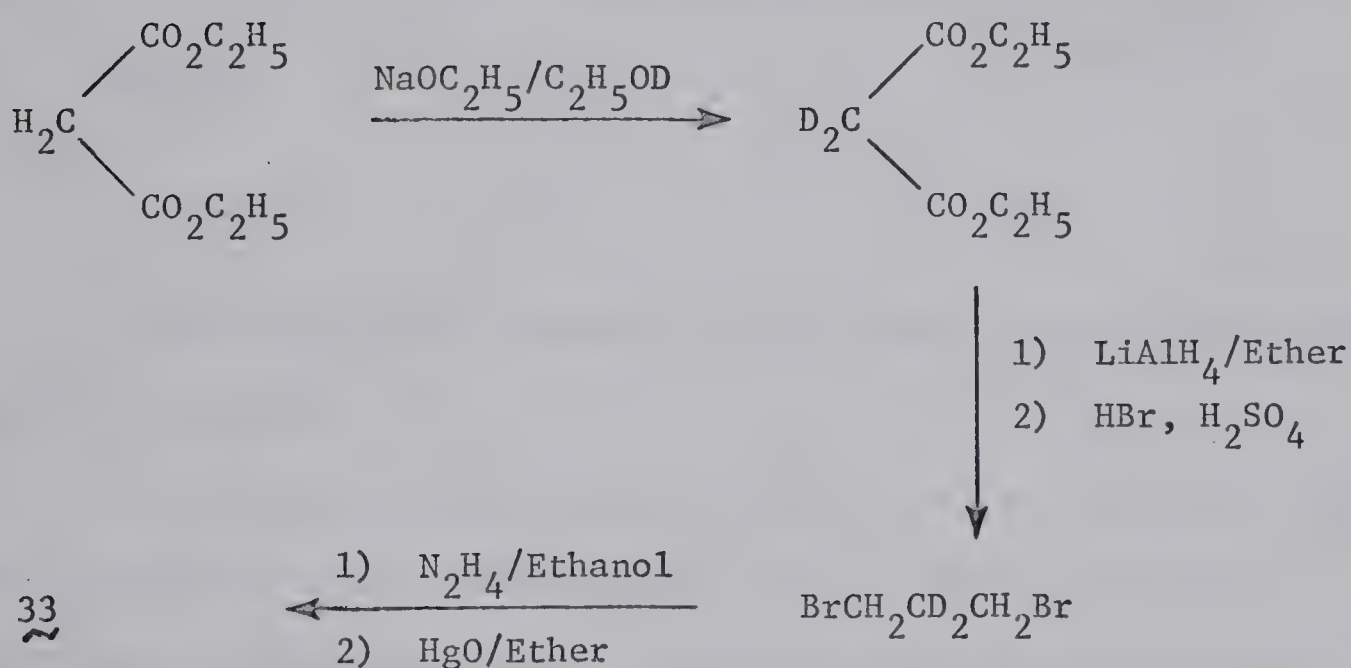
(a) 1,3-Dibromopropane-2-d<sub>1</sub> was prepared by the radical addition of deuterium bromide (56) as described by Kharasch and Mayo (57).



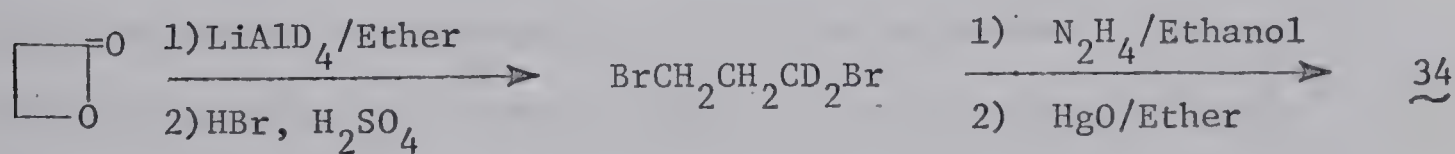
(b) The remaining deuterated dibromides were prepared by refluxing a mixture of 48% hydrobromic acid and sulfuric acid with the corresponding deuterated 1,3-diols, which in turn were prepared as follows:



( i) 1,3-Dihydroxypropane-2,2-d<sub>2</sub> was prepared by the reduction of diethylmalonate-2,2-d<sub>2</sub>, obtained by four successive exchanges of diethylmalonate with sodium ethoxide in ethanol-O-d, with lithium aluminum hydride in dry ether.

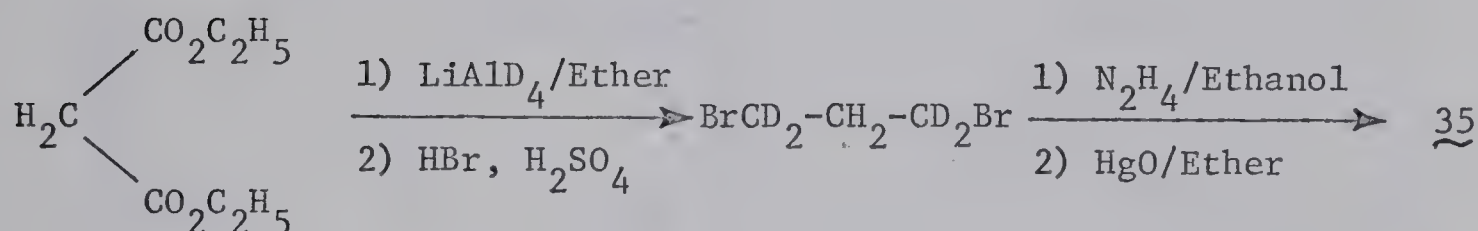


(ii) 1,3-Dihydroxypropane-1,1-d<sub>2</sub> was synthesized by reducing β-propiolactone with lithium aluminum deuteride in dry ether.





(iii) 1,3-Dihydroxypropane-1,1,3,3-d<sub>4</sub> was obtained by the reduction of diethylmalonate with lithium aluminum deuteride in dry ether.



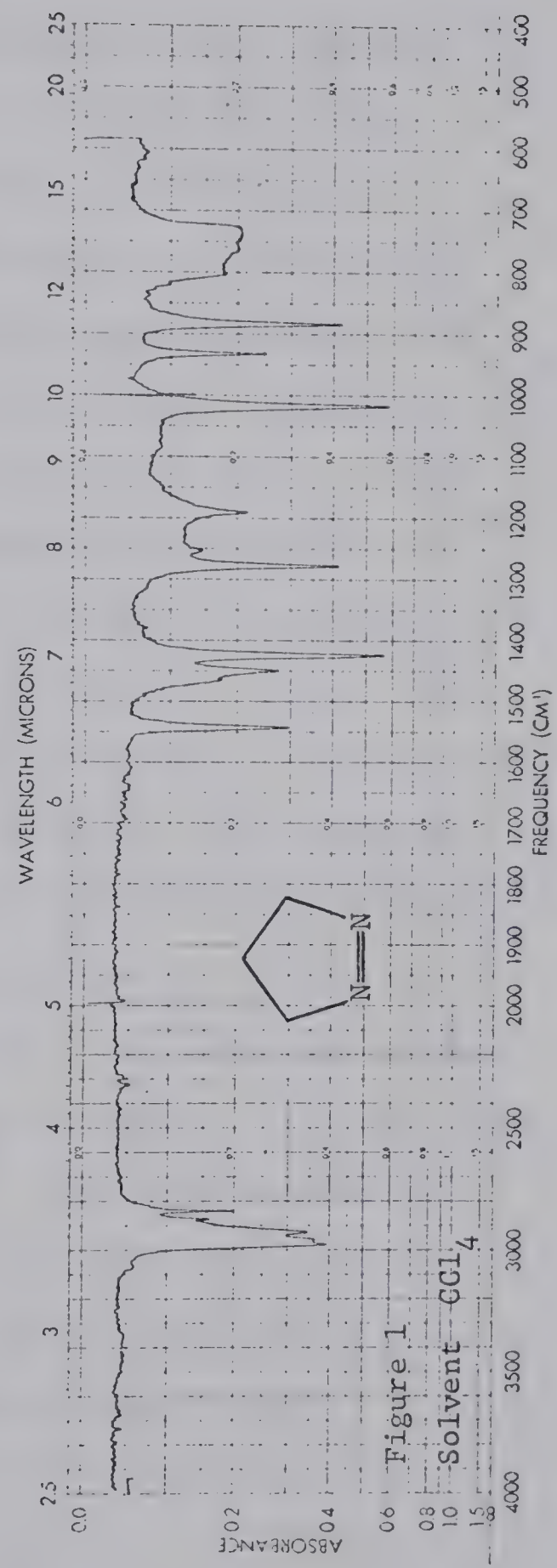
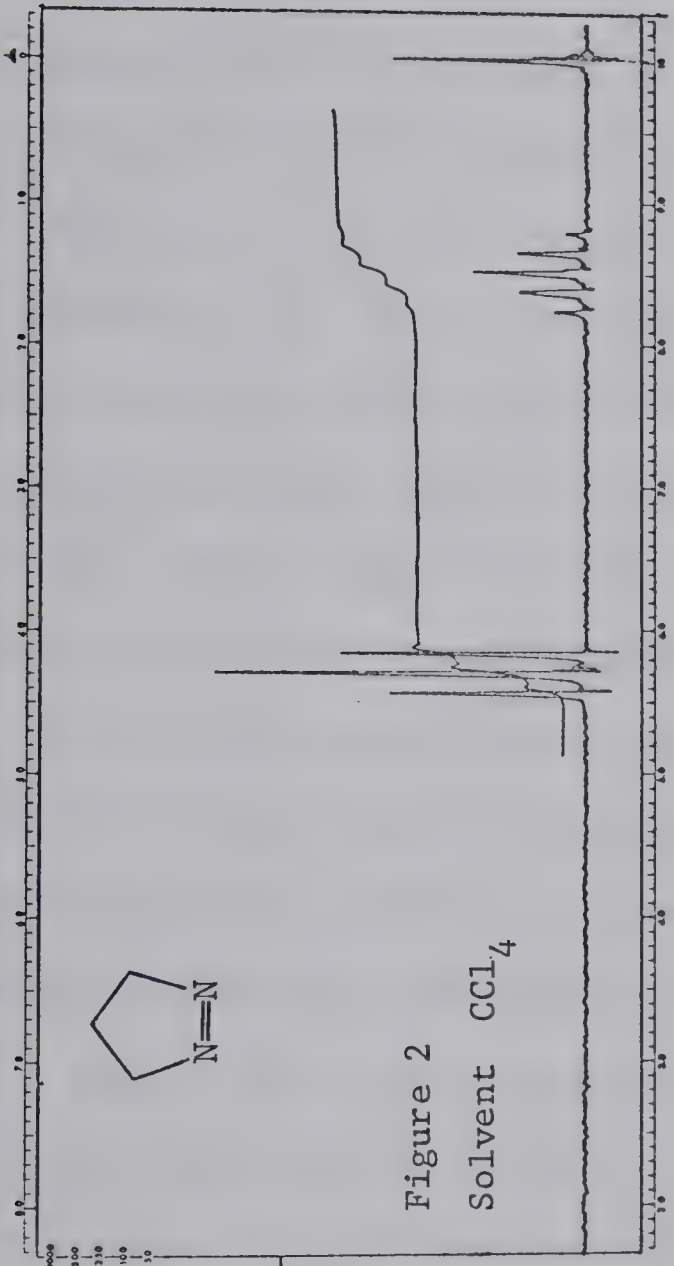
All diols were converted to the corresponding dibromides without isolation.

All of the foregoing deuterated 1-pyrazolines (32 to 35) were purified by gas chromatography, using a 20 ft. 10% Ucon-insoluble on Fluoropak Column. Further purification was carried out by trap to trap distillation under vacuum at  $-80^\circ\text{C}$ .

The infrared (ir) spectra for 32 to 35 in carbon tetrachloride showed no sharp absorption between  $3100\text{-}3600\text{ cm}^{-1}$  and  $1600\text{-}1700\text{ cm}^{-1}$  characteristic for  $>\text{N-H}$  and  $>\text{C=N-}$  groups respectively, but all showed a medium absorption at  $1545\text{ cm}^{-1}$ , which indicates the presence of  $\text{-N=N-}$  group as shown in Figure 1 for 1-pyrazoline (1). Further proof for the presence of  $\text{-N=N-}$  group comes from the ultraviolet (uv) spectra of 32 to 35 which



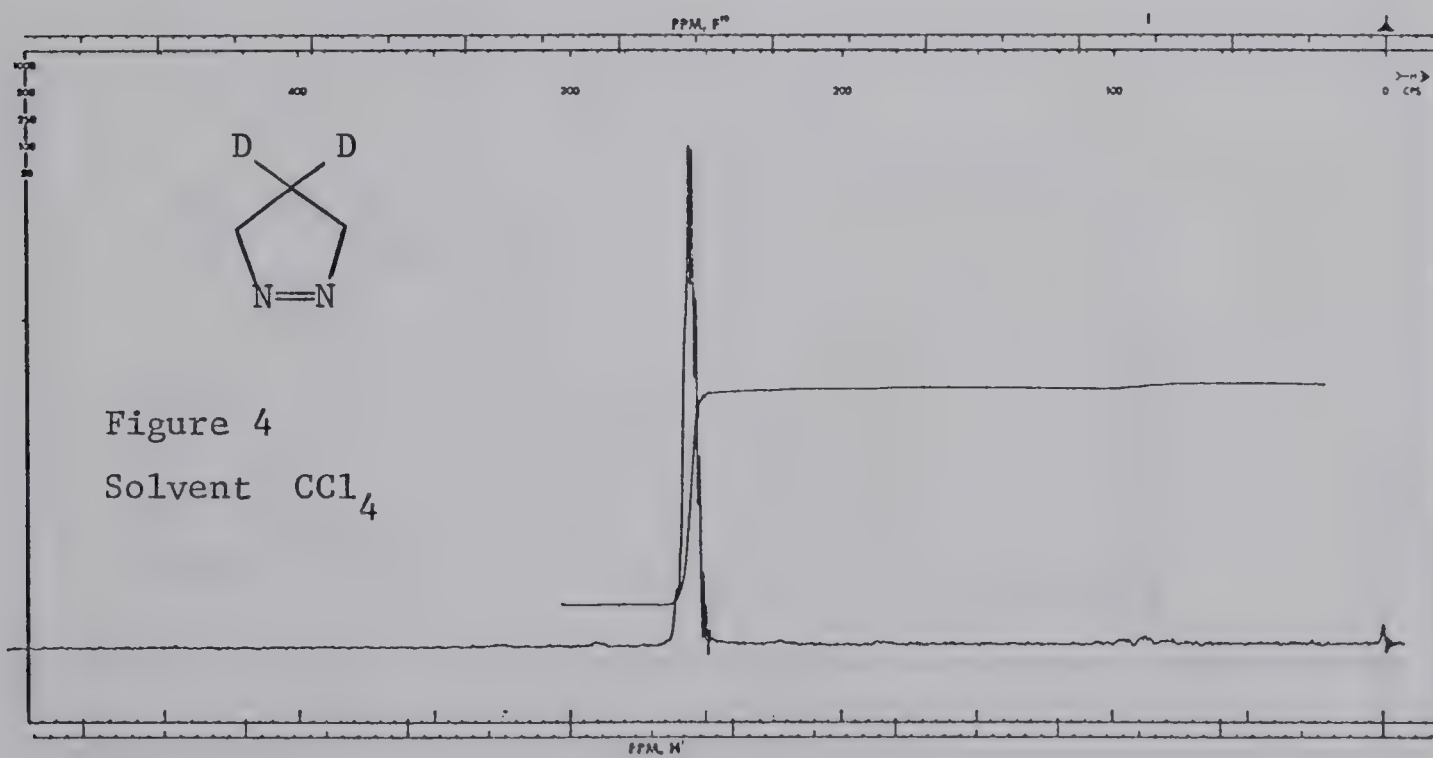
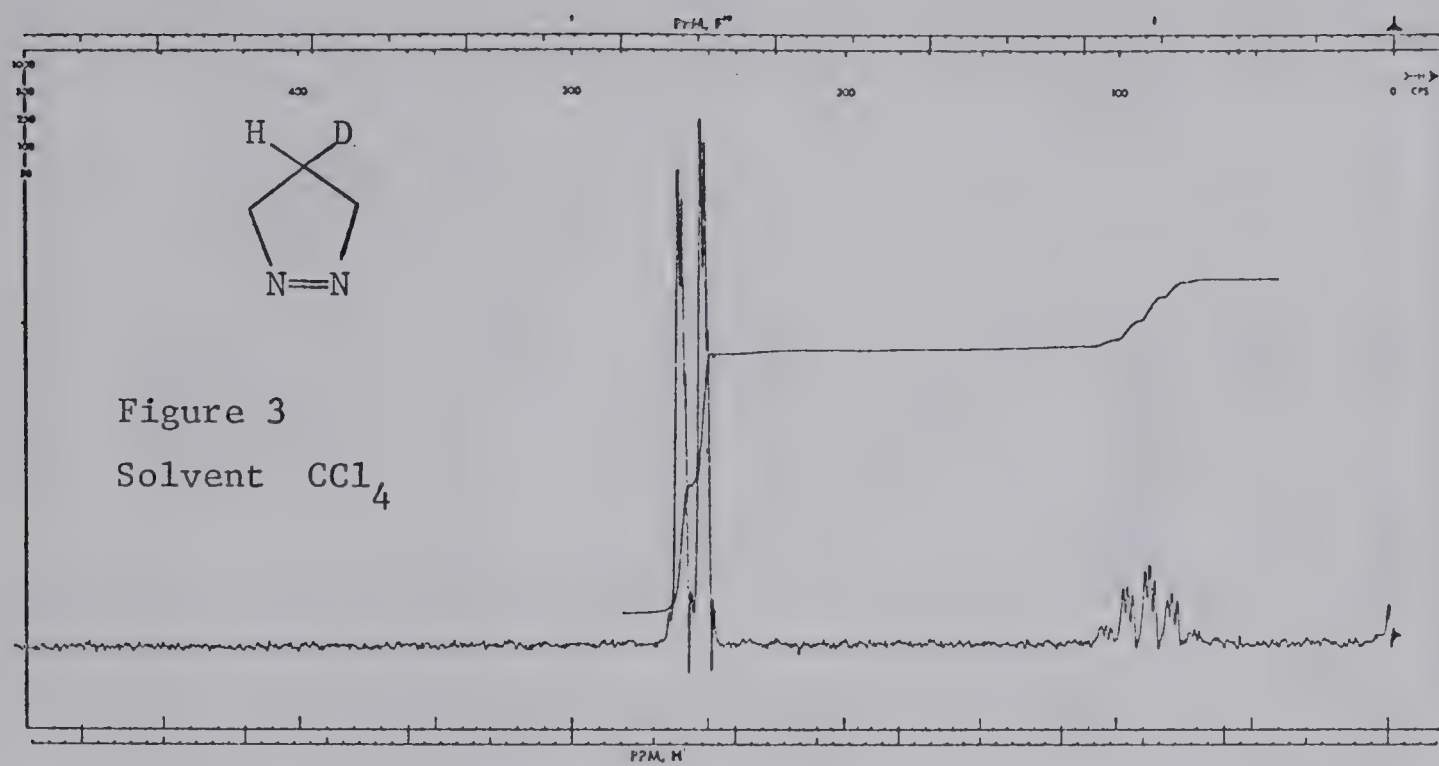






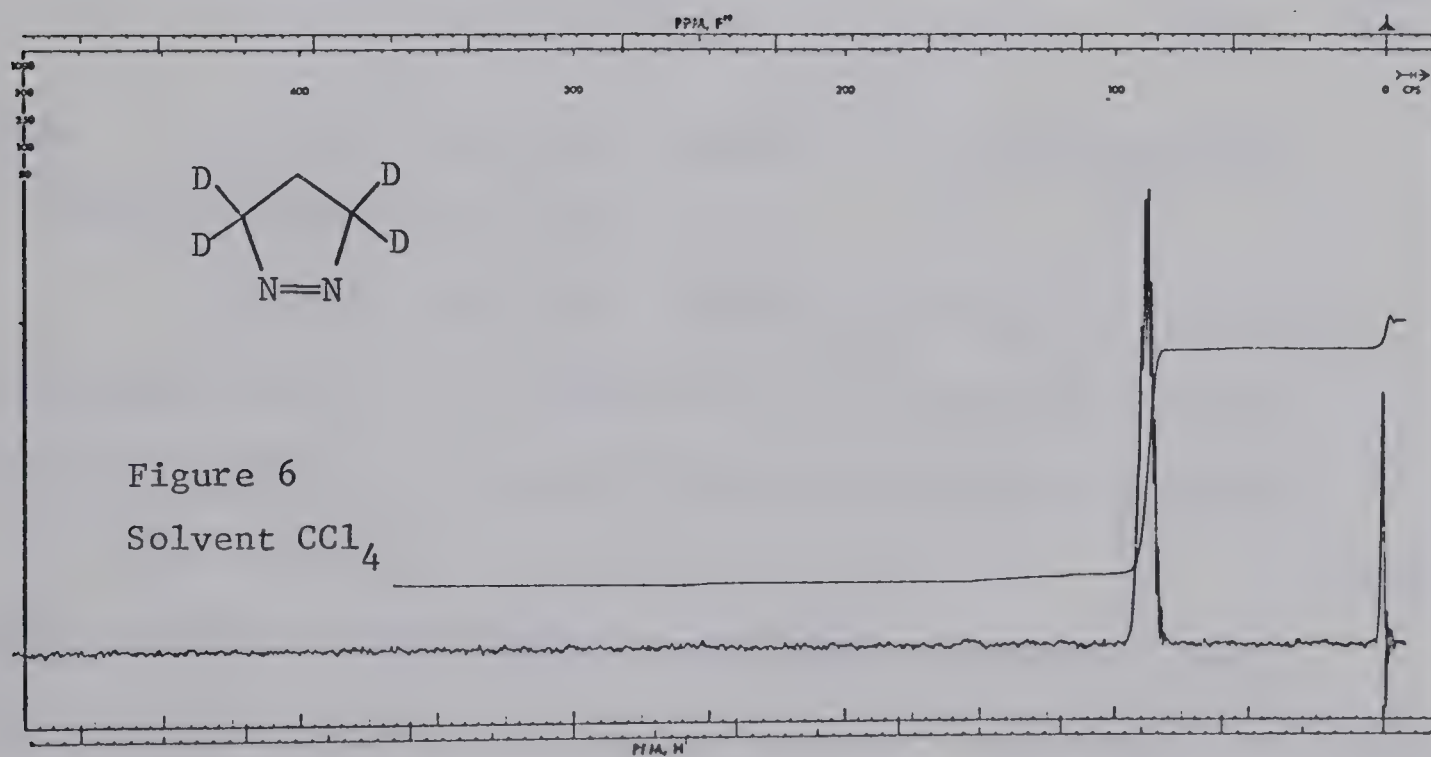
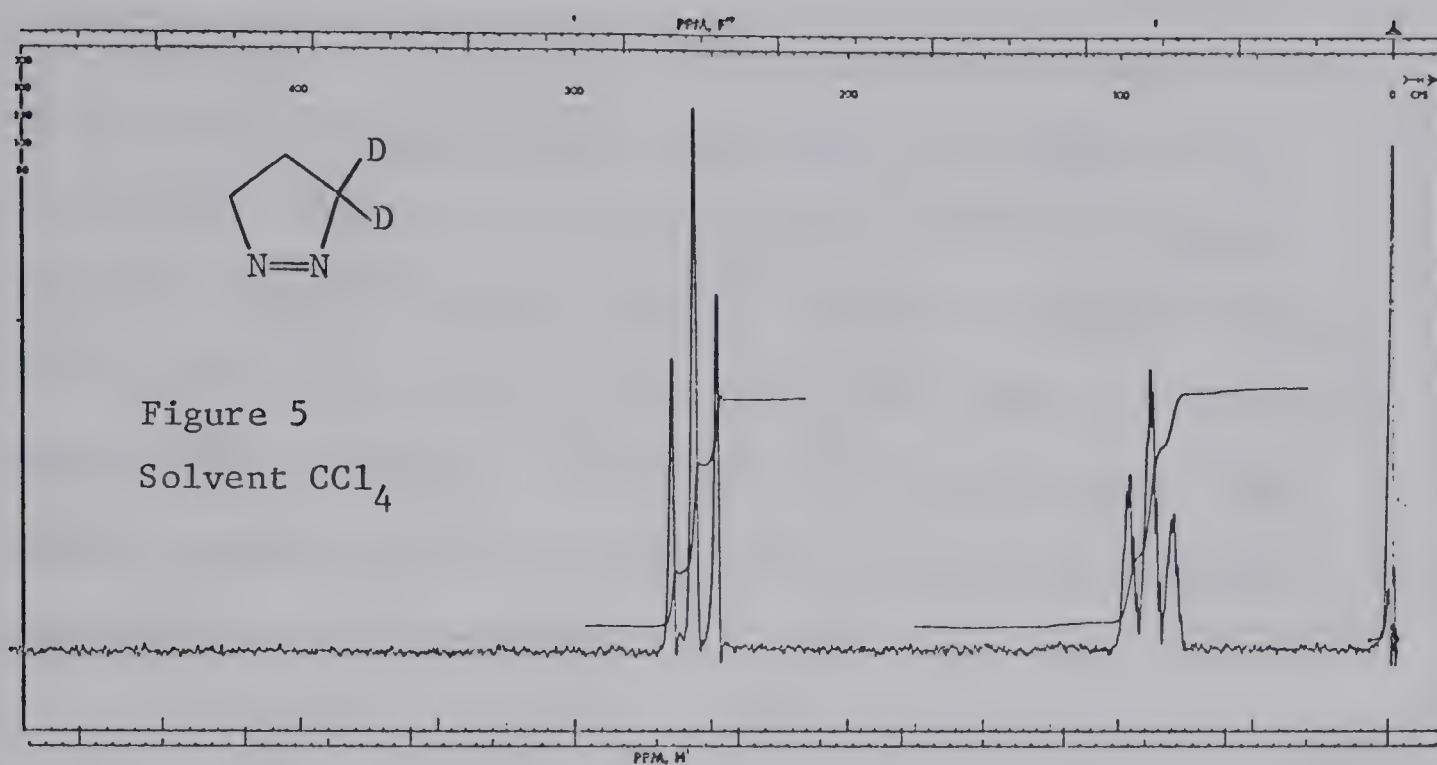
showed an absorption at  $\lambda_{\text{max}} = 315 \text{ nm}$  ( $\epsilon = 446$  in methanol) (11). The nuclear magnetic resonance (nmr) spectrum (Figure 2) for 1 in carbon tetrachloride shows a triplet centered at  $\tau$  5.68 ( $J = 8.3 \text{ Hz}$ ) and a quintet centered at  $\tau$  8.57 ( $J = 8.3 \text{ Hz}$ ) with an integration area of 2.00:1.00 respectively. The nmr spectra for compounds 32 to 35 are shown in Figures 3 to 6 respectively. If coupling by deuterium is ignored then, compound 32 showed that the triplet at  $\tau$  5.68 in the spectrum of 1 becomes a doublet in the spectrum of 32. The integration ratio of the doublet to the quintet was found to be 3.80:1.00, implying that deuterium atom was incorporated into the C-4 position of 1-pyrazoline ring as expected. Compound 33 showed only a singlet at  $\tau$  5.68, and the quintet at  $\tau$  8.57 has almost completely disappeared. This indicates that two deuterium atoms are incorporated at the C-4 position of 1-pyrazoline ring. Compound 34 showed two triplets at  $\tau$  5.68 and  $\tau$  8.57 respectively, with an integration ratio of 1.00:1.00 as expected for complete deuteration of C-3 of the 1-pyrazoline ring. Only a singlet was shown by compound 35 centered at  $\tau$  8.57 and there was no detectable absorption at  $\tau$  5.68. This indicates that C-3 and C-5 of the 1-pyrazoline ring are completely deuterated. The mass spectra of these compounds 32 to 35 were also obtained as a check on the deuterium content of each (see Experimental).













(B) Kinetic Studies

The reactor which was described and used by Mishra (10) and devised by Smith (58) was used to measure the rates of thermolysis of compounds 1, 32, 33, 34, and 35. The reactor was constructed in such a way that the rate of increase of pressure with time inside the system could be measured in terms of the rate of increase of electromotive force (emf) with time as indicated on a strip chart recorder. A transducer was used to convert the pressure reading into emf. First order kinetics were observed to greater than 95% completion.

The rate constants of thermolytic reactions were obtained from the data in the following manner. For a first order gas phase reaction of the type  $A \rightarrow \text{products}$ , it is known (59) that,

$$k = \frac{2.303}{t} \text{Log} \frac{P_{\infty}^a - P_o^a}{P_{\infty}^a - P_t^a} \quad (6)$$

where  $k$  is the first order rate constant,  $t$  is the time,  $P^a$  is the actual pressure inside the reactor.

It is known that the relationship between the emf caused by pressure change on the transducer can be expressed, provided that the pressure is not greater than one atmosphere, as follows,

$$E = ap + b \quad (7)$$

where  $a$  and  $b$  are proportionality constants depending on the particular transducer.

In our system the observed pressure is,

$$P = P^a - P_x \quad (8),$$



where  $P_x$  is the pressure required to push the diaphragm against the needle, a constant quantity.

Then, from equations 7 and 8, we get,

$$E = a[P^a - P_x] + b \quad \text{or} \quad P^a = \frac{E - b}{a} + P_x \quad (9).$$

Substituting equation 9 in 6, we get,

$$k = \frac{2.303}{t} \text{Log} \frac{E_\infty - E_o}{E_\infty - E_t} \quad (10),$$

where  $E_\infty$  is the transducer emf after more than nine half-lives and  $E_t$  is the emf at time  $t$  in seconds.  $E_o$  is not reliable in our measurement, because of insufficient time to allow the system to attain equilibrium after the compound is injected. Therefore,

$$\frac{-kt}{2.303} = \text{Log} [E_\infty - E_t] + C \quad (11).$$

From the linear equation 11, a plot of  $\text{Log} [E_\infty - E_t]$  versus  $t$  gives a straight line with a slope equal to  $-\frac{k}{2.303}$  from which  $k$  is obtained with a high precision since a large number of points can be obtained from the chart record. Generally 10 points were used and the values were taken at regular intervals over the first two half-lives of the reaction. However, to have an indication of the error limits associated with the best fitted values of the constants in a linear equation, the least squares method of numerical solution was used (60).

Equation 11 has the form of

$$y = bx + a \quad (12),$$

where  $y = \text{Log} [E_\infty - E_t]$ ;  $b = -k/2.303$ ;  $x = t$  and  $a=c=\text{Log} [E_\infty - E_o]$ .





The application of the above method is shown in the evaluation of  $k$  for 1-pyrazoline (1), given in Table IX. The graphical plot of  $\text{Log } [E_\infty - E_t]$  versus  $t$  is shown in Figure 7 and illustrates the good first order behaviour. The least squares method gives the following best fit values:

$$b = -\frac{k}{2.303} = \frac{n\sum xy - \sum x \sum y}{n\sum x^2 - (\sum x)^2} = -0.06205 \text{ min}^{-1} \quad (13)$$

$$\text{or } k = 23.82 \times 10^{-4} \text{ sec}^{-1},$$

$$\text{and } a = \text{Log } [E_\infty - E_0] = \frac{\sum x^2 \sum y - \sum x \sum xy}{n\sum x^2 - (\sum x)^2} = 0.9949 \quad (14).$$

The probable error in  $b$  is  $P_b$ , given by

$$P_b = P_y \sqrt{\frac{n}{n\sum x^2 - (\sum x)^2}} \quad (15)$$

where

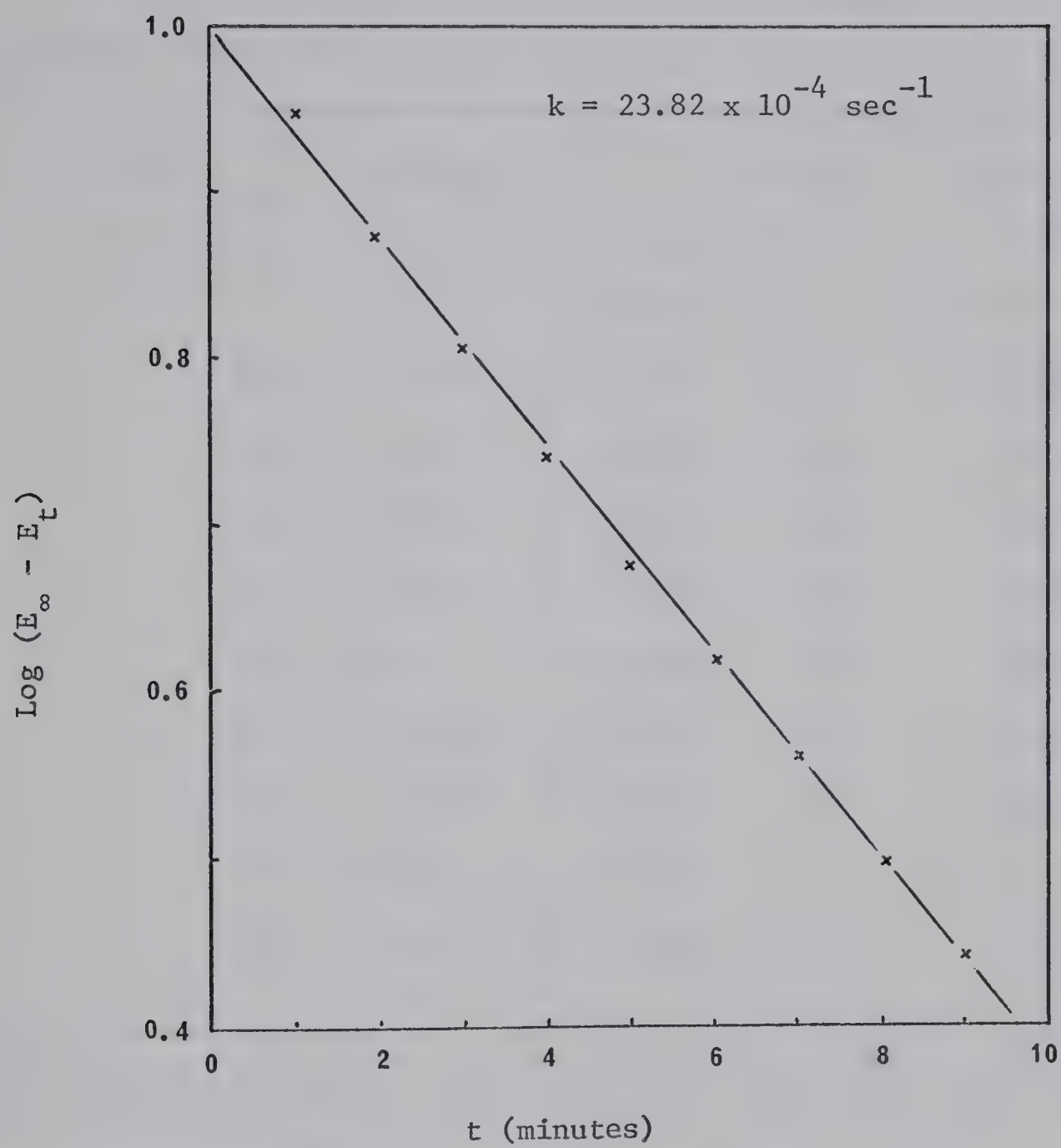
$$P_y = 0.6745 \sqrt{\frac{\sum (y - a - bx)^2}{n-2}} = 0.00429 \quad (16)$$

From 15 and 16,  $P_b = 5.53 \times 10^{-4}$ , giving the corresponding error in  $k$  as  $\frac{2.303 \times 5.53}{6} \times 10^{-4} \text{ sec}^{-1} = 0.21 \times 10^{-4} \text{ sec}^{-1}$ . Thus,  $k = (23.82 \pm 0.21) \times 10^{-4} \text{ sec}^{-1}$  obtained by the least squares method agrees well with the value of  $23.82 \times 10^{-4} \text{ sec}^{-1}$  obtained from the graphical plot. The largest error is derived from difficulty in maintaining a constant high temperature for a long period of time, which was found to vary within  $\pm 0.05^\circ\text{C}$ ; thus causing a probable error of about 0.8% in rate constants near  $502^\circ\text{K}$  (61).



Figure 7

Plot of  $\log (E_{\infty} - E_t)$  vs.  $t$  for the  
thermolysis of 1-pyrazoline at  $229.40 \pm 0.05^{\circ}$





## T A B L E I X

The thermolysis of 1-pyrazoline (1) and the  
least squares calculation for the rate constant

Temperature =  $229.40 \pm 0.05^\circ$ ; Initial pressure  $\approx 170$  Torr;  $E_\infty = 24.25$

No. of obs. n	Time(min) = x	$E_\infty - E_t$	$\text{Log}[E_\infty - E_t]$ = y	$x^2$	xy	$(y-a-bx) \times 10^{-4}$	$(y-a-bx)^2 \times 10^{-8}$
1	1	8.80	0.9445	1	0.9445	+116	13456
2	2	7.45	0.8722	4	1.7444	+ 14	196
3	3	6.37	0.8041	9	2.4123	- 46	2116
4	4	5.50	0.7404	16	2.9616	- 63	3969
5	5	4.75	0.6767	25	3.3835	- 79	6241
6	6	4.15	0.6180	36	3.7080	- 46	2116
7	7	3.65	0.5623	49	3.9361	+ 17	289
8	8	3.15	0.4983	64	3.9864	- 2	4
9	9	2.79	0.4456	81	4.0104	- 8	64

$$(\Sigma x)^2 = 2025; \quad \Sigma x^2 = 285; \quad \Sigma xy = 27.0872; \quad \Sigma x = 45; \quad \Sigma y = 6.1621;$$

$$\Sigma x \Sigma y = 277.2945; \quad n \Sigma x^2 = 2565; \quad n \Sigma xy = 243.7848;$$

$$\Sigma (y-a-bx)^2 = 28451 \times 10^{-8}.$$





The over-all precision in each run is excellent as indicated by the data in Table IX and Figure 7.

The rate constants and the secondary  $\alpha$ - and  $\beta$ -deuterium isotope effects of the 1-pyrazolines studied are given in Tables X and XI.

T A B L E X

Rate constants and secondary kinetic isotope effects for the thermolysis of  $\alpha$ -deuterated 1-pyrazolines at  $229.40 \pm 0.05^\circ$

Compound	$10^4 k$ ( $\text{sec}^{-1}$ )	$k_H/k_D$		$\Delta\Delta G^\ddagger/n$ (cal)
		obs.	corr. to $105^\circ$	
<u>1</u>	23.82			
	23.98			
	23.77			
	Av. 23.86 $\pm$ 0.11			
<u>34</u> <sup>a</sup>	20.06			
	19.87			
	Av. 19.96 $\pm$ 0.13	1.19 $\pm$ 0.01	1.26 $\pm$ 0.01	86 $\pm$ 6
<u>35</u> <sup>a</sup>	16.94			
	17.20			
	Av. 17.07 $\pm$ 0.18	1.40 $\pm$ 0.02	1.55 $\pm$ 0.02	84 $\pm$ 6

<sup>a</sup> Mass spectral and nmr analysis indicate samples to have greater than 98% deuteration in the positions indicated.



T A B L E X I

Rate constants and secondary kinetic  
isotope effects for the thermolysis of  $\beta$ -deuterated 1-pyrazolines

Compound	Temp.	$10^4 k$ (sec <sup>-1</sup> )	$k_H/k_D$		$\Delta\Delta G^\ddagger/n$ (cal)
			obs.	corr. to 105°	
<u>1</u>	224.0	15.3			
	226.9	19.3			
<u>32</u>	224.0	14.76 <sup>a</sup>			
		14.24			
		Av. 14.50±0.36	1.05±0.02	1.06±0.02	52±10
<u>33</u>	226.9	17.00 <sup>b</sup>			
		17.30			
		Av. 17.15±0.21	1.12±0.01	1.14±0.01	56±10

<sup>a</sup> Corrected for 4.9% C<sub>3</sub>H<sub>6</sub>N<sub>2</sub> (mass spectral analysis).

<sup>b</sup> Corrected for 11.3% C<sub>3</sub>H<sub>5</sub>DN<sub>2</sub> and 0.1% C<sub>3</sub>H<sub>6</sub>N<sub>2</sub> (mass spectral analysis).



(C) Product Analysis and Isotopic Labeling Studies

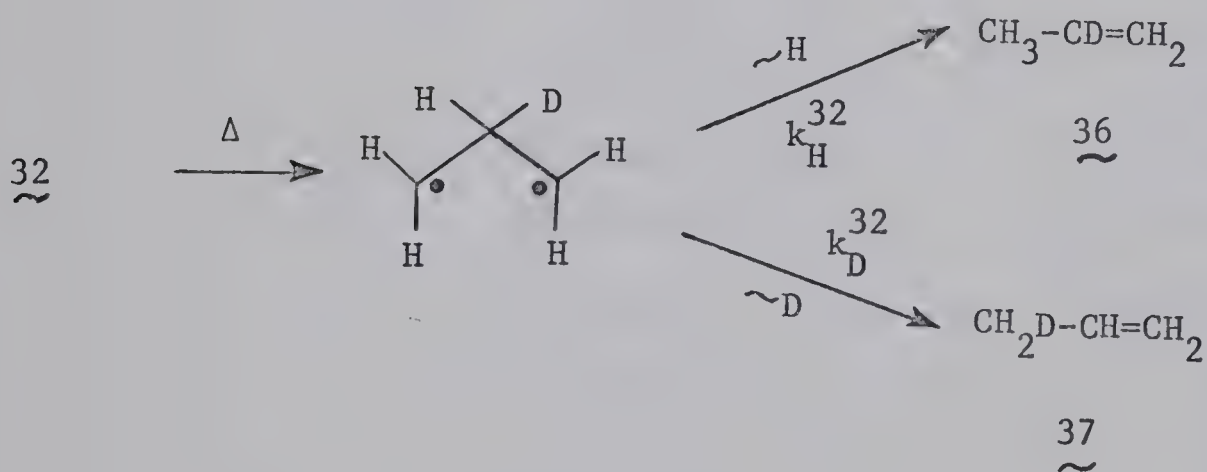
1-Pyrazoline (1) has been reported by Mishra (12) to give cyclopropane, propylene and nitrogen upon thermolysis. The determination of product composition was not carried out on sample trapped directly from the reactor after each kinetic run, because of the gaseous nature of these products and the uncertainty associated with their complete trapping. Instead, samples of 2.0-2.4  $\mu$ -litres of 1, 32, 33, 34 and 35 were introduced by means of a microsyringe inside pyrex bulbs of approximate capacity of 0.5 millilitre. Each sample was then completely degassed by means of a high vacuum system and subsequently sealed. Then the samples were heated by suspending the degassed tube inside the vapour of refluxing n-butyl benzoate at 241°C for greater than nine half-lives. After the thermolysis was complete each bulb was placed inside a bulb crusher, Figure 10, connected to a gas chromatograph. Helium was allowed to flow through until the system reached equilibrium. Then the bulb was crushed in the stream of helium which carried the products directly onto a 20 foot column of mineral oil on firebrick in tandem with a 20 foot column of 10% diethylmalonate on Diatoport for separation. The retention time of each component was compared with that of an authentic sample for identification. Product proportions were determined by integrating the area of each peak using a planimeter. Four determinations were made on each compound, and the results are the average of at least five integrations. The results of these





determinations are given in Table XII.

It has been demonstrated by Mishra (12) that propylene formation in 1-pyrazoline (1) thermolysis arises by hydrogen migration from the central methylene of the trimethylene intermediate to the terminal one. Thus, upon thermolysis of 32 one would expect propylenes to be formed from either hydrogen or deuterium migration, and in proportion depending on the migratory aptitude of hydrogen relative to deuterium (i.e., the magnitude of the isotope effect) as shown in Scheme III. In the case



Scheme III

of 34 thermolysis hydrogen can migrate either to the deuterated terminal methylene or to the undeuterated one. The ratio of the propylenes formed depends then on the rate of hydrogen migration to the deuterated methylene group relative to the rate of hydrogen migration to the natural methylene group, as shown in Scheme IV.

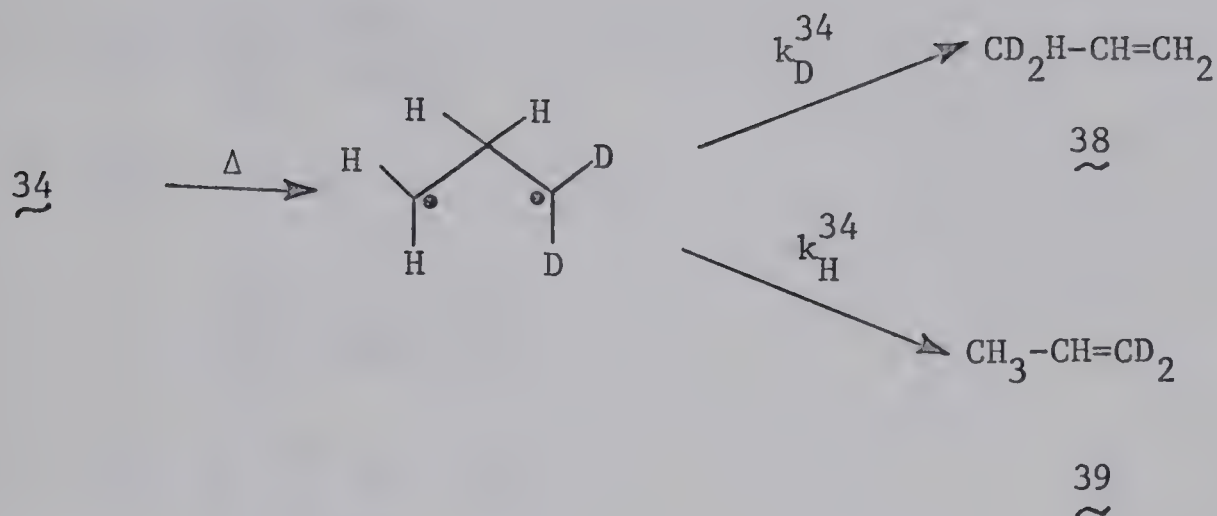


T A B L E X I I

Cyclopropane and propylene  
yields on thermolysis of pyrazolines at 241°

Compound	Cyclopropane	Propylene
<u>1</u>	88.45	11.55
	88.34	11.66
	88.51	11.49
	88.40	11.60
	Av. 88.43±0.07	11.57±0.07
<u>32</u>	89.23	10.77
	89.32	10.68
	89.07	10.93
	Av. 89.21±0.13	10.79±0.13
<u>33</u>	90.43	9.57
	90.17	9.83
	90.29	9.71
	90.17	9.83
	Av. 90.27±0.12	9.73±0.12
<u>34</u>	87.98	12.02
	87.99	12.01
	87.99	12.01
	Av. 87.99±0.01	12.01±0.01
<u>35</u>	87.29	12.71
	87.51	12.49
	87.49	12.51
	Av. 87.43±0.17	12.57±0.17





Scheme IV

These expectations were examined, by isolating the propylenes formed from 32 and 34 after each kinetic run using the same column and gas chromatographic technique as mentioned earlier. Then each sample was distilled under vacuum into an nmr tube, containing carbon disulfide and tetramethylsilane, at liquid nitrogen temperature. The tube was then removed from the vacuum rack and submitted for nmr analysis so as to determine the position of deuterium in the propylenes. Because of the low boiling point of propylene the nmr analyses were carried out at  $-50^\circ\text{C}$  so as to ensure that all the propylenes are condensed and dissolved in the solvent.

The relative proportions of isomeric propylenes 36 and 37 were determined in the following manner; if  $n_{36}$  is the mole fraction of 36 present and  $n_{37}$  is the mole fraction of 37 then R, the integration ratio of aliphatic to olefinic protons may be expressed as:





$$R = \frac{2n_{36} + 3n_{37}}{3n_{36} + 2n_{37}}$$

and the ratio of 36:37 is

$$\frac{n_{36}}{n_{37}} = \frac{(3 - 2R)}{(3R - 2)}$$

Similarly for  $\underline{38}$  and  $\underline{39}$  we get

$$R = \frac{n_{38} + 3n_{39}}{3n_{38} + n_{39}}$$

and

$$\frac{n_{38}}{n_{39}} = \frac{(3 - R)}{(3R - 1)}$$

Integration of the nmr spectrum of the propylene produced from  $\underline{32}$  indicates a 60:40 mixture of  $\underline{36}$  to  $\underline{37}$ , thus an intramolecular isotope effect,  $k_H^{32}/k_D^{32}$ , of  $1.50 \pm 0.08$ . Similarly from the integration of the nmr spectrum of the propylene produced from  $\underline{34}$ , a ratio of 52:48 of  $\underline{38}$  to  $\underline{39}$  was obtained, thus an inverse intramolecular secondary isotope effect,  $k_H^{34}/k_D^{34}$ , of  $0.92 \pm 0.04$ .



## D I S C U S S I O N

The rate constants and the secondary  $\alpha$ -deuterium isotope effects in the thermolysis of  $\alpha$ -deuterated 1-pyrazolines 34 and 35 are recorded in Table X.

The thermal decomposition of 1-pyrazolines to nitrogen cyclopropanes and olefins can proceed by two possible mechanisms.

- ( i ) A concerted two-bond cleavage.
- (ii) A stepwise or one-bond cleavage.

As was stated in the historical section, Seltzer and co-workers (15) have established that deuterium substitution in the  $\alpha$ -position of azoalkanes brings about 89 to 114 cal mole<sup>-1</sup> per deuterium increase in  $\Delta\Delta G^\ddagger$  when that position is undergoing a hybridization change from  $sp^3$  to  $sp^2$  in the rate-determining transition state. If we accept these values of  $\Delta\Delta G^\ddagger$  as a limit, then we can effectively calculate the predicted values of the isotope effects, in the thermolysis of 34 and 35, in terms of the above mechanisms. The isotope effects will be calculated by making use of the following equation (15a),

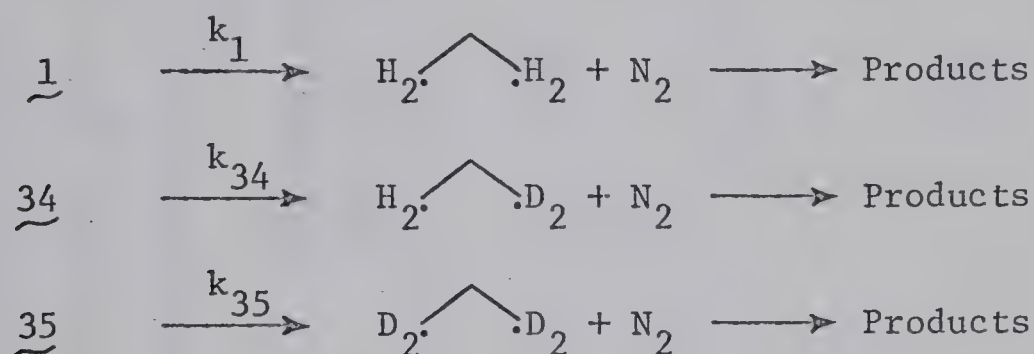
$$\Delta\Delta G^\ddagger = \frac{2.303 RT}{n} \text{ Log } \frac{k_H}{k_D} \quad (17)$$

where  $\Delta\Delta G^\ddagger$  is the change in the free energy of activation, n is



the number of deuterium atoms per molecule,  $R$  is the gas constant,  $T$  is the absolute temperature and  $k_H$  and  $k_D$  are the rate constants for breaking a  $\text{CH}_2\text{-N}$  bond and a  $\text{CD}_2\text{-N}$  bond respectively.

(i) The concerted two-bond cleavage mechanism wherein both carbon-nitrogen bonds of 1-pyrazoline are being cleaved simultaneously in the rate-determining step as shown in Scheme V,  $k_1$ ,  $k_{34}$  and  $k_{35}$  are the observed rate constants for the thermolysis of 1, 34, and 35 respectively.



Scheme V

If we use the lower limit of  $\Delta\Delta G^\ddagger$  (i.e., 89 cal mole<sup>-1</sup> per deuterium) and make the substitution in equation (17), then a concerted two-bond cleavage mechanism would be predicted to yield the isotope effects shown in Table XIII. On the other hand if we substituted the upper limit of  $\Delta\Delta G^\ddagger$  (i.e., 114 cal per deuterium), then the above mechanism would be predicted to yield values of isotope effects as shown in Table XIII.





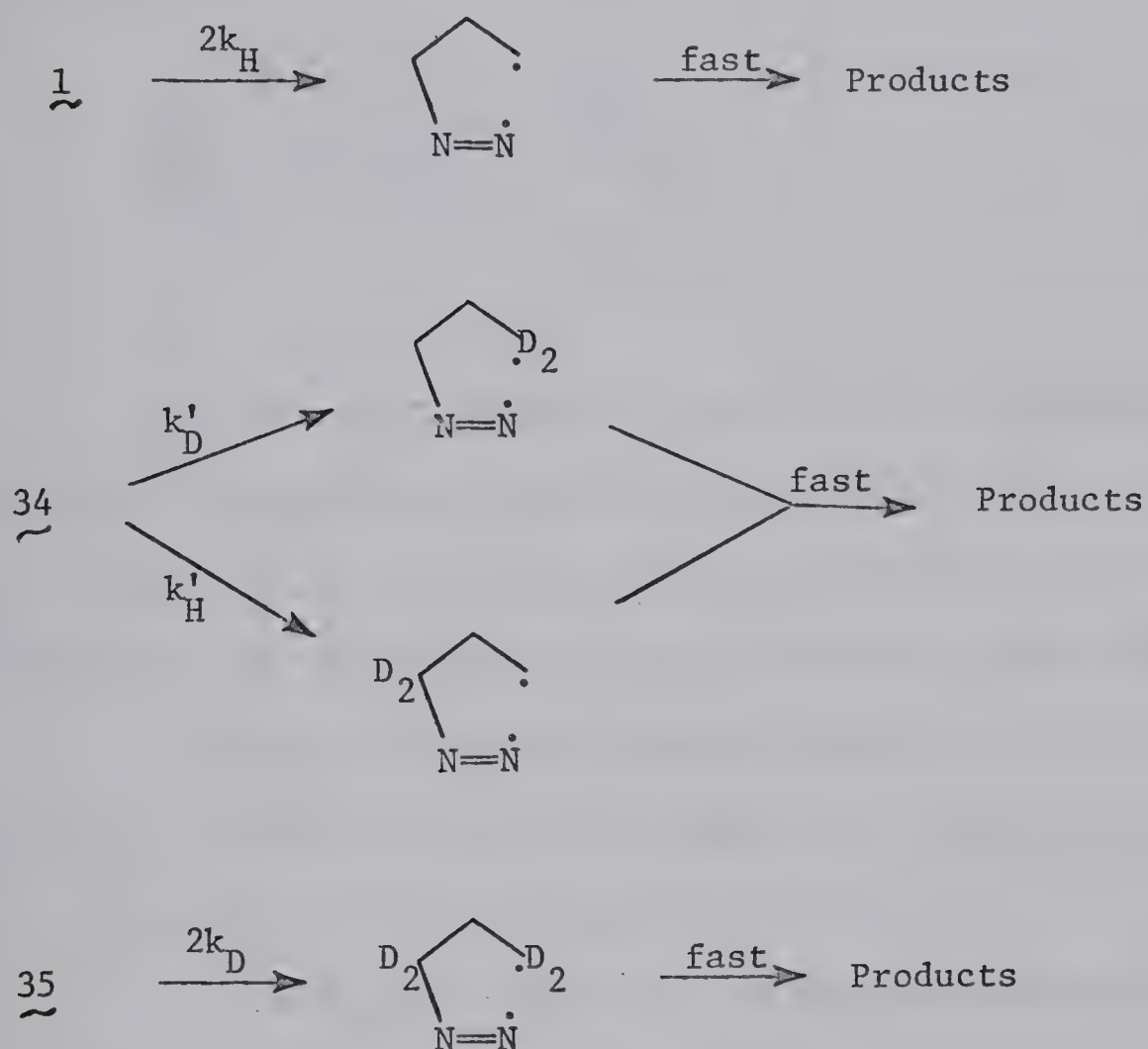
T A B L E X I I I

The predicted and the observed  $\alpha$ -deuterium isotope effects in the thermolysis of  $\alpha$ -deuterated-1-pyrazolines  $\underline{34}$  and  $\underline{35}$  at 229.5°C

Ratio of rate constants	<u>Two-bond cleavage</u>		<u>One-bond cleavage</u>		Observed
	$\Delta G^\ddagger=89\text{cal mole}^{-1}$ per deuterium	$\Delta G^\ddagger=114\text{cal mole}^{-1}$ per deuterium	$\Delta G^\ddagger=89\text{cal mole}^{-1}$ per deuterium	$\Delta G^\ddagger=114\text{cal mole}^{-1}$ per deuterium	
$\frac{k_1}{k_{34}}$	1.19	1.26	1.09	1.12	$1.19 \pm 0.02$
$\frac{k_1}{k_{35}}$	1.43	1.58	1.19	1.26	$1.40 \pm 0.03$
$\frac{k_{34}}{k_{35}}$	1.19	1.26	1.10	1.13	$1.17 \pm 0.02$



(ii) The stepwise or one-bond cleavage mechanism wherein only one carbon-nitrogen bond is breaking in the rate-determining step and the second carbon-nitrogen bond cleaves in a faster succeeding step as shown in Scheme VI.



Scheme VI

If we assume  $k'_H = k_H$  and  $k'_D = k_D$ , then by considering Scheme VI,

$$k_1 = 2k_H, \quad k_{34} = k_H + k_D \quad \text{and} \quad k_{35} = 2k_D, \quad \text{then}$$



$$\frac{k_1}{k_{34}} = \frac{2k_H}{k_H + k_D} = \frac{2 \frac{k_H}{k_D}}{\frac{k_H}{k_D} + 1} \quad (18),$$

$$\frac{k_1}{k_{35}} = \frac{k_H}{k_D} \quad (19).$$

and

$$\frac{k_{34}}{k_{35}} = \frac{k_H + k_D}{2k_D} = \frac{\frac{k_H}{k_D} + 1}{2} \quad (20).$$

If we accept the same values of  $\Delta\Delta G^\ddagger$  as limits and then substitute the predicted values of  $k_H/k_D$ , at 229.4°C, in equations 18, 19 and 20 we can calculate the observed ratio of rate constants for the one-bond cleavage mechanism as shown in Table XIII.

It may be seen from Table XIII that our observed values of isotope effects are consistent with those predicted in terms of a concerted two-bond cleavage mechanism.

An additional argument can be presented from the data in Table X. If we assume that 1-pyrazolines thermolyzed via a one-bond cleavage mechanism, then from the observed value of the  $\alpha$ -effect in the thermolysis of 35, equation 17 would yield an increase in  $\Delta\Delta G^\ddagger$  equal to 168 cal per deuterium. This is larger than any value of  $\Delta\Delta G^\ddagger$  encountered in other "unimolecular" reactions (see Table IV and VI). But if we assume that both carbon-nitrogen bonds are being cleaved simultaneously in the rate-determining step, then the value of  $\Delta\Delta G^\ddagger$  reported in Table X



is in good agreement with those values of  $\Delta\Delta G^\ddagger$  recorded in Tables IV and VI.

The rate constants and the secondary  $\beta$ -deuterium isotope effects observed in the thermolysis of compounds 32 and 33 are reported in Table XI.

The  $\beta$ -effect per deuterium atom observed in the thermolysis of 33 and the  $\beta$ -deuterium isotope effect observed in the thermolysis of 32 (Table XI) are similar in magnitude to those observed by Mishra (12) in the thermolysis of 15 and Erickson (18) in the thermolysis of 20 and 21 respectively, Table VII. The magnitude of these  $\beta$ -deuterium isotope effects are somewhat larger than those normally found in other radical reactions, see Table VII. However, comparisons with other systems are difficult in that in the trimethylene species produced the hydrogens attached to the central methylene are  $\beta$  to both newly formed  $sp^2$  centers. It has been pointed out by Hoffmann\* (22), that hyperconjugative interactions play an important role in stabilizing the trimethylene species. It may be in fact just this hyperconjugative interaction that is giving rise to the enhanced  $\beta$ -deuterium isotope effects. Hodnett (62) has observed, in the photochlorination of isobutane a value for the secondary  $\beta$ -tritium isotope effect on the isobutyl radical. This would tend to suggest  $18 \text{ cal mole}^{-1}$  for the  $\beta$ -deuterium effect.<sup>†</sup> A considerably smaller effect has been

---

\* (See page 16, in the Historical section).

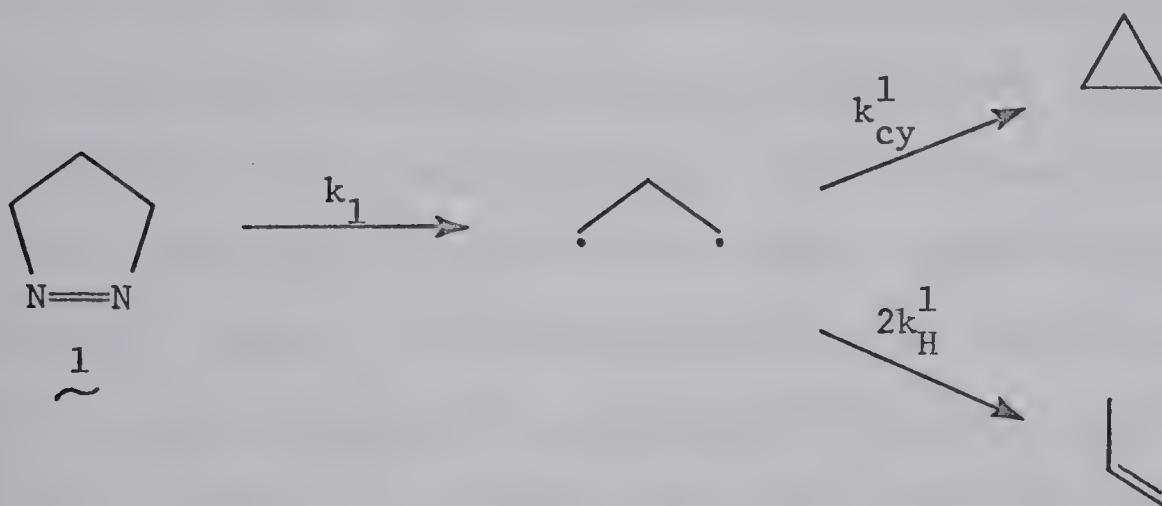
† Data for deuterium and tritium can be related by the equation derived by Swain, et al. (63a); and by Bigeleisen (63b);  $\frac{k_H}{k_T} = \left( \frac{k_H}{k_D} \right)^{1.44}$ .





observed by Seltzer and Hamilton (45) for the 1-phenylethyl-2,2,2-d<sub>3</sub> radical; (see Table VII), however, delocalization of the radical may account for the suppression of hyperconjugation in this system.

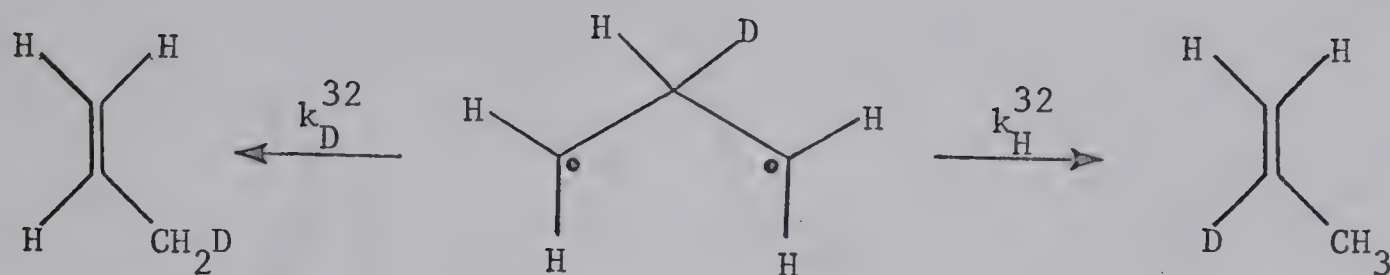
The proportion of cyclopropane and propylene formed on the thermolysis of each of the pyrazolines is indicated in Table XII. Deuterium substitutions on the pyrazoline ring tend to alter these product proportions. These proportions are controlled by the product-determining steps (Scheme VII)(12, 13).



Scheme VII

The decrease in propylene yield on going from 1 to 32 can be explained in terms of the trimethylene intermediate wherein hydrogen has a greater propensity to migrate from the central methylene to the terminal one than does deuterium. This is consistent with the ratio of 60:40 for  $CH_2=CD-CH_3$  to  $CH_2=CH-CH_2D$  calculated from the integration of the nmr spectrum of the propylene.





This ratio corresponds to an intramolecular mechanistic isotope effect  $k_H^{32}/k_D^{32}$  of  $1.50 \pm 0.08$ , which is similar with the value 1.50 obtained by Setser and Rabinovitch (2d) in the thermolysis of 1,2-dideuterio-3-methylcyclopropane. The further decrease in propylene yield on going from 32 to 33 is consistent with the above observation. There may be a small secondary isotope effect upon  $k_H^{32}$ . However, this is not expected to be greater than 1 to 2%, since, using Hammond's postulate (64) which states, "If two states, as for example, a transition state and an unstable intermediate, occur consecutively during a reaction process and have nearly the same energy content, their interconversion will only involve a small reorganization of the molecular structures." We would expect the transition state to resemble strongly the intermediate rather than propylene. This can be shown graphically in Figure 8.

It has been suggested (12) that cyclopropane arises from the cyclization of the trimethylene intermediate. We desired further studies of the effect of deuterium substitution at C-4 of the 1-pyrazoline ring on the rate of the cyclization of trimethylene species to cyclopropane. In the case of the trimethylene



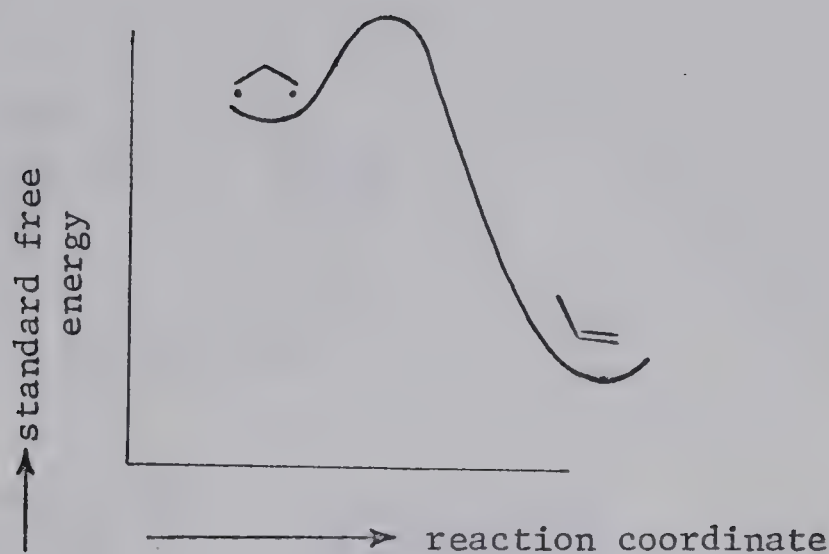


Figure 8 .

intermediate produced from 32, the analytical data from Table XII indicate that:

$$\frac{k_{cy}^{32}}{k_H^{32} + k_D^{32}} = \frac{89.21}{10.79} \quad (21),$$

where  $k_{cy}^{32}$  is the rate constant for cyclization of the trimethylene intermediate produced from 32 to cyclopropane,  $k_H^{32}$  and  $k_D^{32}$  are the rate constants for propylenes formation by migration of hydrogen or deuterium, respectively and

$$\frac{k_{cy}^1}{2k_H^1} = \frac{88.43}{11.57} \quad (22).$$

From the aforementioned nmr data  $k_H^{32}/k_D^{32} = 1.50$ , then by substituting this value in equation 21 we get;





$$\frac{k_{cy}^{32}}{2.5 k_H^{32}} = \frac{89.21}{10.79} \quad (23).$$

Then dividing 22 by 23 we get

$$\frac{k_{cy}^1 \times 2.5 k_H^{32}}{2 k_H^1 \times k_{cy}^{32}} = \frac{88.43 \times 10.79}{89.21 \times 11.57} \quad (24).$$

There may be an isotope effect on  $k_H^{32}$ , due to the non-migrating deuterium when compared with  $k_D^{32}$ . Wiberg has shown that isotope effects of this type are in the order of 1% (65). Therefore we can assume that  $k_H^1 = 1.01 k_H^{32}$ , and by substituting this value in equation 24, we find that:

$$k_{cy}^1 = 1.13 k_{cy}^{32}$$

Similarly if we go through the same type of calculations assuming  $k_D^{32} = 1.01 k_D^{33}$  we find that:

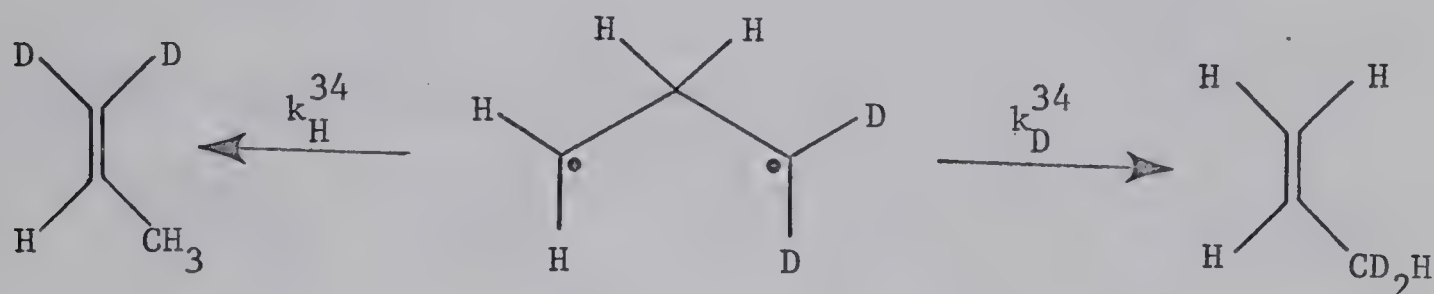
$$k_{cy}^{32} = 1.13 k_{cy}^{33}.$$

Thus deuterium substitution at the 4-position of the pyrazolines slows down the rate at which the trimethylene intermediate cyclizes to cyclopropane. The quantity is similar to that observed for  $sp^3$  carbons going to  $sp^2$ .

Integration of the nmr spectrum of the propylene produced from 34 indicates a 52:48 ratio of  $CD_2H-CH=CH_2$  to  $CD_2=CH-CH_3$ , thus an inverse intramolecular kinetic isotope effect for  $k_H^{34}/k_D^{34}$  of 0.92.



This is consistent with the observed increase in propylene formed from 34 relative to 1, Table XII. Inverse isotope effects of this magnitude have been observed earlier in reactions involving the change of hybridization of a deuterated carbon from  $sp^2$  to  $sp^3$  (Table VIII) (6b).



The further increase in propylene yield on going from 34 to 35 is consistent with an isotope effect of 0.92 in the product-determining step. The magnitudes of these inverse secondary isotope effects are smaller than those normally observed from an  $sp^2$  to  $sp^3$  conversion in the transition state (see Table VIII reactions 1 to 7), but are similar to those observed by Szwarc (53, 54) and Takahasi (55) (Table VIII reactions 8 to 10). These observations provide additional evidence that the transition state resembles the trimethylene intermediate rather than propylene. The isotope effects on the cyclization reactions of the trimethylene intermediate produced from 34 and 35 are calculated in the following manner:

The analytical data in Table XII indicate

$$\frac{k_{cy}^{34}}{k_H^{34} + k_D^{34}} = \frac{87.99}{12.01} \quad (25).$$



Then by dividing both the numerator and the denominator of the left side of equation 25 by  $k_H^{34}$ , we get

$$\frac{k_{cy}^{34}}{\left(1 + \frac{k_D^{34}}{k_H^{34}}\right) k_H^{34}} = \frac{87.99}{12.01} \quad (26).$$

But  $k_H^{34}/k_D^{34} = 0.92$  from the nmr observations, then

$$\frac{k_{cy}^{34}}{2.09 k_H^{34}} = \frac{87.99}{12.01} \quad (27).$$

Then by dividing equation 22 by equation 27, we get,

$$\frac{k_{cy}^1 \times 2.09 k_H^{34}}{k_{cy}^{34} \times 2 k_H^1} = \frac{88.43 \times 12.01}{87.99 \times 11.57} \quad (28).$$

Assuming that  $k_H^1 = k_H^{34}$ , on the basis that the changes in hybridization occurring are the same in each case, then we find that:

$$k_{cy}^1 = 1.00 k_{cy}^{34}$$

Similarly by assuming\* that  $k_D^{34} = k_D^{35}$ , we find that:

$$k_{cy}^{34} = 1.01 k_{cy}^{35}$$

---

\* This assumption seems justified on the basis that any secondary  $\beta$ -isotope effect would be expected to be smaller than the secondary  $\alpha$ -isotope effect which is itself very small (see the previous assumption).





These observations suggest that there is little or no change in the C-H force constants of the terminal methylene groups of the trimethylene intermediate on going to cyclopropane; a fact borne out by the very similar frequencies of the C-H stretching vibration of cyclopropane (3075 and 3009  $\text{cm}^{-1}$ ) (67) and the terminal methylene stretching frequencies of propylene (3089 and 2991  $\text{cm}^{-1}$ ) (68).

The  $\text{CH}_2$  bending, wagging, and rocking modes for cyclopropane (1475, 975, and 854  $\text{cm}^{-1}$ ) (67) and the terminal  $\text{CH}_2$  of propylene (1420, 963, and 921  $\text{cm}^{-1}$ ) (68) similarly have a compensatory effect such that the total change in the C-H force constants on going from the trimethylene species to cyclopropane is negligible.

It is evident that this study of secondary kinetic isotope effects is consistent with the proposed formation of the trimethylene intermediate in the thermolysis of 1-pyrazoline, and provides a strong case for the cleavage of both carbon-nitrogen bonds in the rate-determining transition state.





## E X P E R I M E N T A L

All boiling points are uncorrected.

The deuterated and natural 1-pyrazolines were purified by gas-liquid chromatography (glc) using a Wilkens Aerograph Autoprep Model A-700 with a 20 ft column of 10% Ucon-insoluble on Fluoropak support. Product analyses were carried out on a gas chromatograph consisting of a Gow-Mac Model TR-2-B,W thermal conductivity cell with a Gow-Mac Model 40-50 power supply in conjunction with a Sargent Model SR recorder.

Deuterium analyses were carried out on a Metropolitan-Vickers MS-2, single focussing mass spectrometer. The infrared spectra were obtained on a Perkin-Elmer Model 421 spectrophotometer. The ultraviolet spectra were obtained on a Carey Model 14M Spectrophotometer. The nuclear magnetic resonance spectra were obtained using a Varian A-60 and an HR-100 spectrometer.

(A) Preparations

(a) Pyrazolidine. To a well stirred solution of 97% anhydrous hydrazine (20.5 ml, 0.591 mole) and 98% ethyl alcohol (150 ml), under nitrogen atmosphere and at 70°C, was added dropwise (over a period of four hours) a solution of 1,3-dibromopropane (29.59 g, 0.1478 mole) in 98% ethyl alcohol (15 ml). The stirring was continued for an additional half-hour. During the reaction an oily precipitate of hydrazinemonohydrobromide settled



out. The mixture was then cooled for several hours while stirring, and the crystalline hydrazinemonohydrobromide was filtered off. A slight excess of solid potassium hydroxide was added to the cooled filtrate and the precipitated potassium bromide was removed by filtration. The alcohol and unreacted hydrazine were evaporated under reduced pressure and the residue was vacuum distilled through a 30 cm Vigreux column as quickly as possible. The yield was 6.5 g (50%), collected between 60-71°C (54 mm).

(b) 1-Pyrazoline (1). To a cooled (0°C) stirred mixture of mercuric oxide (33.0 g, 0.15 mole) and anhydrous sodium sulfate (24.0 g) in dry ether (125 ml), was added dropwise a mixture of the pyrazolidine in dry ether (20 ml). After the addition was completed the mixture was allowed to slowly warm, with stirring, to room temperature over a period of two hours. The mercury, excess mercuric oxide, and sodium sulfate were then filtered off. Most of the ether was then removed by distillation through a 30 cm Vigreux column. The residue was subsequently separated on a gas chromatograph and the 1-pyrazoline was collected as a pure fraction. The yield was 2.9 g (30% over all yield from 1,3-dibromopropane). The nmr and ir spectra are shown in Figures 1 and 2 respectively. The uv spectrum has a  $\lambda_{\text{max}}$  at 315 nm ( $\epsilon = 446$  in methanol).

(c) Deuterated 1-pyrazolines. The deuterated 1-pyrazolines 32, 33, 34, and 35 were prepared from the corresponding pyrazolidines which in turn were synthesized from the 1,3-dibromopropanes by the same method described above for the preparation of natural





1-pyrazoline (1). The deuterated 1,3-dibromopropanes were synthesized as below.

1,3-Dibromopropane-2-d<sub>1</sub>. Deuterium bromide, generated by the addition of deuterium oxide to freshly distilled phosphorous tribromide as described by Leitch et al. (56), was added photochemically to freshly distilled allyl bromide using the procedure of Kharasch and Mayo (57). In a typical run allyl bromide (22.08 g, 0.1825 mole) was dried by distillation in vacuo over phosphorous pentoxide, then distilled in vacuo into a 2 litre flask. Deuterium oxide, in a quantity large enough to saturate the allyl bromide was also distilled into the flask. Deuterium bromide was generated and trapped over phosphorous pentoxide. It was then distilled in vacuo into the reaction flask containing the allyl bromide. The flask was allowed to come to room temperature, and was then illuminated with a 500-watt incandescent projection lamp at a distance of 13 cm. Dibromopropane began to condense on the interior wall of the flask a few minutes after illumination. The yield of 1,3-dibromopropane was 35.3 g (95%), bp 165°C. The nmr spectrum showed a doublet centered at  $\tau$  6.48 and a quintet at  $\tau$  7.68. The areas under each curve were found to be in the ratio of 3.82:1.00.

1,3-Dibromopropane-1,1,3,3-d<sub>4</sub>. A solution of freshly distilled diethylmalonate (24.5 g, 0.15 mole) in dry ether (160 ml.) was added dropwise to a well stirred solution of lithium aluminum





deuteride (99 atom % D) (6.75 g, 0.16 mole) in dry ether (350 ml ) at such a rate as to maintain steady reflux. After completion of addition, the refluxing was continued for an additional three hours, cooled to 0°C, and water was added slowly to decompose the excess deuteride. The solution was then acidified with dilute hydrobromic acid, the ether layer removed by distillation, and the crude product in the aqueous layer converted, without isolation, to the dibromide by the addition of 48% hydrobromic acid (116 g) and concentrated sulfuric acid (50 ml). The mixture was then refluxed for seven hours. Ten to 15 ml of 48% hydrobromic acid was added at the end of each hour. The 1,3-dibromopropane was then distilled out of the solution, the organic layer was washed several times with potassium carbonate solution and dried over anhydrous sodium sulfate. Distillation gave 12.7 g (40% yield based on diethylmalonate), bp 165°C. The nmr spectrum showed just a singlet at  $\tau$  7.68.

Ethanol-O-d. Deuterium oxide 99.7% (70 g, 3.5 mole) was added with stirring under anhydrous conditions to boron triethoxide (180 g, 1.166 mole). The mixture was then heated to 50°C for a period of two hours. The ethanol-O-d was then distilled off using a fractionating column. The distillate was redistilled and collected to yield 156 g of alcohol, bp 77.8°C. The nmr spectrum displayed no absorption for the O-H group. The ir spectrum showed a strong absorption at 2470-2490  $\text{cm}^{-1}$  which is characteristic of O-D absorption. No detectable absorption was found between 3590-3650  $\text{cm}^{-1}$  for the O-H group.



Diethylmalonate-2,2-d<sub>2</sub>. A mixture of freshly distilled diethyl malonate (54 g, 0.337 mole) bp 94-96° (18 mm) and ethanol-O-d (69.1 g, 1.47 mole) containing sodium metal (0.18 g) was heated in the absence of water to 45°C for a period of 9-10 hours. The deuterated diethyl malonate and alcohol were then separated by use of a Vigreux column. A total of four exchange reactions were carried out using fresh ethanol-O-d each time. The extent of the exchange reaction was followed by observing the nmr spectrum for the disappearance of the methylene signal at  $\tau$  6.92 after each successive exchange. The deuterated diethyl malonate was finally distilled and dried over anhydrous sodium sulfate.

1,3-Dibromopropane-2,2-d<sub>2</sub>. A solution of freshly distilled diethyl malonate-2,2-d<sub>2</sub> (39.0 g, 0.253 mole) in 224 ml of dry ether was reduced with lithium aluminum hydride (11.85 g, 0.253 mole) in 515 ml dry ether. The work-up and conversion to the dibromide was carried out in the same manner as previously mentioned for the tetradeuterio compound. Distillation gave 29.5 g (57% overall yield) bp 165°. The nmr spectrum showed a singlet at  $\tau$  6.53.

1,3-Dibromopropane-1,1-d<sub>2</sub>. A solution of freshly distilled  $\beta$ -propiolactone (14.4 g, 0.2 mole) in dry ether (160 ml) was added, with stirring, to a solution of lithium aluminum deuteride (< 99 atom % D) (4.2 g, 0.1 mole) in dry ether (300 ml). The work-up and conversion to the dibromide was carried out in the same manner as for the aforementioned tetradeuterio sample. Distillation gave 16.5 g (40.4% yield based on  $\beta$ -propiolactone), bp 165°C. The nmr



spectrum showed a triplet centered at  $\tau$  6.48 and a triplet centered at  $\tau$  7.68. The areas under each curve were found to be in the ratio of 1.00:1.00.

#### (B) Deuterium analysis

The nmr spectra for the deuterated 1-pyrazolines 32, 33, 34 and 35 are shown in Figures 3, 4, 5, and 6 respectively. The low voltage (10 ev) MS-2-H mass spectra showed that the molecular ions have a mass of 71, 72, 72 and 74 for compounds 32, 33, 34, and 35 respectively. Mass spectral and nuclear magnetic resonance analysis indicated that compound 32 is 95.1% deuterated in the desired position, compounds 34 and 35 are greater than 98% deuterated in the positions indicated. The mass spectral analysis for compound 33 gave the following results 88.6%  $C_3H_4D_2N_2$ , 11.3%  $C_3H_5DN_2$ , and 0.1%  $C_3H_6N_2$ .

#### (C) Kinetic Measurements

All kinetic studies were carried out on the reactor which is shown diagrammatically in Figure 9. The reactor system is essentially the same as that designed by Smith (58), and used by Mishra (10). The working procedure was also that used by Mishra (10). Some variation in the attached glass apparatus have been made by Cameron (69). Samples were injected into the reactor as neat liquids.





nitrogen

K

A B

M

N

Q

R

F

G

S

J

C

D

E

H

L

T

U

V

P

O

to vacuum

A = Reactor	B = Diaphragm
C = Relay	D = Transducer
E = Recorder	F = Calibrated needle valve
G = Solenoid valve	H = Manometers
J = Small ballast	K = Large ballast
L = Cold traps	M = Heaters
N = Thermocouples	O = Cold junction
P = Potentiometer	Q, R, S, T, U, V = Stopcocks

B = Diaphragm

D = Transducer

F = Calibrated needle valve

H = Manometers

K = Large ballast

M = Heaters

0 = Cold junction

Q,R,S,T,U,V = Stopcocks





(D) Product Analysis

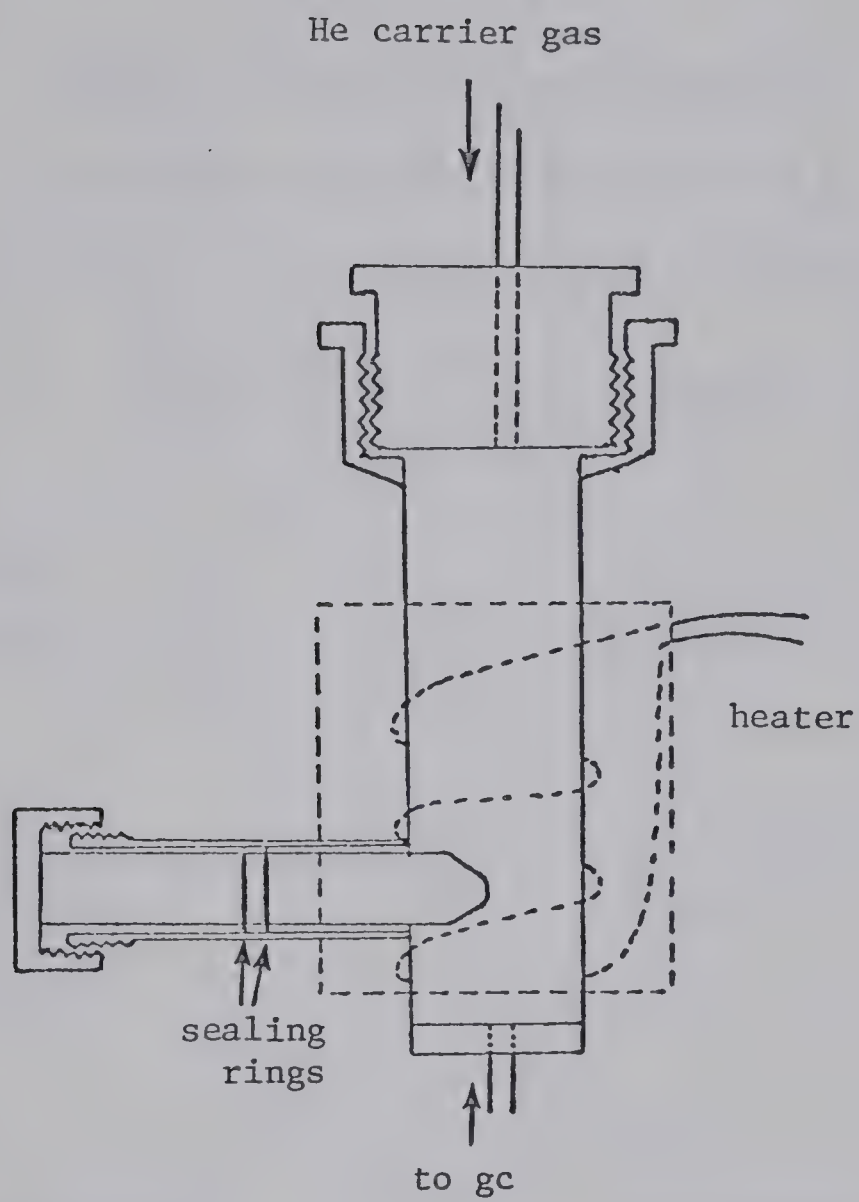
( i) The bulb crusher. Product compositions were studied by pyrolyzing degassed samples in sealed pyrex bulbs which were heated and then crushed directly in the helium carrier gas flow by the use of a bulb crusher, Figure 10, and the products were analyzed by gas chromatography.

(ii) Identification and quantitative analysis of the products.

All products were identified by comparison of their relative retention times with those of authentic samples on three different columns; 8 ft 20% di-n-butylmaleate on Fluoropak, 20 ft mineral oil on fire brick in tandem with a 20 ft 10% di-n-butylmaleate on Diatoport, and 20 ft saturated silver nitrate in propylene glycol on Diatoport in tandem with 20 ft 10% 1,2,3-tris(2-cyanoethoxy)-propene (TCP) on fire brick. The second column was more useful for better separation and quantitative estimation of the products. The relative retention times for the products on these three columns are given in Table XIV.



Figure 10



Schematic diagram for the bulb crusher



T A B L E X I V

Relative retention data for the  
thermolysis products of 1-pyrazoline 1

Column	Column temp. (C°)	Helium flow rate (ml min <sup>-1</sup> )	Compound	Relative re- tention time (N <sub>2</sub> = 1.000)
8', 20% n-butyl- maleate on fluoro- pak	25	23	Cyclopropane	1.83
			Propylene	1.26
20', mineral oil on firebrick in tandem with a 20', 10% n- butylmaleate on Diatoport	25	43	Cyclopropane	2.67
			Propylene	1.75
20', saturated silver nitrate in propylene glycol on Diatoport in tandem with a 20', 10% TCP on firebrick	25	50	Cyclopropane	1.25
			Propylene	2.30



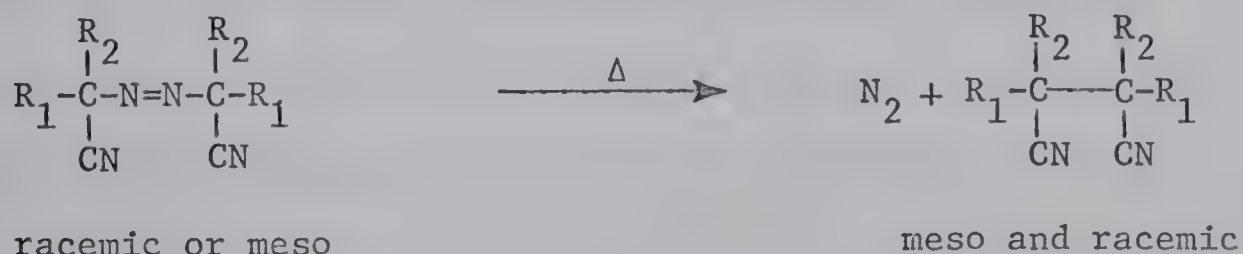


## CHAPTER II

## I N T R O D U C T I O N

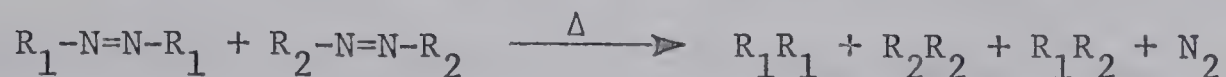
(A) Gas Phase Thermolysis of Azoalkanes

The most important reaction of azoalkanes is their tendency to decompose into alkyl free radicals and molecular nitrogen under the influence of heat or light (70). Azomethane, the parent compound of the azoalkanes was found to produce upon thermolysis, apart from nitrogen, ethane as the main product with some ethylene, methane, and higher hydrocarbons being formed concomitantly (70). There is a large body of information to indicate the presence of methyl radicals in the thermolysis of azomethane (70,71). It has been shown that the initial products of thermal and photochemical decomposition are capable of removing metallic mirrors(72) and that azomethane initiates the thermal decomposition of ethane and propane (73). Overberger and Berenbaum (74) have shown that the racemic and the meso forms of diastereomeric azonitriles not only decompose at the same rate, but yield identical mixtures of diastereomeric succinonitrile derivatives, as shown below.



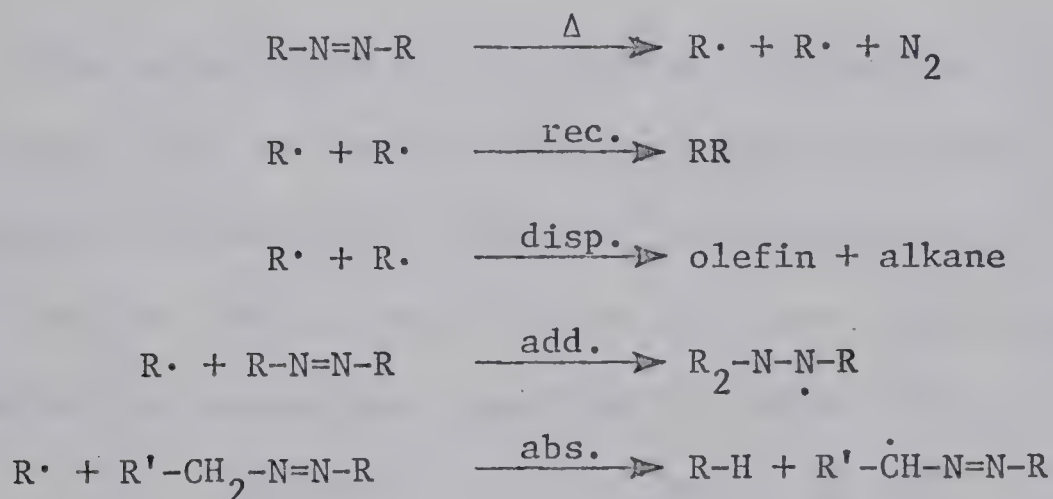


Also, a mixture of two azonitriles bearing different substituents yields not only the symmetric products, but also the unsymmetric one.



This class of compounds has been used as a source of radicals to initiate polymerization reactions.

It has been shown (70) that the gas phase thermal decomposition of azoalkanes produces molecular nitrogen and alkyl free radicals. The initially formed radicals not only combine to give the corresponding alkane, but can also undergo further processes such as radical disproportionation, addition to the nitrogen-nitrogen double bond (70, 75, 78a) of the azoalkane, or hydrogen abstraction from the azoalkane<sup>\*</sup>, as shown below.




---

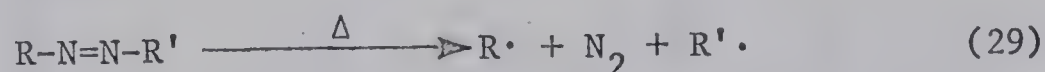
\* When the alkyl groups are larger than methyl, resonance stabilization of the resulting radical suggests preferential abstraction of  $\alpha$ -hydrogen atoms from the azoalkane.



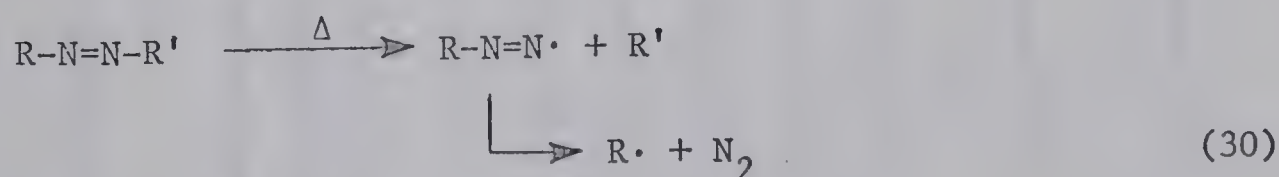
Frost and Rice (75a) found that the addition of ethylene, propylene, and nitric oxide to the thermolysis of azomethane (40) reduced the rates of nitrogen and methane formation and that nitric oxide is a more efficient inhibitor than are the olefins. The yields of methane, ethane, and ethylene were reduced to almost zero upon the addition of a sufficient amount of nitric oxide. These observations led the authors to suggest a short chain in azomethane thermolysis.

Activation energies for the unimolecular decomposition of azoalkanes indicate that the more stable radicals are more readily produced (Table XV). Thus an increase in the reactivity of azoalkanes can be achieved by means of stabilizing groups such as phenyl, cyano, and alkoxycarbonyl groups at one or both  $\alpha$ -carbon atoms.

The unimolecular decompositions of azomethane (40), methyl-azo-2-propane (41), and azo-bis-2-propane (42) were first studied by Ramsperger (76) and their activation parameters are in Table XV. He concluded that both carbon-nitrogen bonds are being cleaved in the rate-determining step (equation 29) rather than by a process



of one bond at a time (equation 30).







T A B L E X V

Kinetic parameters in the thermal decomposition of some azo compounds

Compound	Solvent	E <sub>a</sub> kcal/mole	Log A	ΔS <sup>‡</sup> e.u.	T°C	k x 10 <sup>4</sup> sec <sup>-1</sup>	Reference
(40) <chem>CH3-N=N-CH3</chem>	Gas phase	51.2	15.7	12.2	300	5.6	75b
(40) <chem>CH3-N=N-CH3</chem>	Gas phase	55.5			303	1.78*	75a
(41) <chem>(CH3)2CH-N=N-CH3</chem>	Gas phase	47.5	14.5	11.0	250	0.4	76
(42) <chem>(CH3)2CH-N=N-CH(CH3)2</chem>	Gas phase	40.9	13.7	1	120	0.0001	76
(43) <chem>CH3CH2-N=N-CH2CH3</chem>	Gas phase	48.5	15.8	12.2	250	0.3	78b
(43) <chem>CH3CH2-N=N-CH2CH3</chem>	Gas phase	47.0					78a
(44) <chem>(CH3)3C-N=N-C(CH3)3</chem>	Gas phase	42.8	15.3	15.2	250	280	79
(45) <chem>C6H5-CH2-N=N-CH2-C6H5</chem>	Gas phase	35.0	-	5	120	0.045*	81a
(46) <chem>C6H5-CH(CH3)-N=N-CH(CH3)-CH3</chem>	Diphenylether	36.5	-	9.3	120	0.132*	41
(47) <chem>C6H5-CH(CH3)-N=N-CH(CH3)-C6H5</chem>	Ethylbenzene	32.6	-	7	120	4.85*	41

cont'd





T A B L E X V

cont'd

(48)	$\begin{array}{c} \text{C}_6\text{H}_5-\text{CH}-\text{N}=\text{N}-\text{CH}-\text{C}_6\text{H}_5 \\   \qquad \qquad   \\ \text{C}_2\text{H}_5 \qquad \text{C}_2\text{H}_5 \end{array}$	Ethylbenzene	32.3	-	-	120	2.06*	41
(49)	$\begin{array}{c} \text{CH}_3 \qquad \text{CH}_3 \\   \qquad   \\ \text{CH}_3-\text{C}-\text{N}=\text{N}-\text{C}-\text{CH}_3 \\   \qquad   \\ \text{CN} \qquad \text{CN} \end{array}$	Toluene	31.1	-	3	80.4	1.55	81b
(50)	$\begin{array}{c} \text{CH}_3 \qquad \text{CH}_3 \\   \qquad   \\ \text{CH}_3-\text{C}-\text{N}=\text{N}-\text{C}-\text{CH}_3 \\   \qquad   \\ \text{C}_2\text{H}_5\text{O}_2\text{C} \qquad \text{CO}_2\text{C}_2\text{H}_5 \end{array}$	Nitrobenzene	30.9	-	5	80	1.57	81c
(51)	$(\text{C}_6\text{H}_5)_2\text{CH}-\text{N}=\text{N}-\text{C}_6\text{H}_5$	Decalin	34.0±1.3	-	3.9±3.1	124.5	0.344	40
(52)	$(\text{C}_6\text{H}_5)_3-\text{C}-\text{N}=\text{N}-\text{C}_6\text{H}_5$	Toluene	27.0±1	-	5.2±3	53.3	2.25	40
(53)	$(\text{C}_6\text{H}_5)_2\text{CH}-\text{N}=\text{N}-\text{CH}-(\text{C}_6\text{H}_5)_2$	Toluene	26.6±1.3	-	2.2±3.3	64.0	3.40	40

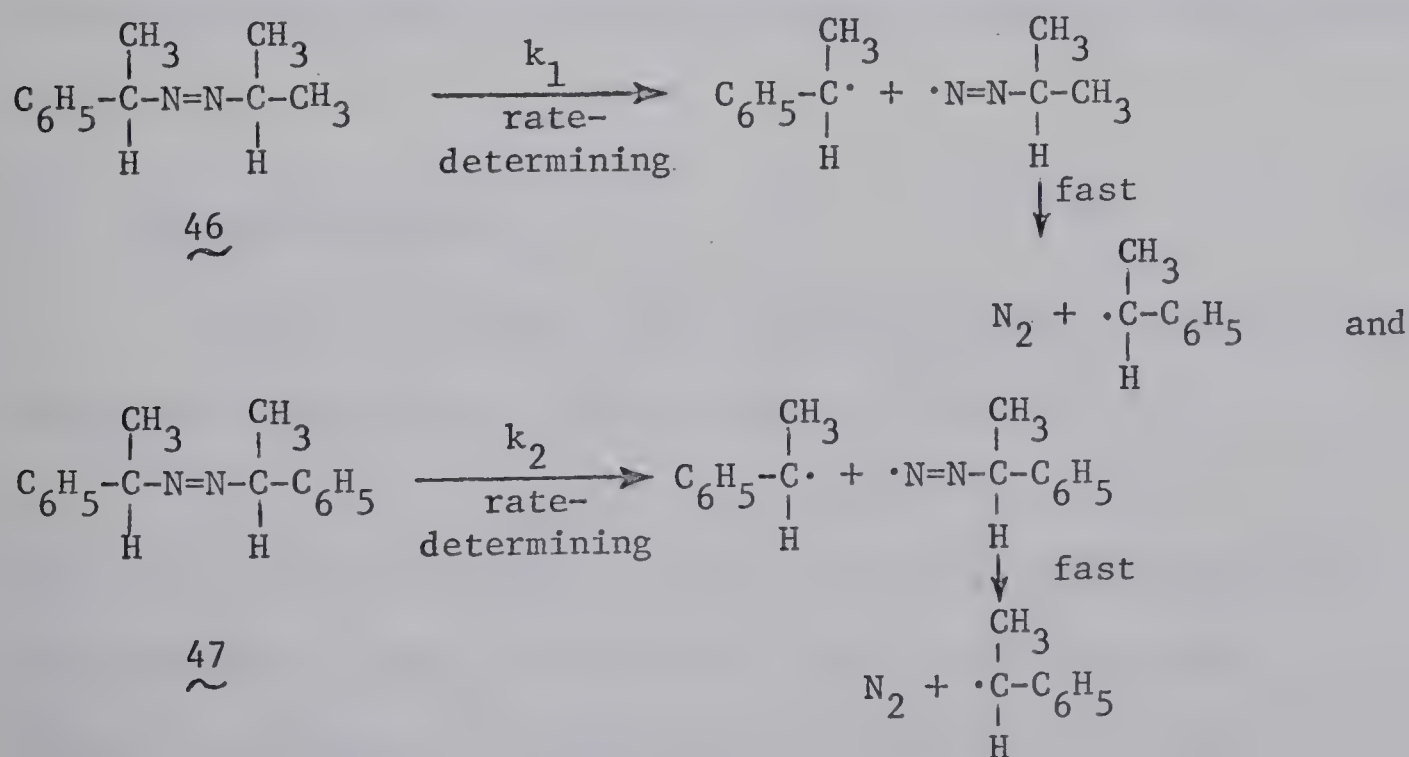
† "net inhibited rate."

\* Extrapolated to 120°.



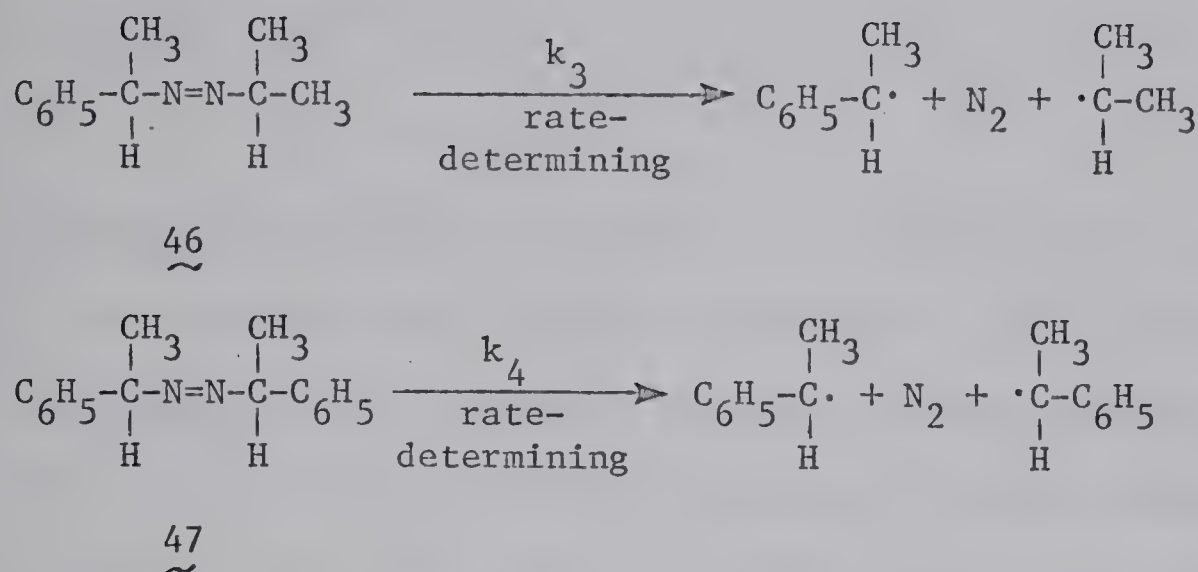
Cohen and Wang (40, 80) noted that in a comparison of azomethane (40), azo-bis-2-propane (42), azo-bis-1-phenylethane (47), and azo-bis-diphenylmethane (53), that symmetrical substitution of a pair of methyls or a pair of phenyls for  $\alpha$ -hydrogens had an approximate additive effect on lowering of the activation energy (see Table XV). This observation, in conjunction with an additional comparison of phenylazodiphenylmethane (51) with phenylazotriphenylmethane (52) and azo-bis-diphenylmethane (53) (Table XV), led them to conclude that the contribution of radical stabilizing groups, in both alkyl fragments, are observed as decreases in activation energy in the rate-determining step, consistent with a simultaneous cleavage of both carbon-nitrogen bonds.

Overberger and DiGiulio (41) have provided additional support for the conclusion that both alkyl groups attached to the azo linkage participate in the rate-determining step. They have considered compounds 46 and 47 in Schemes VIII and IX.



Scheme VIII





Scheme IX

Scheme VIII predicts that the rate of thermolysis of 47 should be two times that of 46, a simple statistical factor for the breaking of the  $\alpha$ -phenylethyl carbon-nitrogen bond. Scheme IX implies that the resonance stabilization of the second phenyl group should contribute to a decrease in activation energy, on going from 46 to 47, such as to make  $k_4 > 2k_3$ . They observed a difference in the rate of 37-fold on going from 46 to 47 and thus concluded that both carbon-nitrogen bonds are breaking in the rate-determining transition state.

### (B) Polanyi Relations

Evans and Polanyi (82) have carried out a number of reactions of sodium atoms with a series of alkyl halides,



and from examining the shapes of the potential energy curves for these reactions, they deduced that a simple relation exists between the changes in the heat of reaction and in the activation





energies, as shown below.

$$E_a = \alpha \Delta H + C \quad (31)$$

where  $E_a$  is the activation energy,  $\Delta H$  is the heat of reaction, and  $\alpha$  and  $C$  are constants. They found that the reaction holds with variation in  $R$ . The validity of this relationship (equation 31) has been tested by a variety of reactions. Trotman-Dickenson and co-workers have found that the equation holds for the reactions of methyl radicals (83a), bromine atoms (83b, c) and difluoroamino radicals (83d) with alkanes, and the possibility to apply the data for iodine as well was suggested for each of the reactions in the series



( $R = CH_3, C_2H_5, i-C_3H_7, t-C_4H_9$ , etc.)  $\Delta H$  is then represented by the strength of the bond being broken, i.e.,  $D(R-H)$  because the  $HX$  bond is being formed irrespective of the change in the alkyl radical. Then equation 31 takes the form

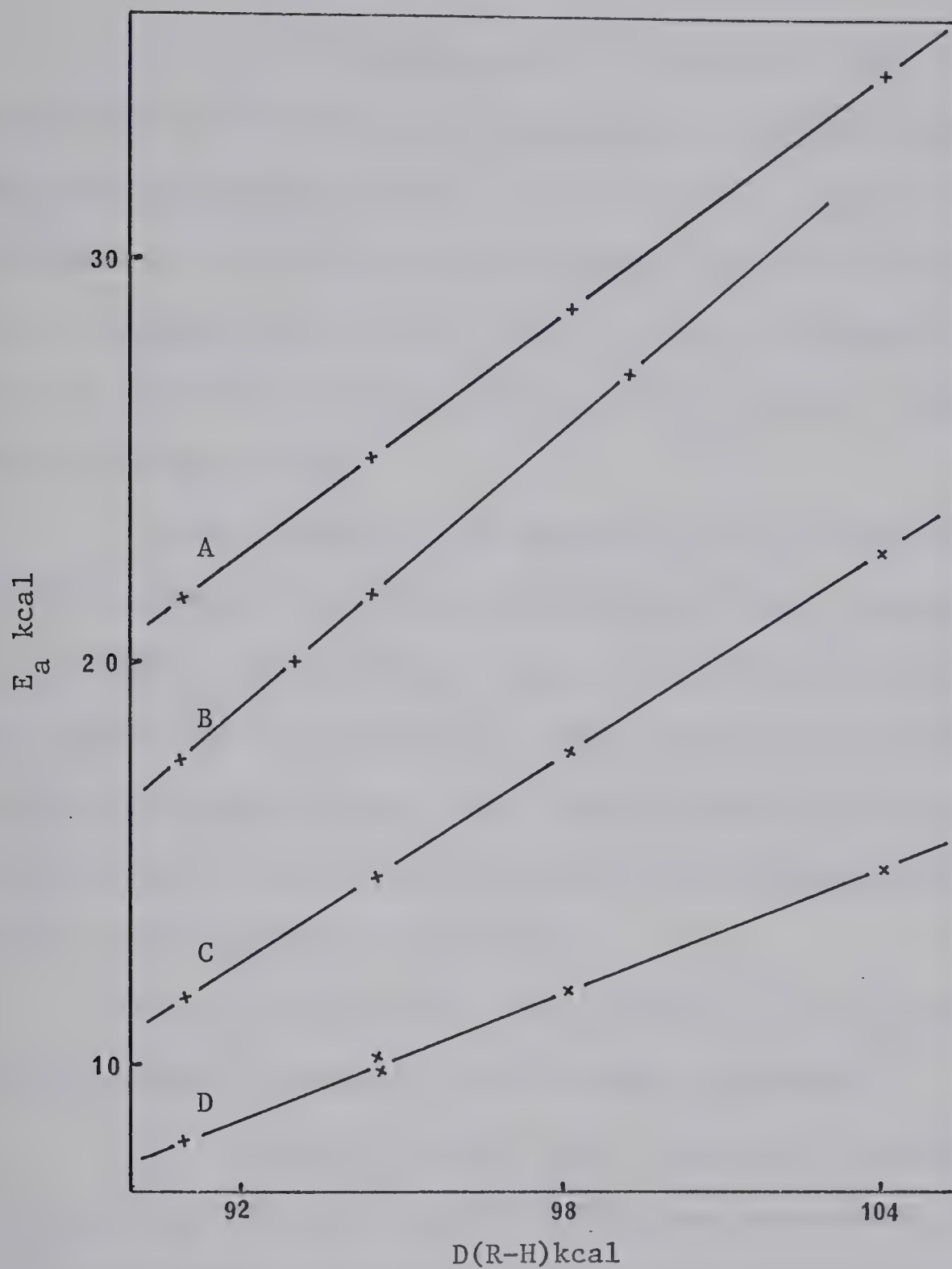
$$E = \alpha [D(R-H) - C]$$

A straight line has been obtained from the plot of  $E_a$  against  $D(R-H)$  for each series of reactions as shown in Figure 11.

The Polanyi relationship is confirmed by the linearity of the plot. Subsequently this relationship has been used to determine the bond dissociation energy of related hydrocarbons by interpolation. It has been emphasized (84) that this type of relationship is only applicable to reactions of radicals or atoms with a series of closely related compounds.



Figure 11



Polanyi plots of  $E_a$  vs.  $D(R-H)$  for reactions  $X + RH = XH + R$ : A, iodine atoms; B, difluoroamino radicals; C, bromine atoms ( $E_a$  displaced by +4kcal; D, methyl radicals.

(Taken from Ref. 84)



## P R O P O S A L

It has been demonstrated by Seltzer et al (15) that the replacement of a hydrogen by a deuterium on a carbon undergoing a hybridization change from  $sp^3$  to  $sp^2$ , during a reaction, produces a decrease in rate of 12-15% per deuterium, at  $105^\circ$ . This represents a change in free energy,  $\Delta\Delta G^\ddagger$ , of 89 to 114 calories per mole per deuterium, and is referred to as a secondary  $\alpha$ -deuterium kinetic isotope effect.

Since our results, in Chapter I, are directly dependent upon the magnitude observed for this effect we have attempted a further test of its validity. If we could enhance the observed  $k_H/k_D$  values to a point where the rates observed by a two-bond cleavage mechanism, Scheme X, are distinguishable from those rates predicted for a stepwise mechanism then such a test exists on simple algebraic grounds (see below).

The selection of the azo compound to be used in such a test must take cognizance of the following conditions:

(a) Since the observed  $k_H/k_D$  values are temperature dependent, i.e.,  $\ln k_H/k_D = \Delta\Delta G^\ddagger/RT$ , then the measurement of rate will be facilitated by using an azo compound that thermolyzes at a conveniently low temperature, e.g.,  $75-150^\circ$ .

(b) The larger the number of  $\alpha$ -deuteriums the larger the observed rate changes.

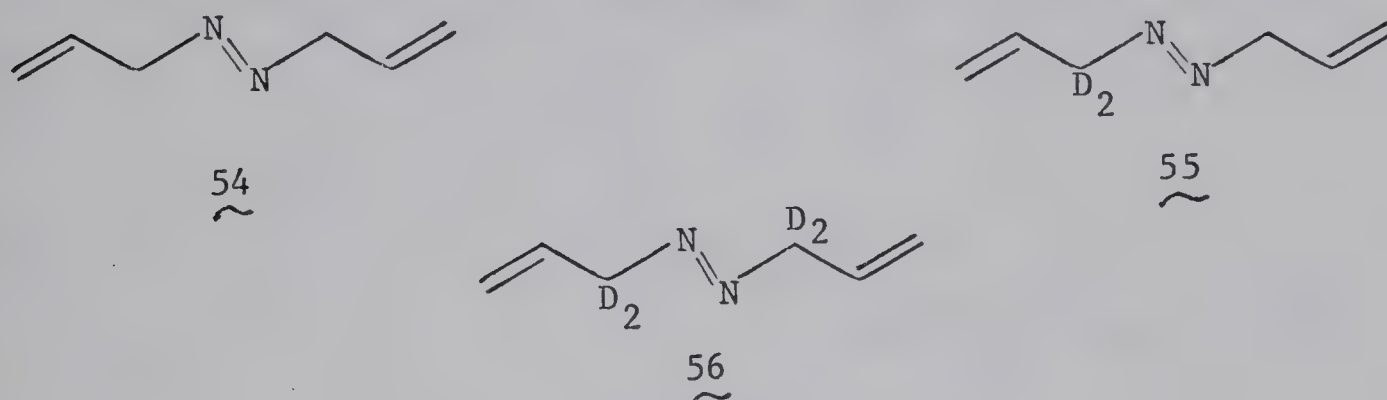
(c) It is desirable to carry out such a reaction in the gas phase since we are less likely to observe possible ionic





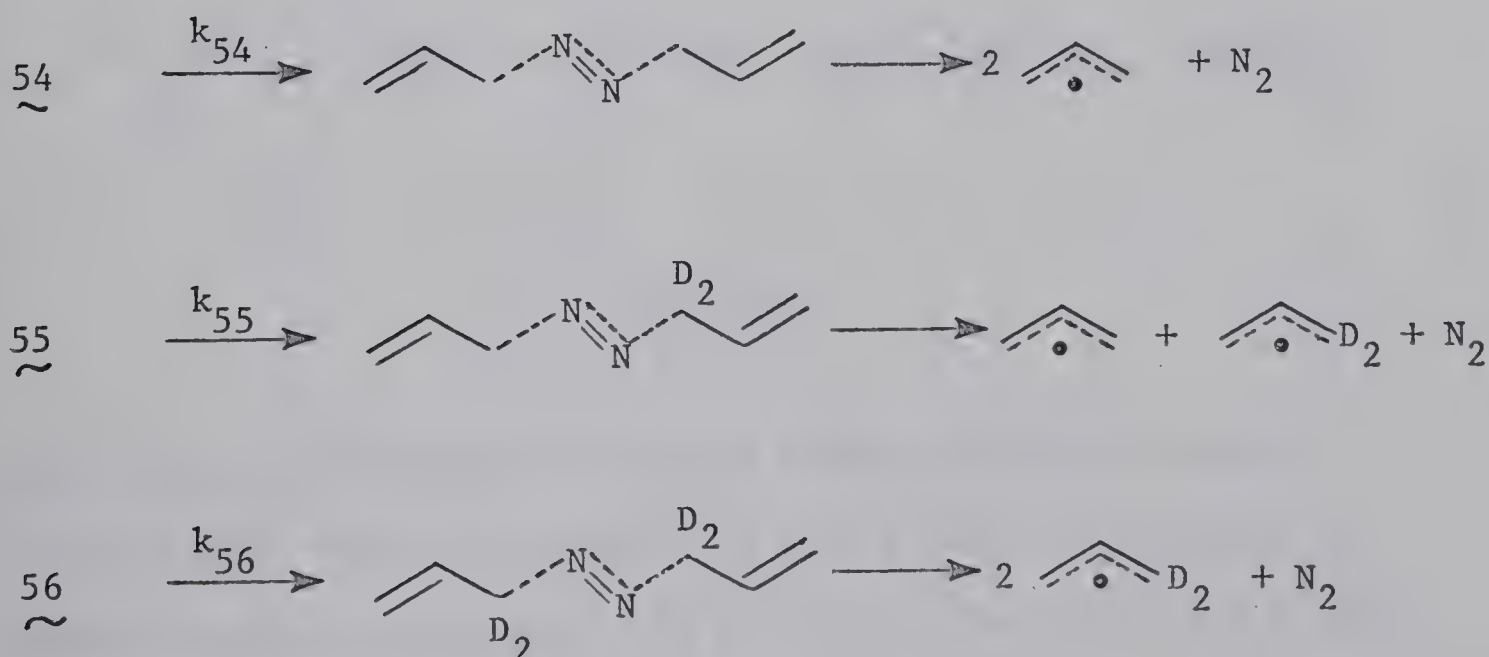
side reactions and since we have available an accurate method of measuring the rate of such gas phase reactions.

Azo-bis-3-propene (54) fulfills the above requirements as closely as possible. We have undertaken the synthesis of 54



along with its  $-d_2$  (55) and  $-d_4$  (56) analogues.

If we examine the  $k_H/k_D$  values predicted for 54, 55, and 56 from Seltzer's values of 89-114 cal mole<sup>-1</sup> per deuterium at 150° we see that the concerted two bond cleavage mechanism, Scheme X, suggests those values of  $k_{54}/k_{55}$ ,  $k_{54}/k_{56}$ , and  $k_{55}/k_{56}$



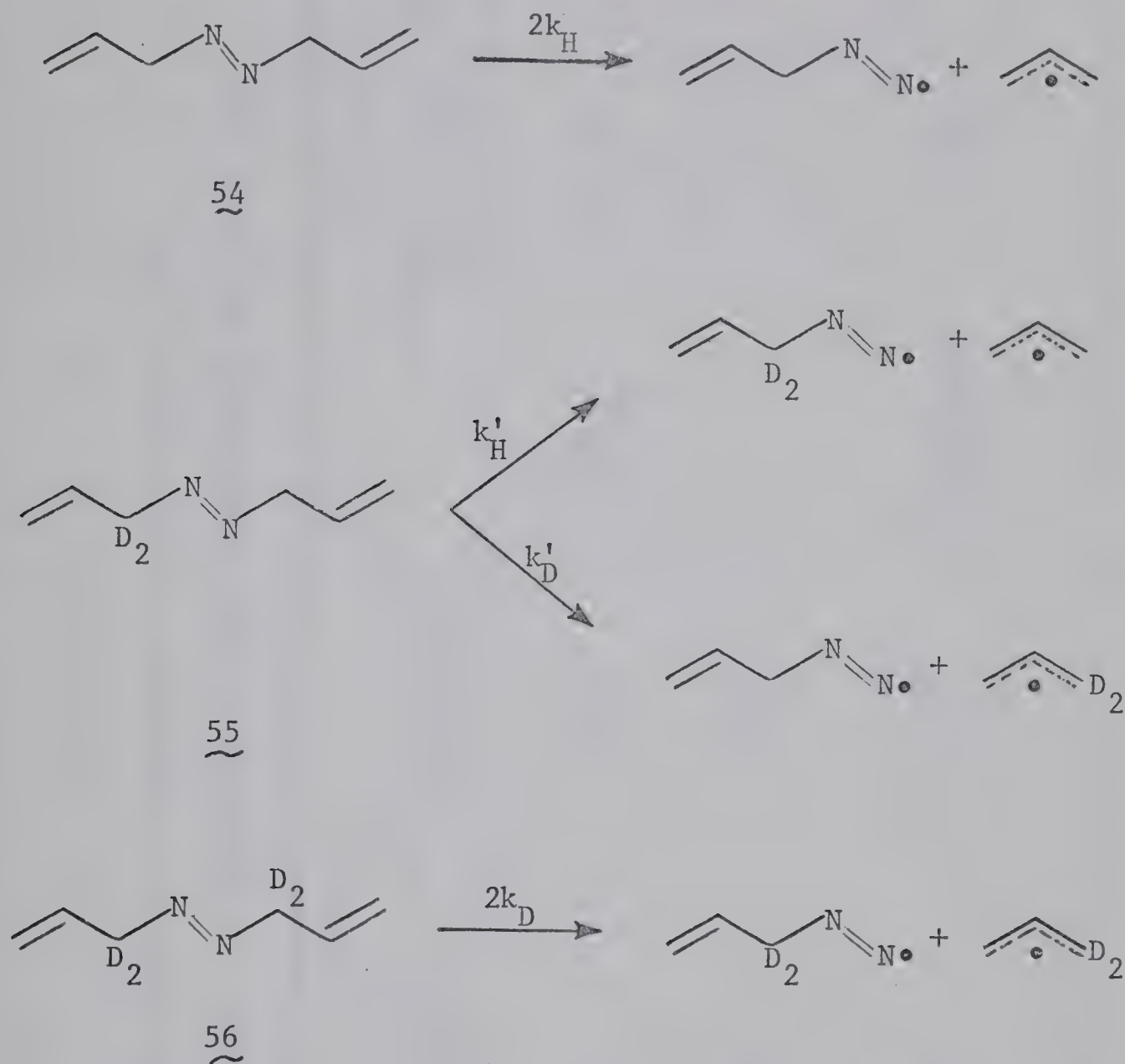
Scheme X





listed in Table XVI.

If however, the mechanism is that analogous to Scheme XI, wherein only one carbon-nitrogen bond is undergoing cleavage



Scheme XI

in the rate-determining step and the magnitude of the kinetic isotope effect for two deuteriums is that given by  $k_{54}/k_{56}$ , then assuming that  $k'_H = k_H$  and  $k'_D = k_D$  we predict the values for  $k_{54}/k_{55}$  and  $k_{55}/k_{56}$ , respectively, by the relationships in Table XVI. The predicted values for those cases wherein  $k_{54}/k_{56}$  is observed to



T A B L E X V I

The predicted  $\alpha$ -deuterium isotope effects in the  
thermolysis of  $\alpha$ -deuterated azo-bis-3-propenes 55 and 56 at 150°C

Ratio of rate constants	Scheme X		Scheme XI	
	$\Delta G^\ddagger = 89 \text{ cal}^{-1} \text{ mole}^{-1}$ per deuterium	$\Delta G^\ddagger = 114 \text{ cal}^{-1} \text{ mole}^{-1}$ per deuterium	$\Delta G^\ddagger = 89 \text{ cal}^{-1} \text{ mole}^{-1}$ per deuterium	$\Delta G^\ddagger = 114 \text{ cal}^{-1} \text{ mole}^{-1}$ per deuterium
$\frac{k_{54}}{k_{55}}$	1.235	1.310	$\frac{2k_{54}}{k_{54}+k_{56}}$	1.21 1.26
$\frac{k_{54}}{k_{56}}$	1.525	1.717		
$\frac{k_{55}}{k_{56}}$	1.235	1.310	$1/2(k_{54}/k_{56}+1)$	1.26 1.36



be 1.525 and 1.717 are listed in Table XVI. It is to be noted that in the concerted symmetrical cleavage process that  $k_{54}/k_{55}$  has the same value as  $k_{55}/k_{56}$  and that  $k_{54}/k_{56}$  is simply the square of this value. For the one bond cleavage scheme the value of  $k_{55}/k_{56}$  is simply the median value between unity and  $k_{54}/k_{56}$ . The larger the value of  $k_H/k_D$  observed the larger the difference between the values of  $k_{55}/k_{56}$  predicted by the two mechanisms.

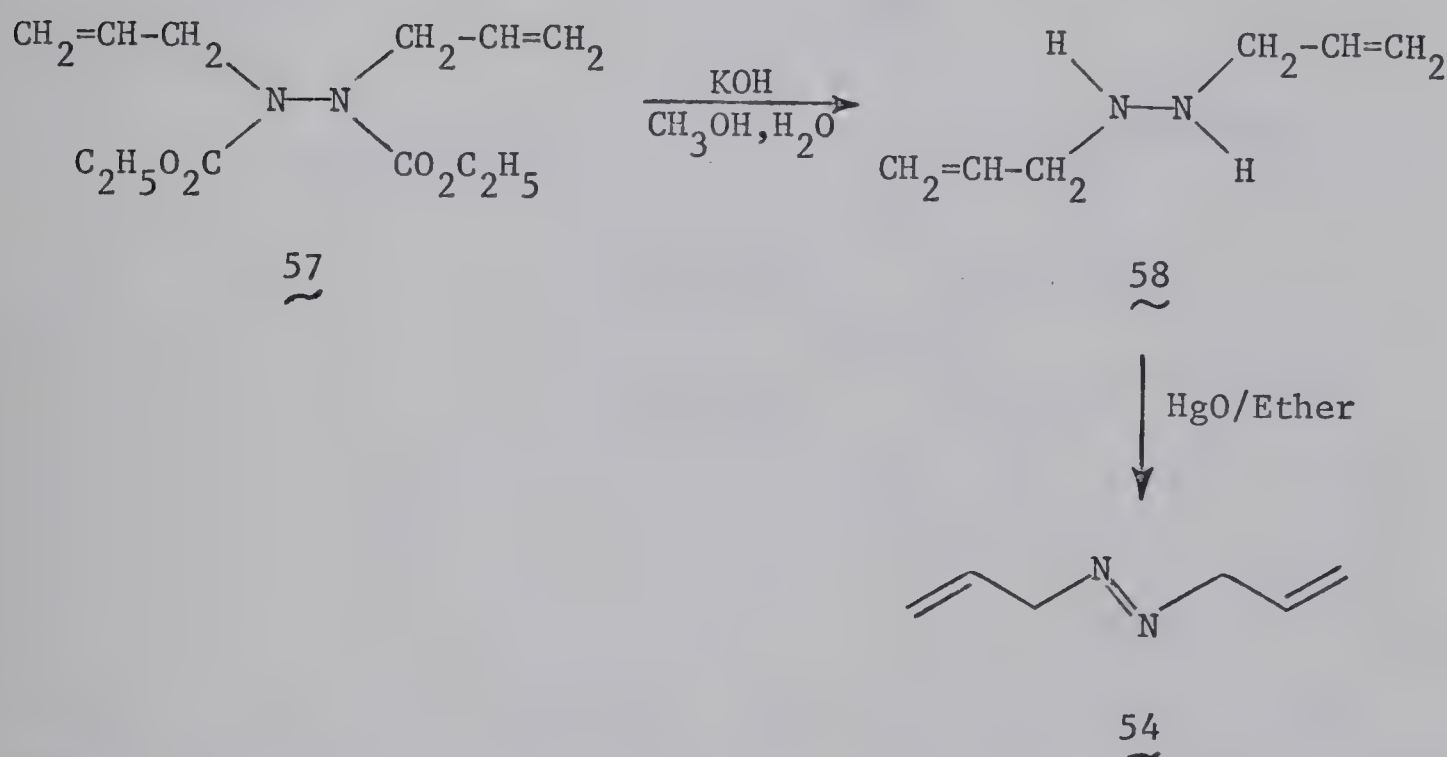




## R E S U L T S

(A) Synthesis

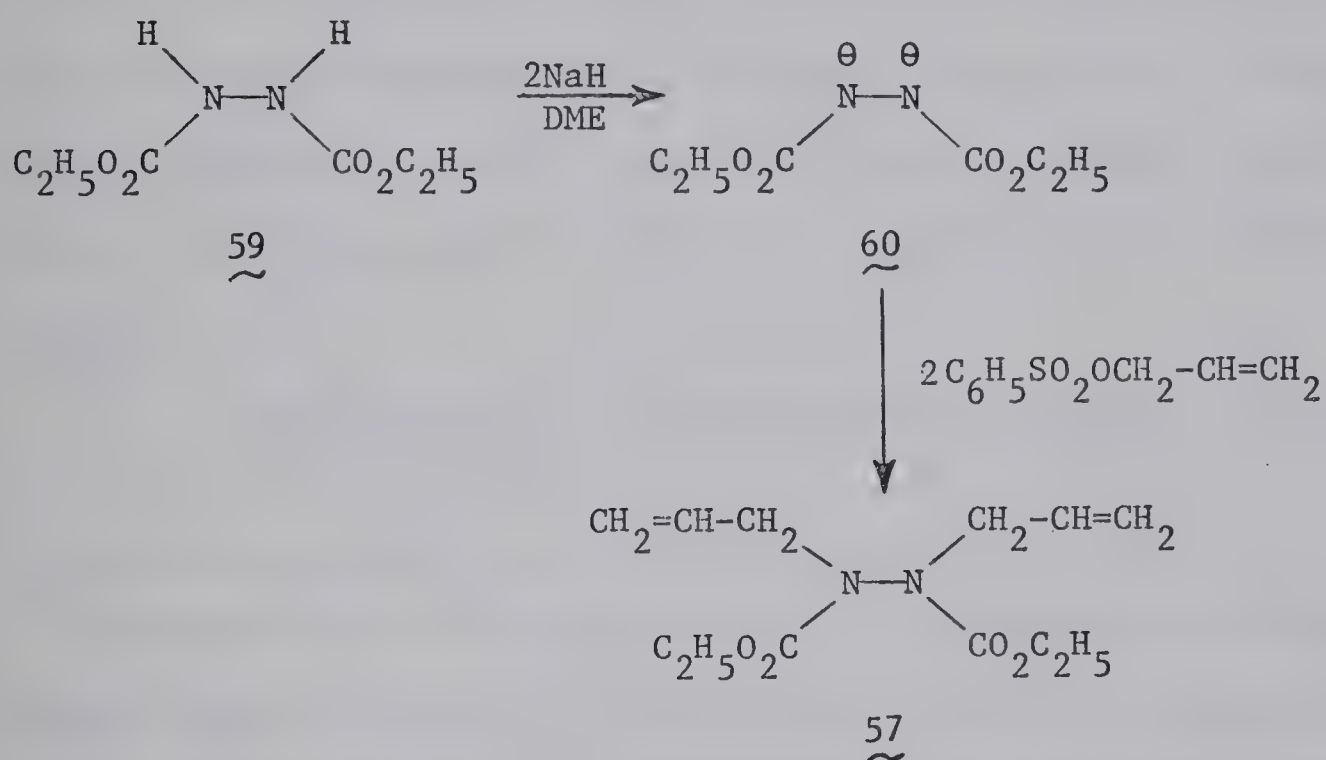
The synthesis of azo-bis-3-propene (54) was achieved by the mercuric oxide oxidation of the corresponding hydrazine (58) which in turn was obtained from the hydrolysis (96) of diethyl-N,N'-diallylbicarbamate (57) with an aqueous solution of potassium hydroxide in methanol.



Diethyl-N,N'-diallylbicarbamate (57) was reported by Zweig and Hoffmann(85) in 1963. They prepared the compound 57 from the reaction of allyl bromide with the dianion(60) of diethyl azodicarboxylate, generated by the reaction of potassium metal with diethyl azodicarboxylate in dry DME(1,2-dimethoxyethane). However, this procedure was not followed due to the low yield (40%)



and the difficulty of preparing a monoallyl derivative needed for subsequent preparations. Instead, the dianion (60) was generated from the addition of sodium hydride to a solution of DEHD (diethyl hydrazodicarboxylate) (59) in dry DME. The dianion (60) solution was then allowed to react with allyl benzenesulfonate in DME under a nitrogen atmosphere; the yield of 57 was 83%.



The nmr spectrum of 57 (Figure 12) displayed signals for the methine (multiplet  $\sim 4.2\tau$ ), vinylidine (multiplet  $\sim 4.9\tau$ ), allyl and methylene (overlapping doublet and quartet  $\sim 6.0\tau$ ), and methyl (triplet centered at  $8.8\tau$ ) protons with integration values of 1.00:2.02:3.98:3.01; calcd. 1:2:4:3.

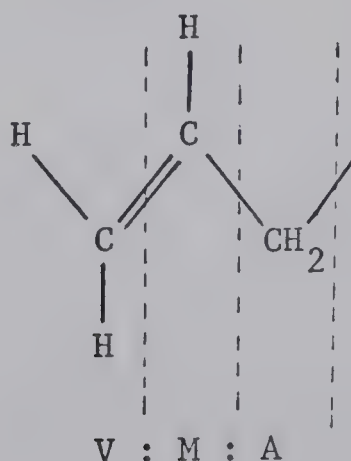


The structure of 54 was established in the following manner. Microanalysis was found to be consistent with the formula  $C_6H_{10}N_2$ . In the mass spectrum the molecular ion has a mass of 110 which is also consistent with the formula  $C_6H_{10}N_2$ . The ultraviolet spectrum shows  $\lambda_{\text{max}}$  at 358 nm ( $\epsilon = 24$  in methanol). The infrared spectrum (Figure 13) has no absorption above  $3100\text{ cm}^{-1}$ , characteristic of nitrogen-hydrogen bonds. The nmr spectrum\* (Figure 14) shows signals corresponding to vinylidine (multiplet at  $\sim 5.48\tau$ ), methine (multiplet  $\sim 4.57\tau$ ), and allyl (doublet at  $6.28\tau$ ), protons with a V:M:A ratio of 2.01:1.00:1.99 as expected for compound 54, calcd. 2:1:2.

The synthesis of 3-propenyl-azo-3'-propene-3',3'-d<sub>2</sub> (55)

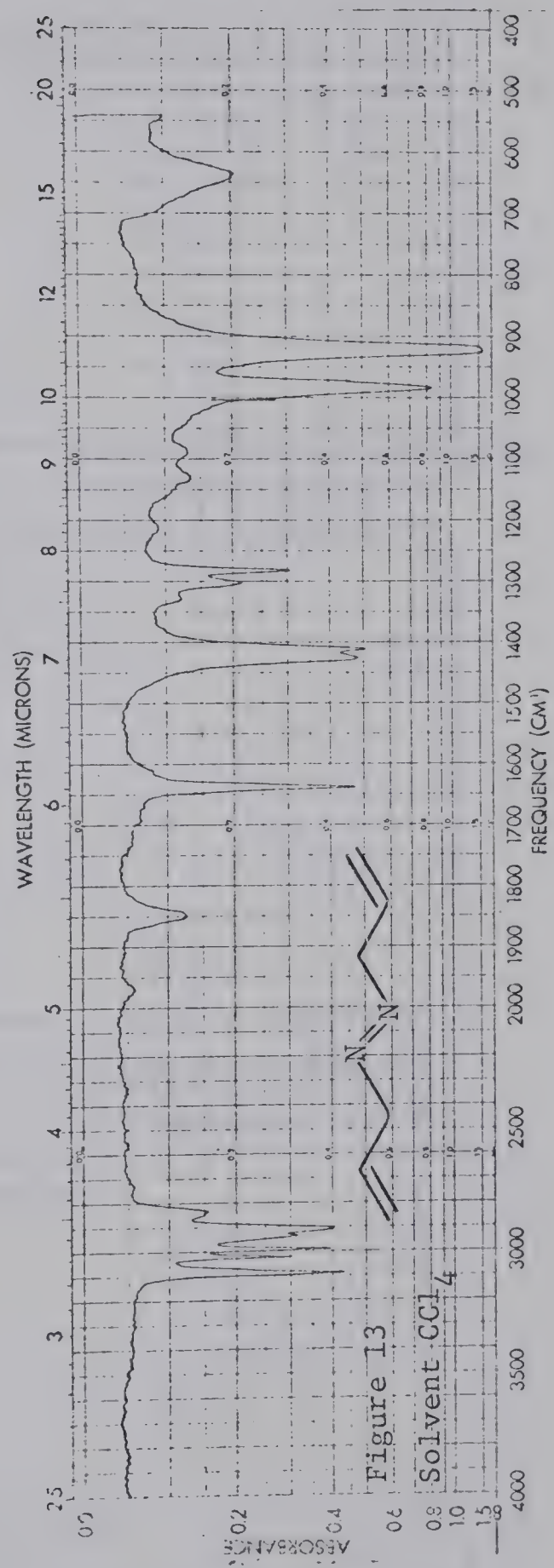
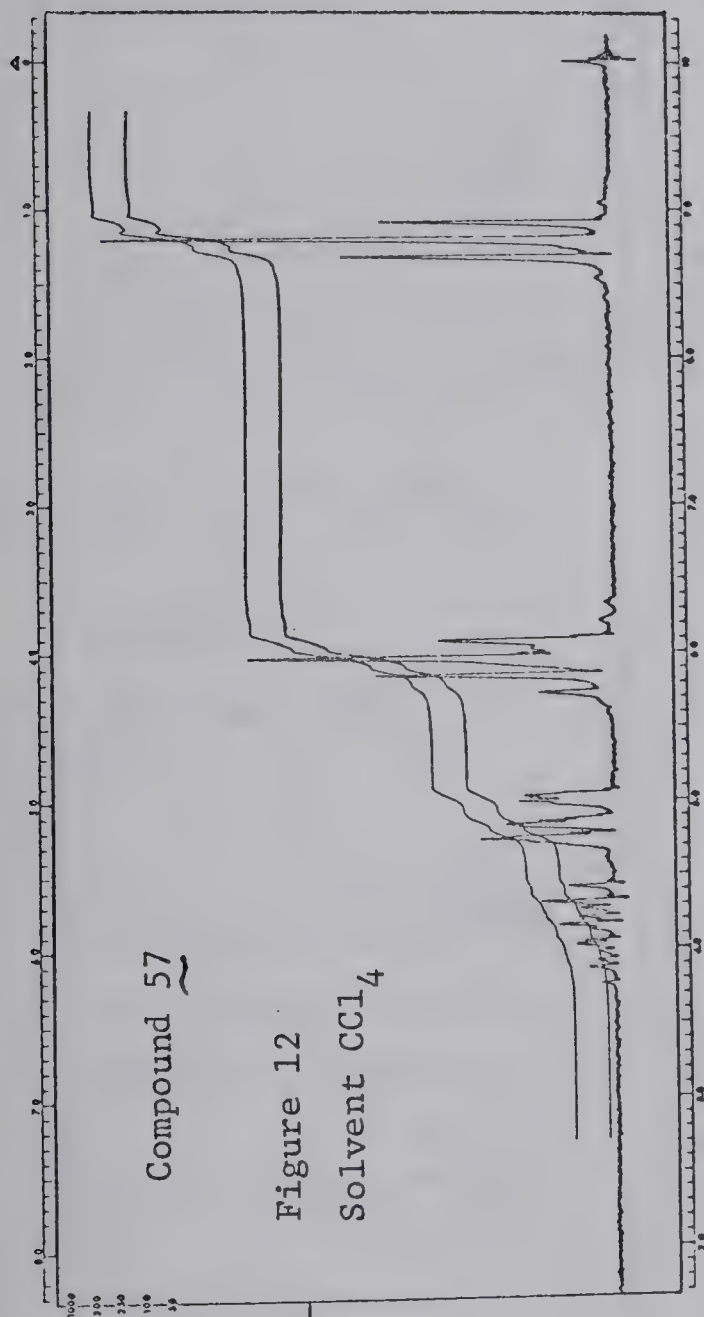
---

\* Throughout this thesis the protons of the terminal methylene groups shall be referred to as vinylidine protons (V) that proton on  $C_2$  will be referred to as the methine proton (M) and the tetrahedral set as the allylic protons (A), and the integration ratios of their nmr spectra will be consistently quoted in the following order:



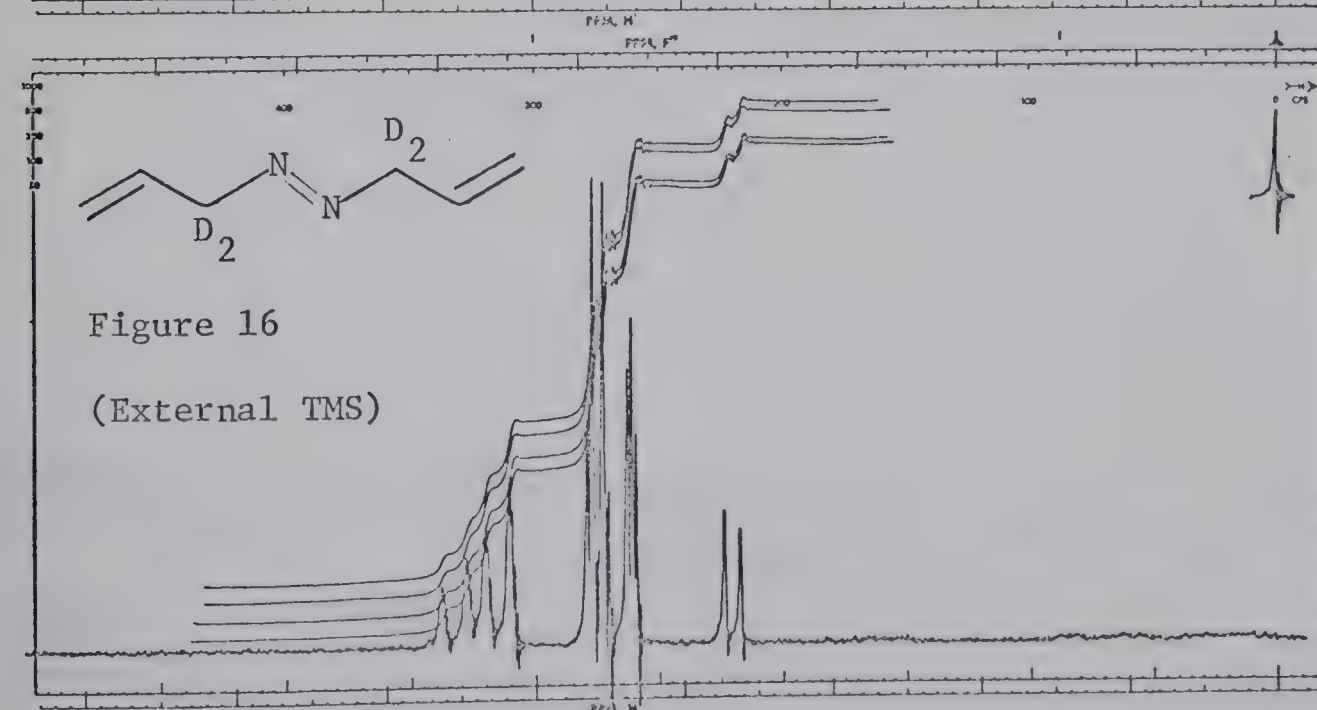
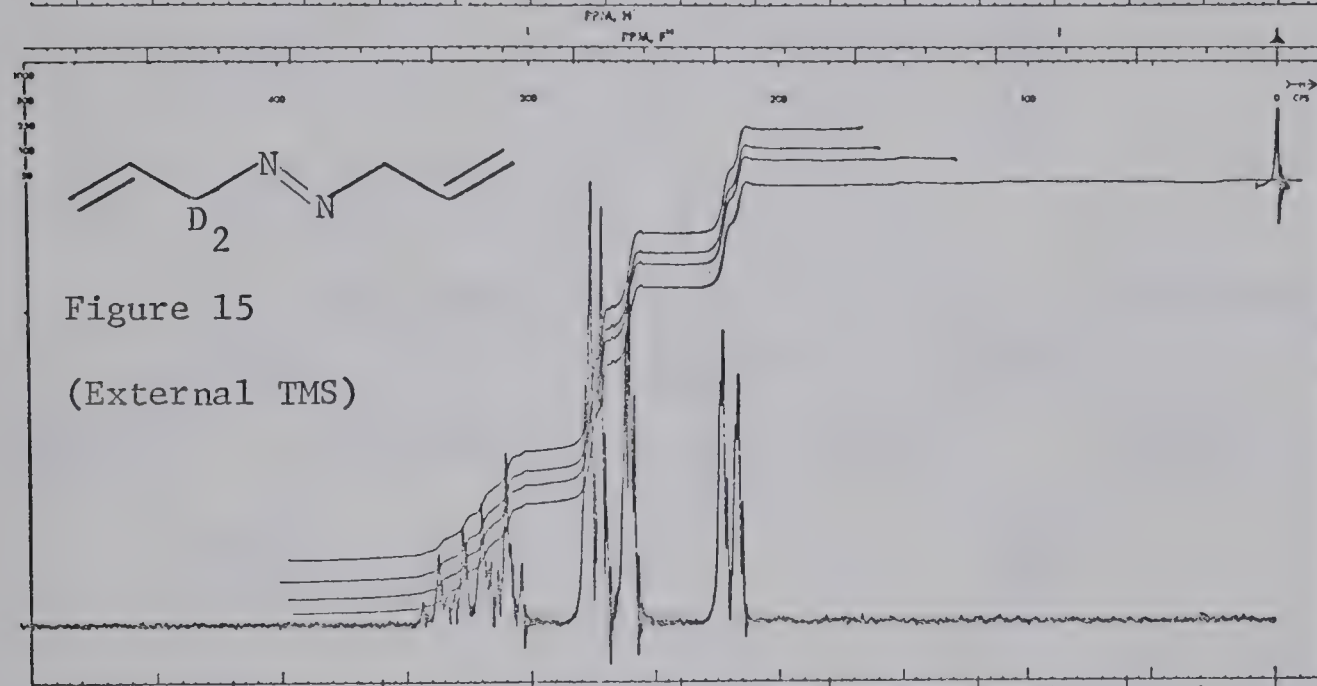
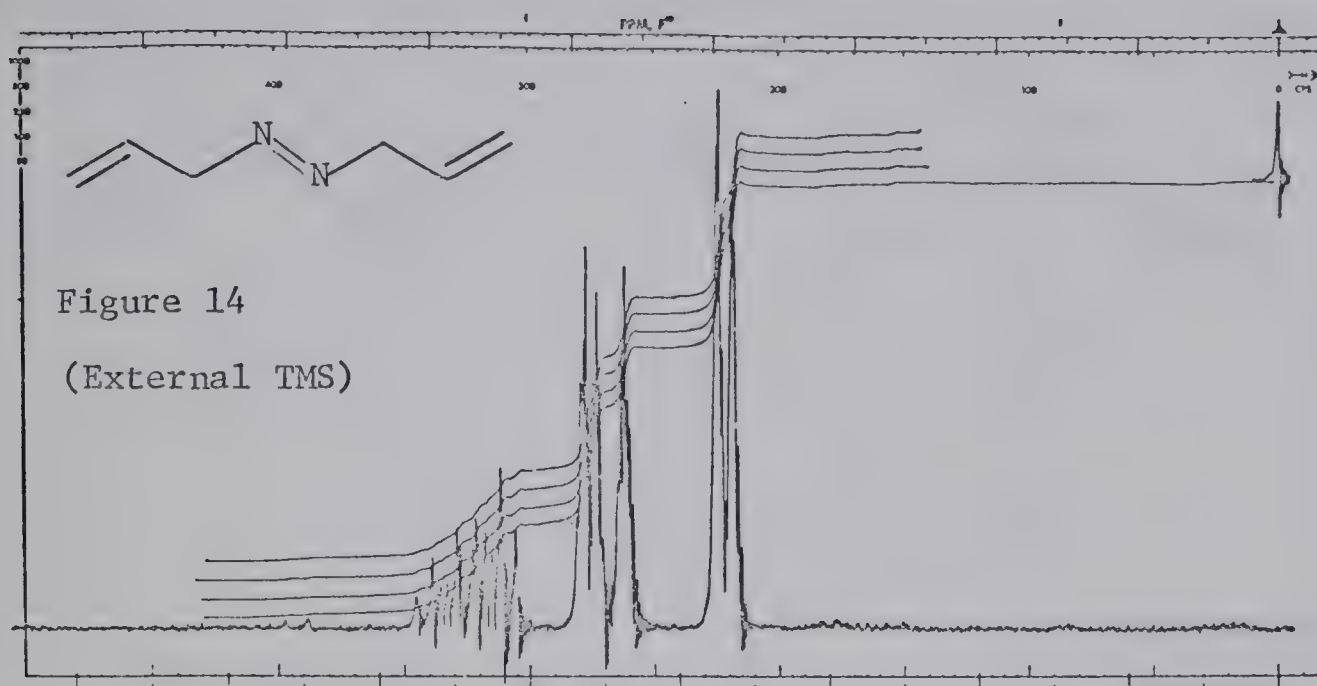






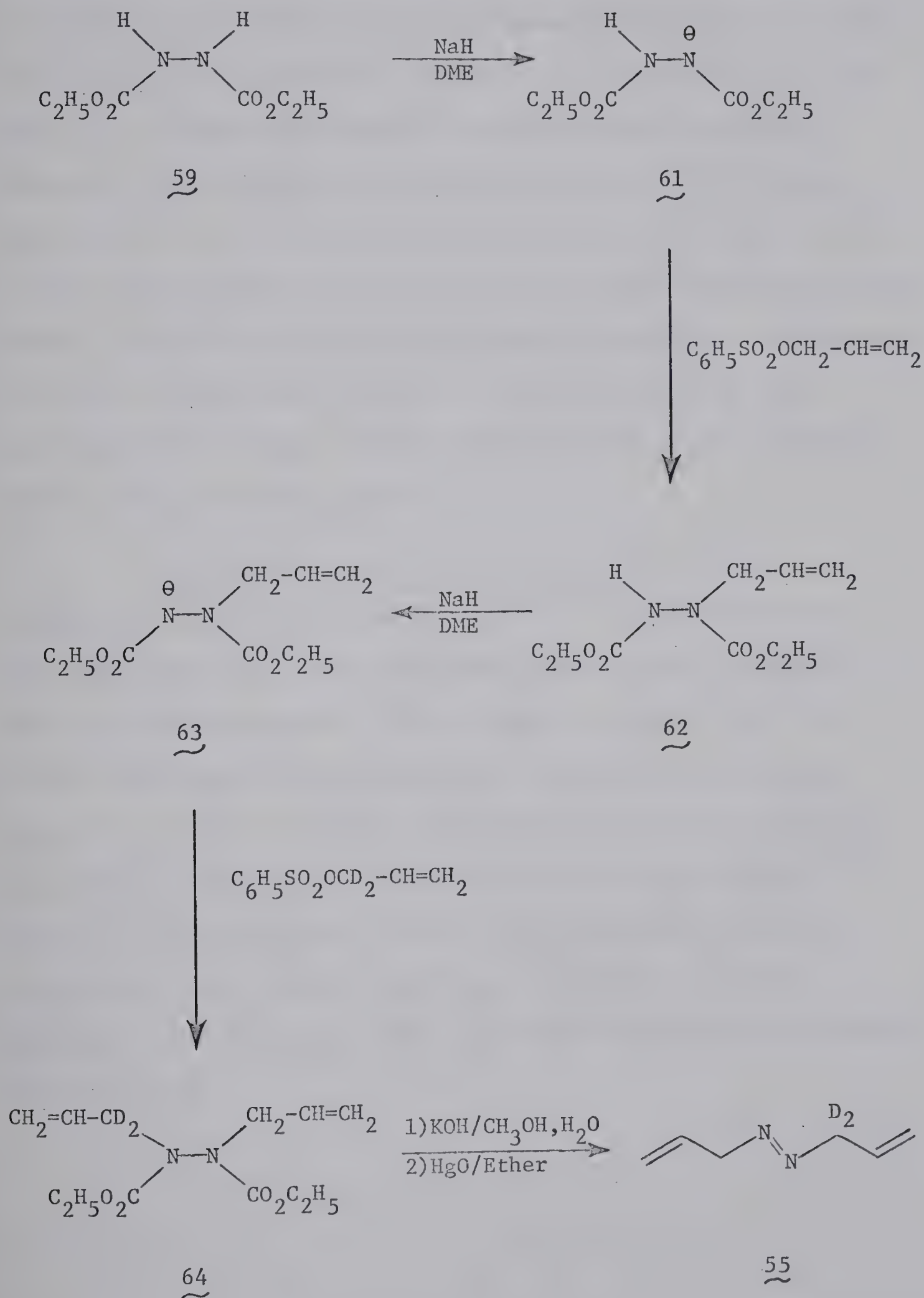








was accomplished in the following manner.



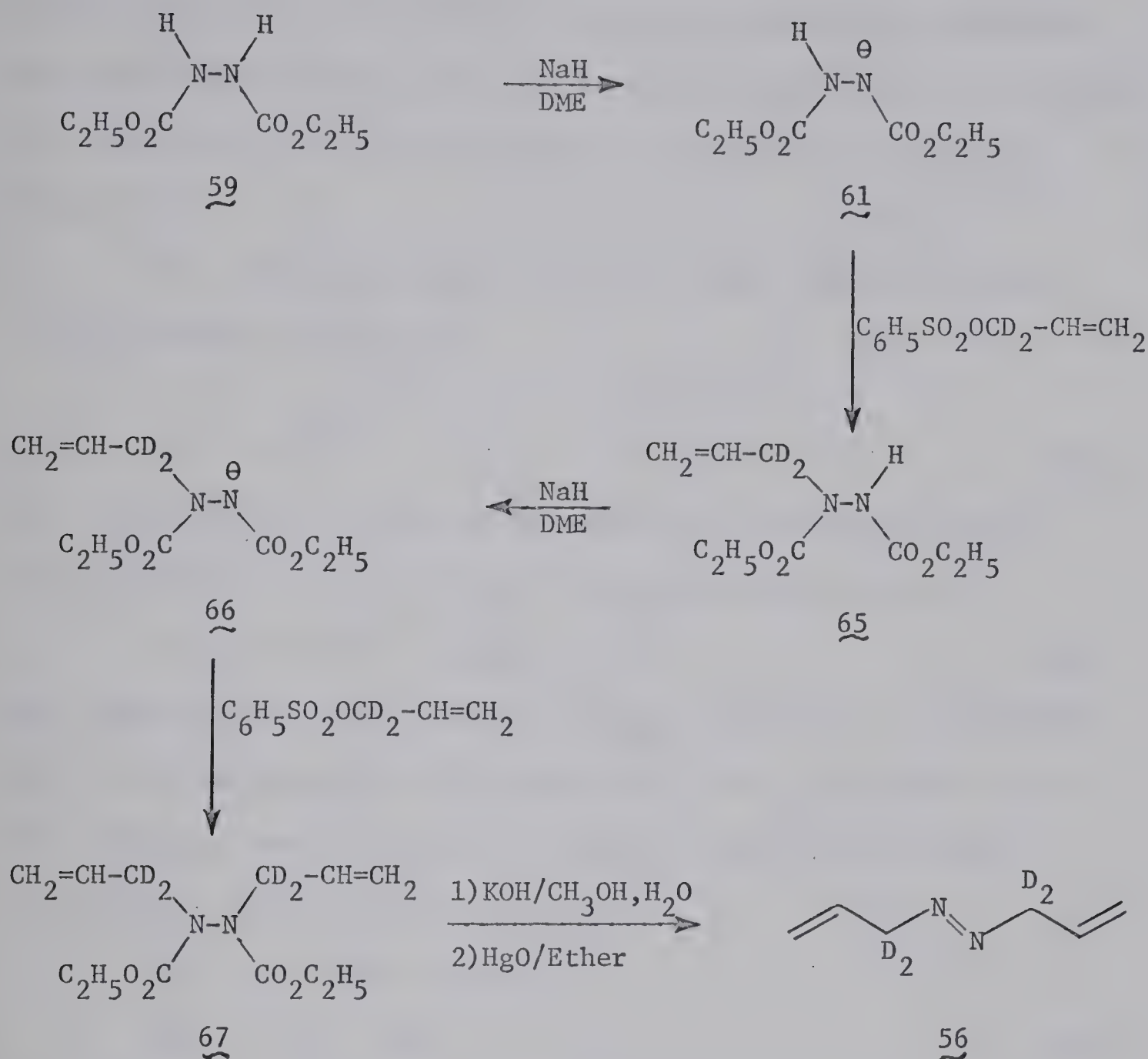


Special precaution was taken to minimize the probability of diallyl 57 formation during the monoallyl 62 synthesis. The crude monoallyl compound 62 was subjected to a careful fractional distillation, by means of a spinning band column, to separate the pure monoallyl compound 62 from traces of the diallyl compound 57. This further purification was a necessary step so as to ensure the absence of any diallyl compound 57 as a source of azo-bis-3-propene (54) in the final product. The nmr spectrum for 55 is shown in Figure 15. Integration of the nmr spectrum gave a V:M:A ratio of 2.02:1.00:0.98. This indicates that deuterium scrambling did not occur to any appreciable extent to the vinylidine position.

The synthesis of azo-bis-3-propene-3,3-d<sub>2</sub> (56) was accomplished in the same manner described for the preparation of 54, except that allyl- $\alpha,\alpha$ -d<sub>2</sub> benzenesulfonate was used instead of the allyl benzenesulfonate. The nmr analysis revealed that 14.5% of the total deuterium was scrambled to the vinylidine position during the reaction. To avoid this scrambling we tried to prepare the diallyl compound 67 by introducing the  $\alpha$ -deuterated allyl groups in a stepwise manner similar to the method used for the preparation of the diallyl compound 64. Hydrolysis of 67 and subsequent oxidation of the hydrazine formed furnished the deuterated azo compound 56.







The nmr spectrum of compound 56 is shown in Figure 16. The allylic protons signal at  $\tau$  6.28 has not completely disappeared and the integration gave a V:M:A ratio of 1.77:1.00:0.275. This ratio indicates that 13.9 % of deuterium also underwent scrambling by this method of preparation.

#### (B) Kinetic Studies

The thermolysis of 54 was carried out in the same reactor as that used for the thermolysis studies in Chapter I. The kinetic



studies were done at six different temperatures, and rate constants were evaluated from the slopes of the plots of  $\text{Log } (E_{\infty} - E_t)$  vs. time. The linearity of the plot confirms the good first order behavior (Figure 17).

The effect of temperature on the rate constant is given by the Arrhenius equation 32,

$$k = A e^{-E_a/RT} \quad (32),$$

where  $E_a$  is the activation energy and  $A$  is the frequency factor.

Equation 32 can also be expressed in the logarithmic form 33.

$$\text{Log } k = \text{Log } A - \frac{E_a}{2.303R} \times \frac{1}{T} \quad (33).$$

Thus, plotting  $\log k$  vs.  $\frac{1}{T}$  gives  $-\frac{E_a}{2.303R}$  as the slope, from which the activation energy  $E_a$  can be obtained. Once  $E_a$  was found,  $\log A$  was calculated from equation 33. However, both parameters were calculated by the least squares method.

For a gas phase reaction

$$\Delta H^{\ddagger} = E_a - nRT \quad (34),$$

where  $\Delta H^{\ddagger}$  is the enthalpy of activation and  $n$  is the order of the reaction (59). For a first order reaction, equation 34 becomes

$$\Delta H^{\ddagger} = E_a - RT \quad (35).$$

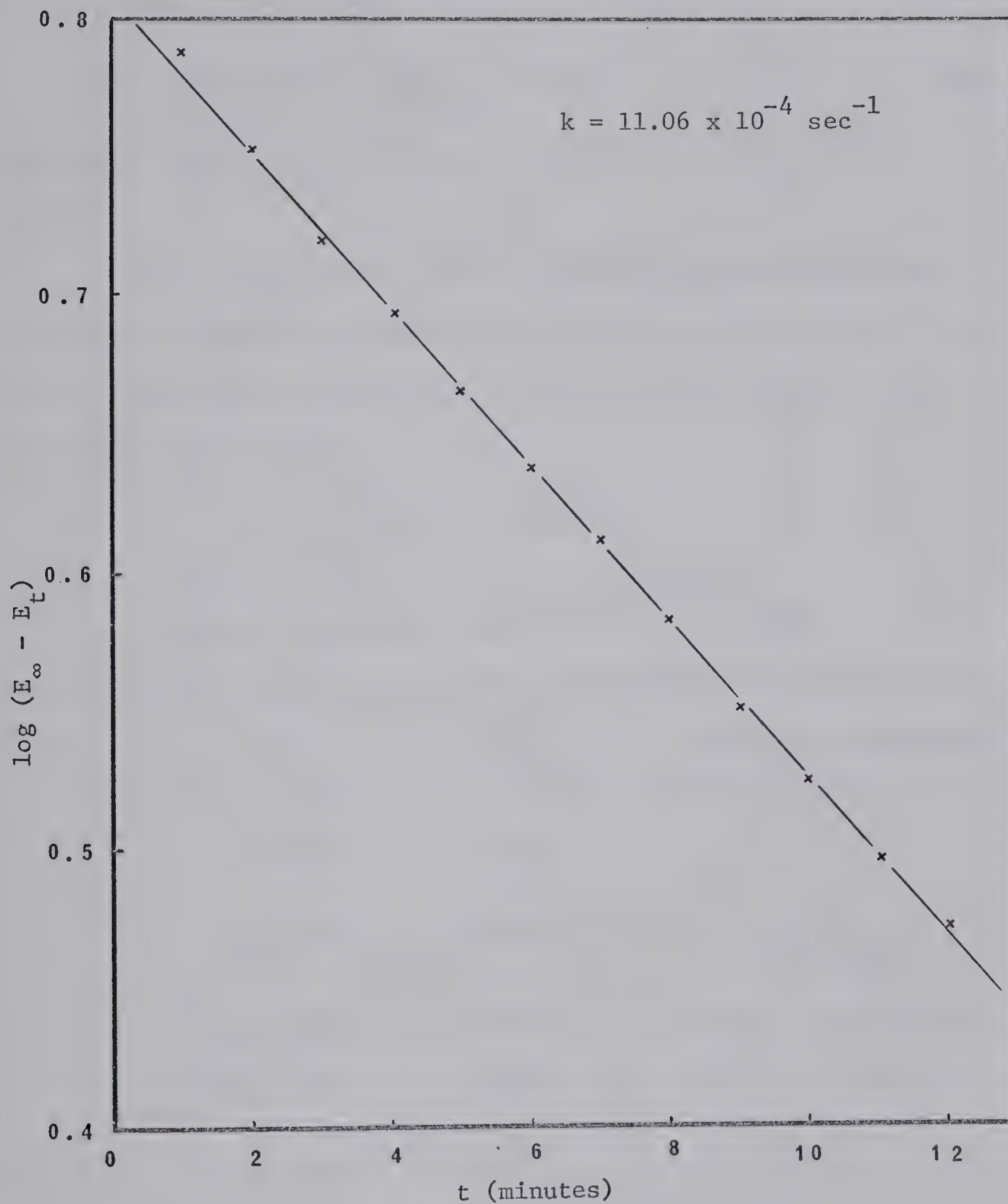
From the transition state theory (59)

$$k = \frac{k'T}{h} \times e^{-\Delta H^{\ddagger}/RT} \times e^{-\Delta S^{\ddagger}/R} \quad (36),$$

where  $k'$ ,  $h$ , and  $T$  are defined as before, and  $\Delta H^{\ddagger}$  and  $\Delta S^{\ddagger}$  are the enthalpy and entropy of activation, respectively. Combining equations 32, 35, and 36 gives an expression for  $\Delta S^{\ddagger}$ ,



Figure 17



Plot of  $\log(E_{\infty} - E_t)$  vs.  $t$  for the  
thermolysis of azo-bis-3-propene at  $152.69^{\circ}$



$$\Delta S^\ddagger = R \ln \frac{Ah}{k'T_e} \quad (37),$$

$$\text{or } \Delta S^\ddagger = 2.303R [\text{Log } \frac{h}{k'T_e} + \text{Log } A] \quad (38).$$

Equation 38 was used to calculate the entropy of activation at 150.0°C.

The rate constants and the activation parameters of the thermolysis of azo-bis-3-propene (54) are given in Table XVII. Data for the least squares calculation (88) of the activation parameters are shown in Table XVIII.

T A B L E X V I I

Rate constants and activation parameters  
for the thermolysis of azo-bis-3-propene (54)

Run No.	T°C	$k \times 10^4$ (sec <sup>-1</sup> )	Activation parameters
1	142.650	3.88	
2	152.687	11.06	$E_a = 36.06 \pm 0.16$ kcal/mole
3	158.812	19.92	Log A = 15.54 ± 0.08
4	161.650	25.90	$\Delta S^\ddagger = +9.88 \pm 0.36$ e.u.
5	161.750	26.2	
6	167.125	44.55	





T A B L E X V I I I

Least squares calculation of the activation parameters

for the thermolysis of azo-bis-3-propene (54)

Run no.	y (Log <sub>10</sub> <sup>k</sup> )	x (1000/T)	x <sup>2</sup>	xy	y-a-bx	(y-a-bx) <sup>2</sup> x 10 <sup>8</sup>
1	-3.4112	2.4049	5.783544	-8.203594	+0.0003	9
2	-2.9562	2.3482	5.514043	-6.941748	-0.0079	6084
3	-2.7007	2.3149	5.358762	-6.251850	-0.0010	100
4	-2.5867	2.2998	5.289080	-5.948892	+0.004	1600
5	-2.5817	2.2993	5.286780	-5.936102	+0.003	900
6	-2.3511	2.2712	5.158349	-5.339818	-0.0062	3844

$$\Sigma y = -16.5876; \quad \Sigma x = 13.9383; \quad \Sigma x^2 = 32.390558; \quad \Sigma xy = -38.622004; \quad \Sigma x \Sigma y = -231.202945;$$

$$(\Sigma x)^2 = 194.276207; \quad \Sigma (y-a-bx)^2 = 12537 \times 10^{-8}$$



From the data in Table XVIII,

$$y = bx + a$$

$$\text{Log } k = \frac{-E_a}{2.303 \times R \times 1000} \frac{1000}{T} + \text{Log } A$$

$$\frac{-E_a}{2.303R} = b = \frac{n\sum(xy) - \sum x\sum y}{n\sum x^2 - (\sum x)^2}$$

$$= \frac{6(-38.622004) - 231.202945}{6(32.390558) - 194.276207}$$

$$= -7.880118$$

$$E_a = 7.880118 \times 2.303 \times 1.987$$

$$= 36.06 \text{ kcal}$$

$$\text{Log } A = a = \frac{\sum x^2 \sum y - \sum x \sum xy}{n\sum x^2 - (\sum x)^2}$$

$$= \frac{(32.390558)(-16.5876) - (13.9383)(-38.622004)}{0.067141}$$

$$= 15.54$$

The Arrhenius equation for thermolysis of 54 therefore becomes

$$k = 10^{15.54} e^{(-36.06/RT)}$$

$$\Delta S_{150.0}^\ddagger = 2.303 R \text{ Log } \frac{Ah}{k'T_e}$$

$$= 4.576 (\text{Log } A - 10.3201 - 2.6265 - 0.4343)$$

$$= 4.576 (15.54 - 13.3809)$$

$$= 9.88 \text{ e.u.}$$

The probable error in the slope (60) ( $P_b$ ) is given by

$$P_b = P_y \sqrt{\frac{n}{n\sum x^2 - (\sum x)^2}}$$



where  $P_y$  is the probable error of the residuals.

$$P_y = 0.6745 \sqrt{\frac{\sum (y - bx - a)^2}{n - 2}}$$

$$P_y = 0.6745 \sqrt{\frac{12537 \times 10^{-8}}{4}}$$

$$= 0.00376$$

$$P_b = 0.03555$$

The error in the activation energy  $E_a$  in kcal/mole can now be calculated.

$$\text{Error} = P_b \times 2.303 \times 1.987 = 0.162 \text{ kcal}$$

$$E_a = 36.06 \pm 0.16 \text{ kcal.mole}$$

The probable error of the intercept (60) ( $P_a$ ) is given by

$$P_a = P_y \sqrt{\frac{\sum x^2}{n \sum x^2 - (\sum x)^2}}$$

$$= 0.00376 \sqrt{\frac{32.390558}{0.067141}}$$

$$= 0.0825$$

$$\text{Log } A = a = 15.54 \pm 0.08$$

$$\text{and } \Delta S^\ddagger = 9.88 \pm 0.36 \text{ e.u.}$$

The rate constants and the secondary  $\alpha$ -deuterium kinetic isotope effects in the thermolysis of the deuterated azo compounds 55 and 56 are recorded in Table XIX.

The rates of thermolysis of compound 54 were determined at three different pressures. The results of these determinations are shown in Table XX. There is no dependence on pressure of the rate of decomposition as expected for a reaction following first order kinetics.





T A B L E X I X

Rate constants and secondary kinetic  
isotope effects for  $\alpha$ -deuterated azo-bis-3-propenes

Compound	T°C	$k \times 10^4$ (sec <sup>-1</sup> )	$\frac{k_H}{k_D}$
54 ~	161.65	25.94	
	161.65	25.86	
		Av. 25.90±0.05	
	161.75	26.23	
	161.75	26.17	
		Av. 26.20±0.04	
55 ~	161.65	22.69	
	161.65	22.78	
		Av. 22.76±0.06	1.14±0.004
56 ~	161.75	20.77	
	161.75	20.65	
	161.75	20.69	
		Av. 20.70±0.06*	1.26±0.004

\* Uncorrected for deuterium scrambling (see Discussion).

T A B L E X X

Rates of thermolysis of azo-bis-3-propene  
(54) at different pressures and 158.812°C

Sample's volume in µlitre	Pressure in Torr	$k \times 10^4$ (sec <sup>-1</sup> )
30	41	19.45
60	82	19.92
90	123	19.32



(C) Control Runs\*

(i) For the nmr analysis of compound 56 special attention was made to obtain high precision in integrating the spectrum. For this reason the nmr spectrometer was calibrated several times against a sample of pure azo-bis-3-propene (54) until the integration ratios were reproducible in every determination and a V:M:A ratio of 2.01:1.00:1.99 was obtained. The nmr analysis was then carried out on a sample of compound 56. The spectrometer was then rechecked by using the sample of pure azo-bis-3-propene (54) which after the averaging of three scans gave a V:M:A ratio of 2.01:1.00:1.99. Compound 56 gave a V:M:A ratio of 1.770:1.000:0.275 corresponding to 13.9% of the total deuteriums being at the vinylidine position. An aliquot was injected into the reactor for 32 minutes at 142°C, corresponding to 40% completion. The reactor was then pumped out and the reactants and products trapped on the vacuum line. The recovered azo compound was then purified by preparative gas chromatography and using the above mentioned procedure a V:M:A ratio of 1.568:1.000:0.323 was observed, corresponding to 17.1% of the deuteriums at the vinylidine position.

---

\* Product stabilities - Doering and Toscano (97) have examined the stability of 1,1,7,6-tetradeuterio-1,5-hexadiene and have found that it does not rearrange until temperatures from 250-350° have been attained. Thus our products are stable under the reaction conditions.



(ii) The mass spectral analysis of compound 55 displayed a molecular ion which has a mass of 112 consistent with  $C_6H_8D_2N_2$ , and a trace of molecular ion at a mass of 113 which corresponds to the natural abundance of  $C^{13}$  and  $N^{15}$  isotopes. The analysis displayed no molecular ions at higher masses than those indicated. The mass spectrum for compound 56 was also determined which showed a molecular ion of a mass 114 consistent with  $C_6H_6D_4N_2$ . Therefore, this method of analysis could be used to examine the possibility of compound 56 formation during the thermolysis of 55. Thus a sample of 55 was heated to 50% decomposition, the recovered sample was then submitted for mass spectral analysis. The analysis showed two molecular ions with masses of 112 and 114, which correspond to the dideuterio 55 and tetradeuterio 56 compounds. The amount of 56 produced judging from the peak intensities was about 2 to 3% of the total amount present.

(D) Product Analysis and Deuterium Labeling Studies

The quantitative yield of the products in the thermolysis of 54 was checked in the following manner. In a particular thermolysis, 65 mg of 54 was injected into the reactor at 150°C. When the thermolysis was completed, the reactor was pumped out, and the weight of the hydrocarbon products trapped from the reactor was found to be 48.7 mg (99.1% yield). Gas chromatographic analysis of this material showed it to be greater than 99.9% 1,5-hexadiene with a trace of propylene. Similar results were obtained using the

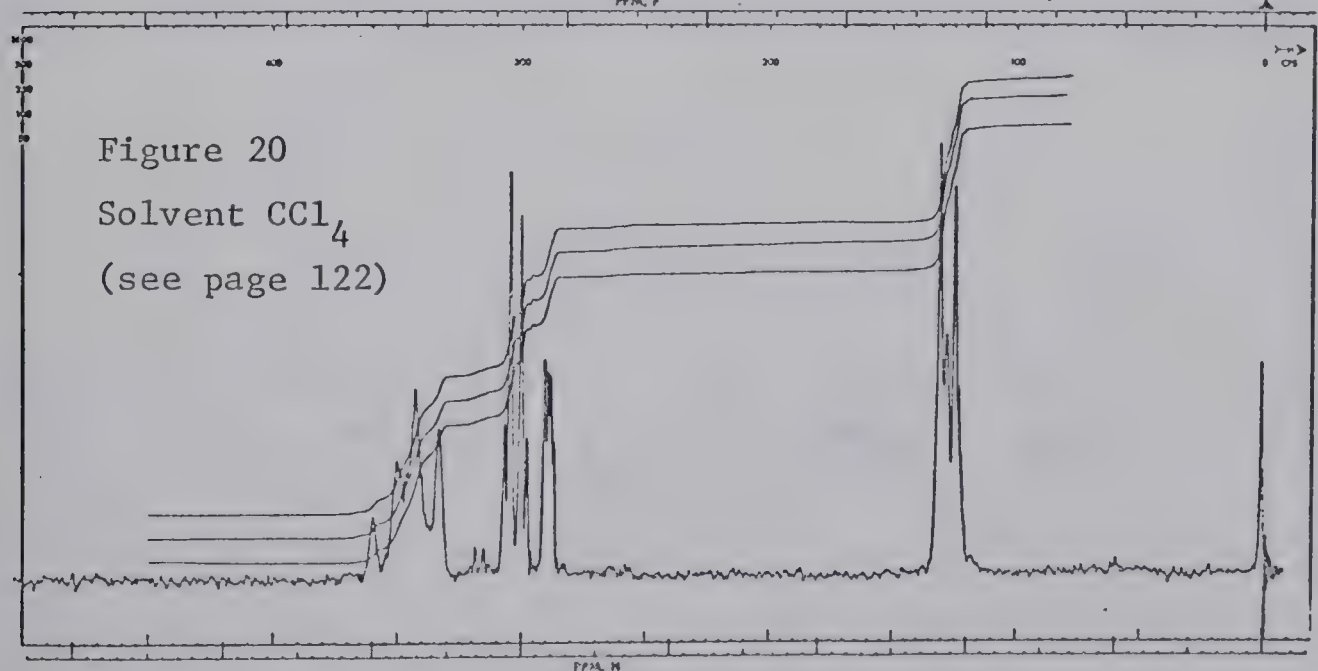
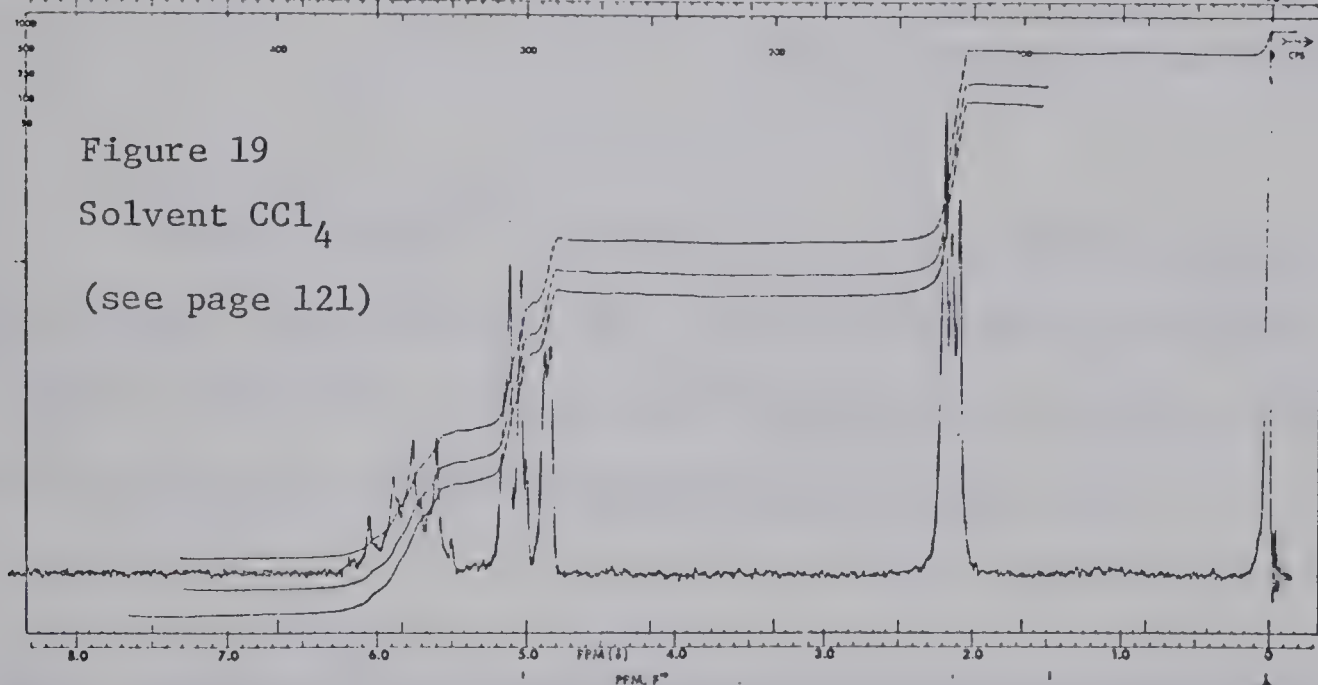
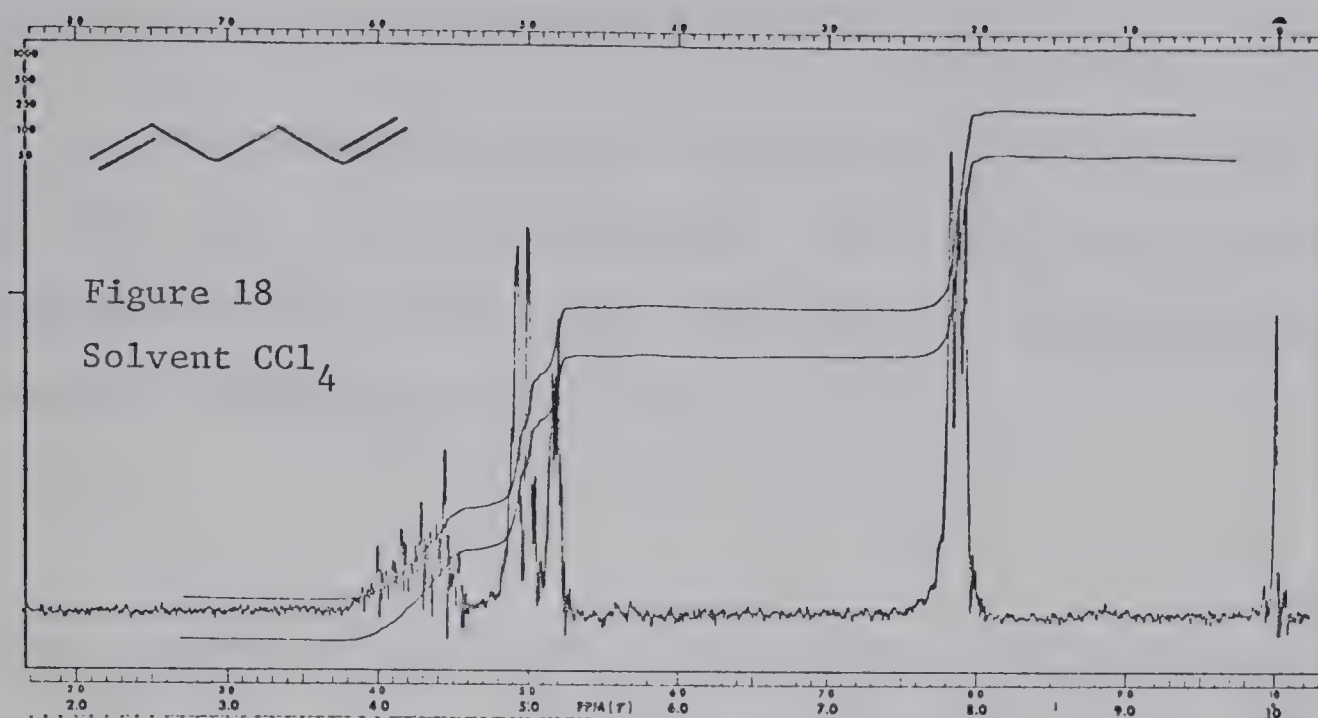




bulb-crusher technique for sample analysis. All products were identified by comparison of their retention times on three different columns with those of an authentic sample. The structure of 1,5-hexadiene was further confirmed from the comparison of its mass spectrum and nmr spectrum with those of an authentic sample. The nmr spectrum (Figure 18) displayed vinylidene (multiplet  $\sim 5.06\tau$ ), methine (multiplet at  $\sim 4.23\tau$ ), and allyl (unresolved triplet centered at  $7.88\tau$ ) protons, with a V:M:A ratio of 2.01:1.00:2.01. The nmr spectrum of the 1,5-hexadiene produced from the thermolysis of 55 is shown in Figure 19. Integration of the nmr spectrum gave a V:M:A ratio of 3.02:2.00:3.03. The nmr spectrum of the 1,5-hexadiene- $d_4$  (Figure 20), produced from the thermolysis of 56 displayed a V:M:A ratio of 1.00:1.00:1.02. The mass spectrum of the 1,5-hexadiene produced from the thermolysis of 55, displayed evidence of three molecular ions with the following masses: 82, 84, and 86 which is consistent with  $C_6H_{10}$ ,  $C_6H_8D_2$ , and  $C_6H_6D_4$  respectively. The mass spectrum of the 1,5-hexadiene produced from 56 thermolysis showed only one molecular ion which has a mass of 86, consistent with  $C_6H_6D_4$ . Quantitative data from the mass spectral results on 1,5-hexadiene were not attempted due to the complexity of the mass spectrum and its sensitivity to changes in ionization potential.



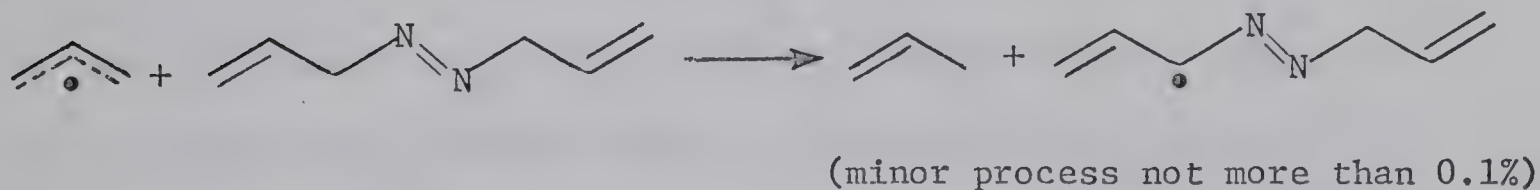




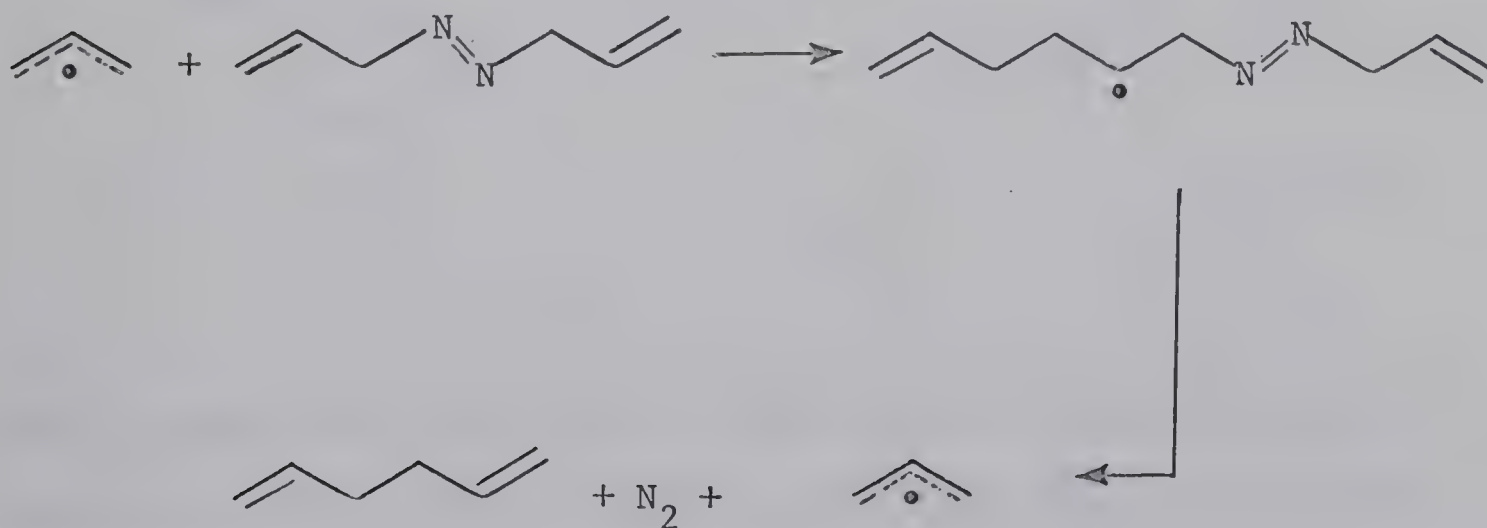


## DISCUSSION

The thermolysis of azo-bis-3-propene (54) is unique in that there is no induced decomposition. The allyl radicals produced in the thermal decomposition seem to be unable to produce propylene by hydrogen abstraction (70, 75, 78).

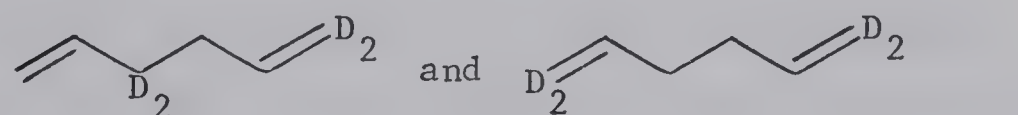


Such a reaction is believed to be the principal type of chain process responsible for the induced decomposition observed by Forst and Rice (75). The azo-bis-3-propene system however allows a different mode of induced decomposition to occur, i.e.,





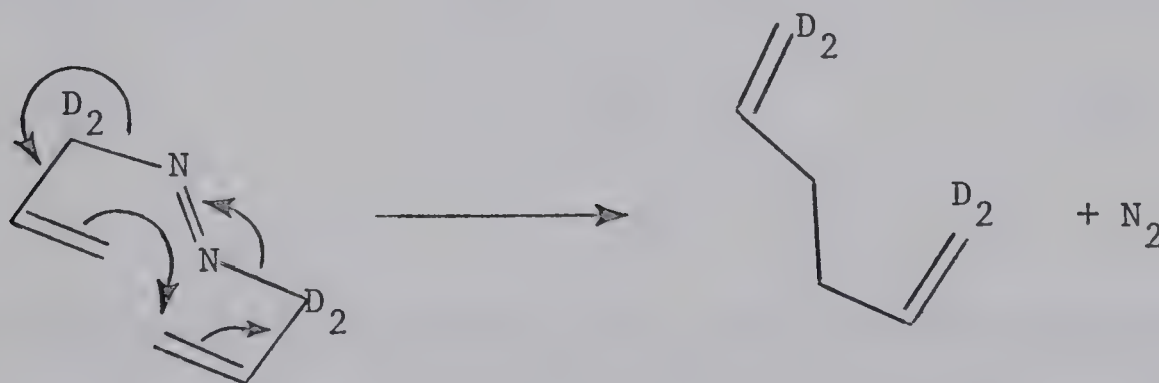
This process however can not be very important since the 1,5-hexadiene- $\underline{d}_4$  produced by such a procedure would consist of essentially equal amounts of isomers:



the nmr spectrum of which would display a V:M:A ratio of 1:2:3.

The 1,5-hexadiene- $\underline{d}_4$  produced from the thermolysis of 56 displayed a V:M:A ratio of 1.00:1.00:1.02. A similar case can be made for the products from the thermolysis of 55.

A case can also be made for a molecular reaction of the type:



Such a process would give rise to 1,5-hexadiene having all of its deuterium in the vinylidene position, and would give a V:M:A ratio of 0:2:4. That this is not operative can be seen from the values of the V:M:A ratio for the 1,5-hexadiene produced from 56 (see

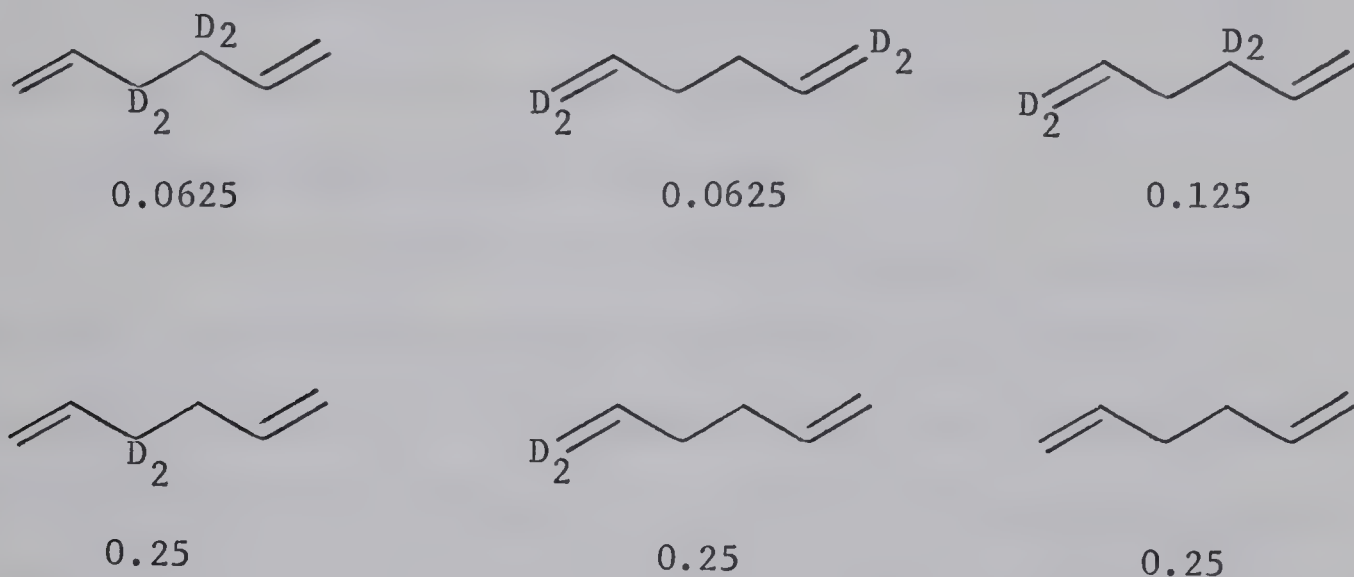




above).

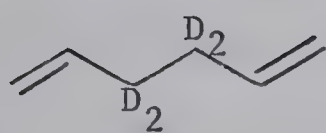
The most probable sequence then seems to be that each labelled allyl group is capable of recombining in such a way as to statistically place either the deuterium bearing end, or the protium bearing end, to the vinylidene position of the product.

If a statistical distribution of products is obtained from the thermolysis of 55 then the expected product proportions (in mole fractions) are:

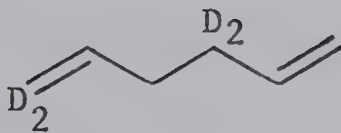


If these proportions exist then a V:M:A ratio of 3.00:2.00:3.00 is expected. The nmr spectrum for the 1,5-hexadiene produced from 55 showed a V:M:A ratio of 3.02:2.00:3.03 for the respective signals. While the 1,5-hexadiene is not readily amenable to mass spectrometry, we were able to observe a molecular ion peak corresponding to  $C_6H_6D_4$  at mass 86. The statistical distribution for the combination of allyl radicals from 56 is:

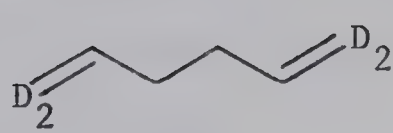




0.25



0.50



0.25

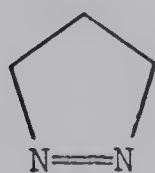
This would predict a V:M:A ratio of 1.00:1.00:1.00 for the intensities of the corresponding signals in the nmr spectrum, the experimentally observed ratio is 1.00:1.00:1.02.

The positive nature of  $\Delta S^\ddagger$ ,  $+9.88 \pm 0.36$  e.u., is such that a dissociative mechanism to produce radicals is more appropriate than an intramolecular concerted process.

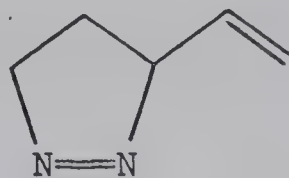
It is of particular interest to compare the activation energy for the azo-bis-3-propene (54) thermolysis ( $36.06 \pm 0.16$  kcal mole<sup>-1</sup>) with that of azomethane ( $55.5$  kcal mole<sup>-1</sup>) (75). The decrease in activation energy,  $19.4$  kcal mole<sup>-1</sup>, is attributed to a contribution from the allylic resonance energy to the rate-determining transition state. There is some doubt as to the correct value for the resonance energy of the allyl radical since theoretical (89) and early experimental results (90, 91) predict a value of 15-18 kcal mole<sup>-1</sup>. More recently Benson (92) and Frey (93) have suggested smaller values of  $13 \pm 1$  and  $12 \pm 1$  kcal mole<sup>-1</sup>. In a recent communication Golden, Gac, and Benson (94) have provided evidence for a value of the allylic resonance energy of  $9.6$  kcal mole<sup>-1</sup>, and have stated that their study of the dissociation and recombination of the 2 allyl  $\rightarrow$  1,5-hexadiene



system "must surely lay to rest any thought that the allyl resonance energy is much greater than 12 kcal mole<sup>-1</sup>." In an earlier study on the thermolysis of 3-vinyl-1-pyrazoline (11), Cameron (13) found a decrease in activation energy of 10.2 kcal mole<sup>-1</sup> upon replacing an allylic hydrogen with a vinyl group.

1

$$E_a = 42.4 \pm 0.3 \text{ kcal}$$

11

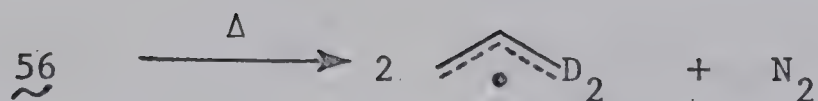
$$E_a = 32.2 \pm 0.2 \text{ kcal}$$

The decrease of activation energy, 19.4 kcal mole<sup>-1</sup>, observed on going from azomethane to azo-bis-3-propene (54) then is essentially 2 x 9.72 and implies that both allylic systems are contributing their resonance energy of stabilization to a decrease of the activation energy.

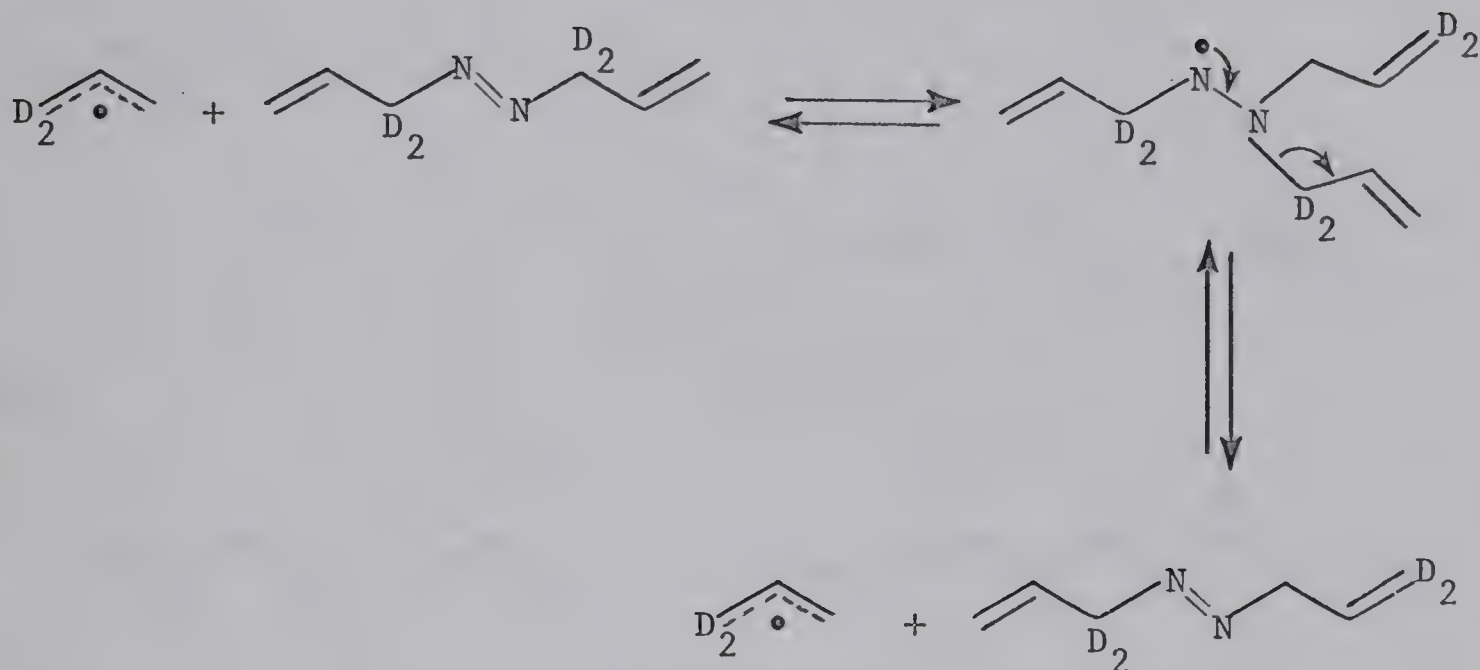
The 3% of scrambling of deuterium from the  $\alpha,\alpha$ - position to the  $\gamma,\gamma$ -position of the allyl groups during the thermolysis of azo-bis-3-propene-3,3-d<sub>2</sub> (56), as revealed from the control run, is of particular importance when discussing the mechanism of the thermolysis reaction. This observation can be rationalized in terms of the following mechanism.





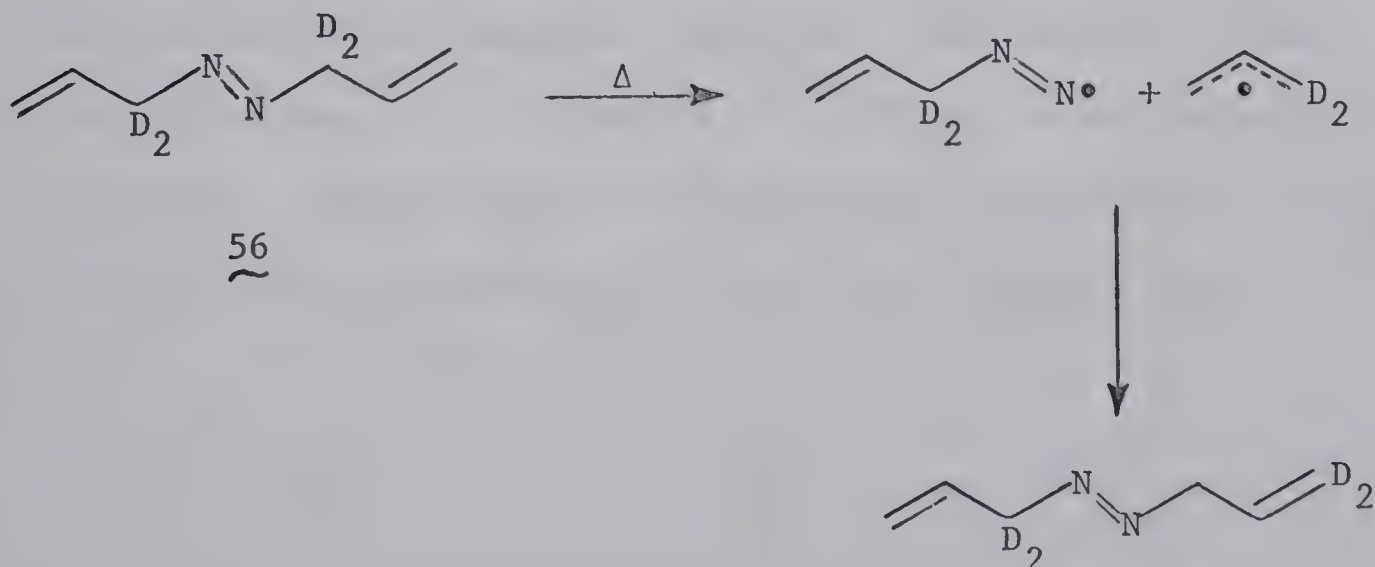


then



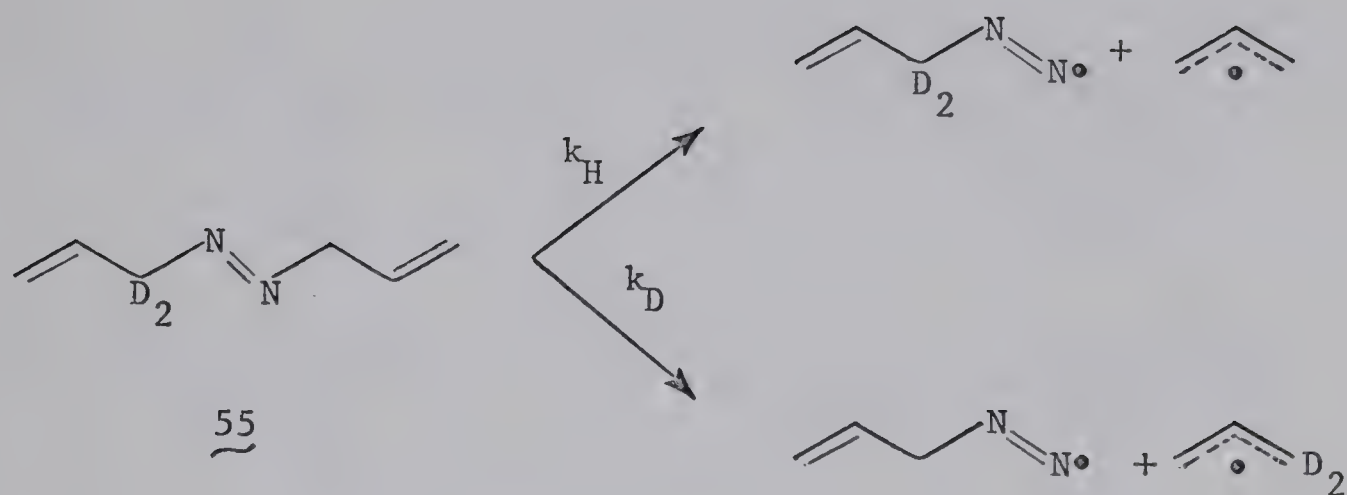
This is supported by the observation of the formation of the tetradeuterio azo compound (56) during the thermolysis of 55.

However, this evidence does not rule out the possibility of deuterium scrambling through a one-bond cleavage mechanism as shown below.

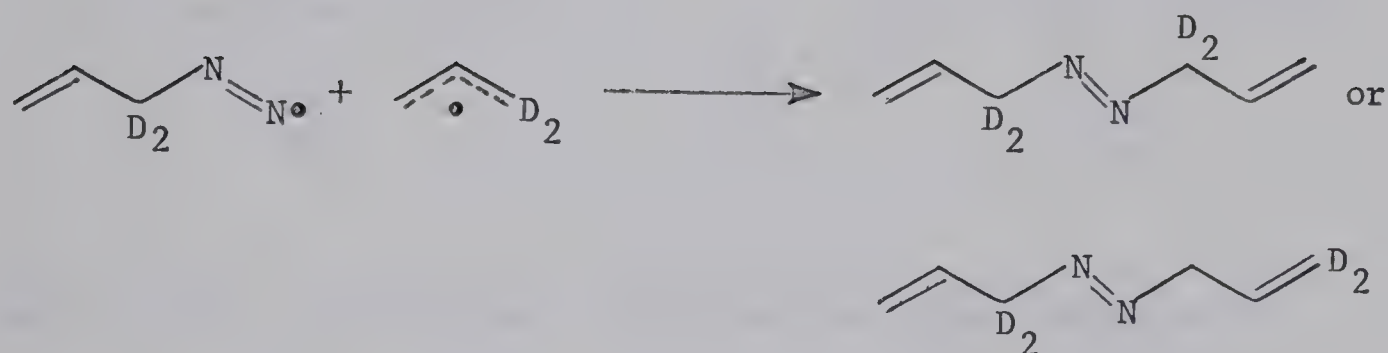






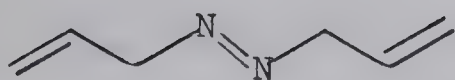
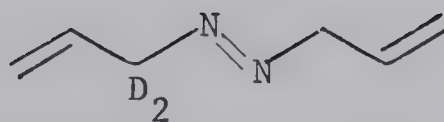
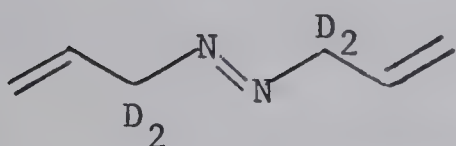
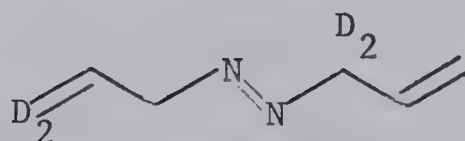
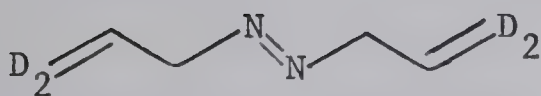
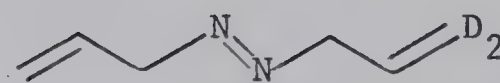


then



The observed rate constants in Table XIX require corrections for (a) the scrambling of the label during the synthesis of 56 and (b) the scrambling of the label during the reaction. The rate constants are measured from points taken between 20 and 80% completion wherein an estimated 10 to 12% of the scrambling process occurs. Thus for 55 there will be the compounds 54, 56, 68, 69, and 70 in mole fractions  $f_{54}$ ,  $f_{56}$ ,  $f_{68}$ ,  $f_{69}$  and  $f_{70}$



54  
~55  
~56  
~68  
~69  
~70  
~

respectively. If we attempt the correction using equation 39

$$k_{\text{obs}}^{55} = f_{54}k_{54} + f_{55}k_{55} + f_{56}k_{56} + f_{68}k_{68} + f_{69}k_{69} + f_{70}k_{70} \quad (39)$$

then we will require several assumptions since many of the mole fractions and rate constants cannot be observed directly. If we assume that deuteriums in the  $\gamma$ -position, as in 68, 69, and 70, give rise to no decrease in rate relative to the corresponding protio compound<sup>\*</sup>, then equation 39 becomes:

---

\* Belanic-Lipovac, Borčić and Sunko have observed a  $k_H/k_D$  value of 1.00 for the ethanolysis of 1,1-dimethylallyl chloride and 1,1-dimethylallyl-3,3-d<sub>2</sub> chloride (95).



$$k_{\text{obs}}^{55} = (f_{69} + f_{70} + f_{54})k_{54} + (f_{55} + f_{68})k_{55} + f_{56}k_{56}.$$

Judging by the values of the control run, p.115, the amount of scrambled material will be approximately 10 to 12%, of which the amount of 69 formed will be less than 1% since it requires two events. If the scrambling process is random then 54, 56, 68, and 70 will be produced in the ratio of 2:1:1:1. This allows a further simplification of the original equation to give:

$$k_{\text{obs}}^{55} = 0.08 k_{54} + 0.90 k_{55} + 0.02 k_{56} \quad (40).$$

If we now divide each component of equation 40 by  $k_{54}$  we obtain:

$$k_{\text{obs}}^{55}/k_{54} = 0.08 + 0.90 k_{55}/k_{54} + 0.02 k_{56}/k_{54}.$$

The values of  $k_{55}/k_{54}$  and  $k_{56}/k_{54}$  are related in the following manner (see p.99):

$$\left( \frac{k_{54}}{k_{55}} \right)^2 = \frac{k_{54}}{k_{56}}$$

By using the value for  $k_{\text{obs}}^{55}$  and  $k_{54}$  in Table XIX, and letting

$k_{55}/k_{54} = x$  we get the quadratic equation 41.

$$0.02 x^2 + 0.90 x - 0.799 = 0 \quad (41)$$

for which the values  $x = 0.87$  and  $-45.9$  are solutions. The former value corresponds to a kinetic isotope effect for 55 of  $k_{\text{H}}/k_{\text{D}} = 1.15$ , the latter is negative and unrealistic. If the amount of scrambled material is as high as 18% then equation 40 becomes:

$$k_{\text{obs}}^{55} = 0.12 k_{54} + 0.85 k_{55} + 0.03 k_{56}$$





and the  $k_H/k_D$  value is 1.16.

The problem of correcting the observed rate constant in Table XIX for the amount of 68 produced during the synthesis of 56 is simplified by the assumption\* that the initial reaction mixture consists of only 56 and 68 with no 69 present. This corresponds to 72.2% of 56 and 27.8% of 68, with 10 - 12% scrambling occurring during the reaction some 69 is likely to be produced. If the allyl groups are again considered to scramble in a random fashion then the average value of mole fractions of 56, 68, and 69 present are 0.66, 0.32 and 0.02 respectively. Using equation 39 and the same assumptions as those used from compound 55, we obtain the equation:

$$k_{\text{obs}}^{56} = 0.02 k_{54} + 0.32 k_{55} + 0.66 k_{56}$$

dividing this by  $k_{54}$  we obtain

$$\frac{k_{\text{obs}}^{56}}{k_{54}} = 0.02 + 0.32 \frac{k_{55}}{k_{54}} + 0.66 \frac{k_{56}}{k_{54}} \quad (42)$$

Using the value 1.15 obtained earlier for  $k_H/k_D$  we can solve equation 42. The value obtained for the  $k_H/k_D$  ratio is 1.35. If an extreme value of 18% scrambling is used the above calculations render an equation corresponding to equation 42 of

---

\* This assumption can be justified on the basis that no deuterium scrambling was observed in the second allylation step, i.e., in going from 63 to 64 in the synthesis of 55 (p.105).



$$\frac{k_{\text{obs}}^{56}}{k_{54}} = 0.06 + 0.32 \frac{k_{55}}{k_{54}} + 0.62 \frac{k_{56}}{k_{54}}$$

This gives a  $k_{\text{H}}/k_{\text{D}}$  value for 56 of 1.38. Thus we can see, Table XXI, that using values that tend to overestimate the amount of rearrangement we get values for the kinetic isotope effect of 55 and 56 that are smaller than those expected on the basis of Seltzer's work.

T A B L E X X I

Corrected isotope effects for the thermolysis of 55 and 56

% deuterium scrambling	$k_{\text{H}}/k_{\text{D}}$ <u>55</u>	$k_{\text{H}}/k_{\text{D}}$ <u>56</u>
12%	1.15	1.35
18%	1.16	1.38
$\Delta\Delta G^{\ddagger}/n \text{ cal mole}^{-1}$	60-64	65-69

It may be seen that the correction in Table XXI is significant, however we feel that the magnitude of our kinetic isotope effect measurements are meaningful. We were hoping to get precision in our measurements in the order of 1 to 2%, but because of the scrambling of deuterium the precision would not



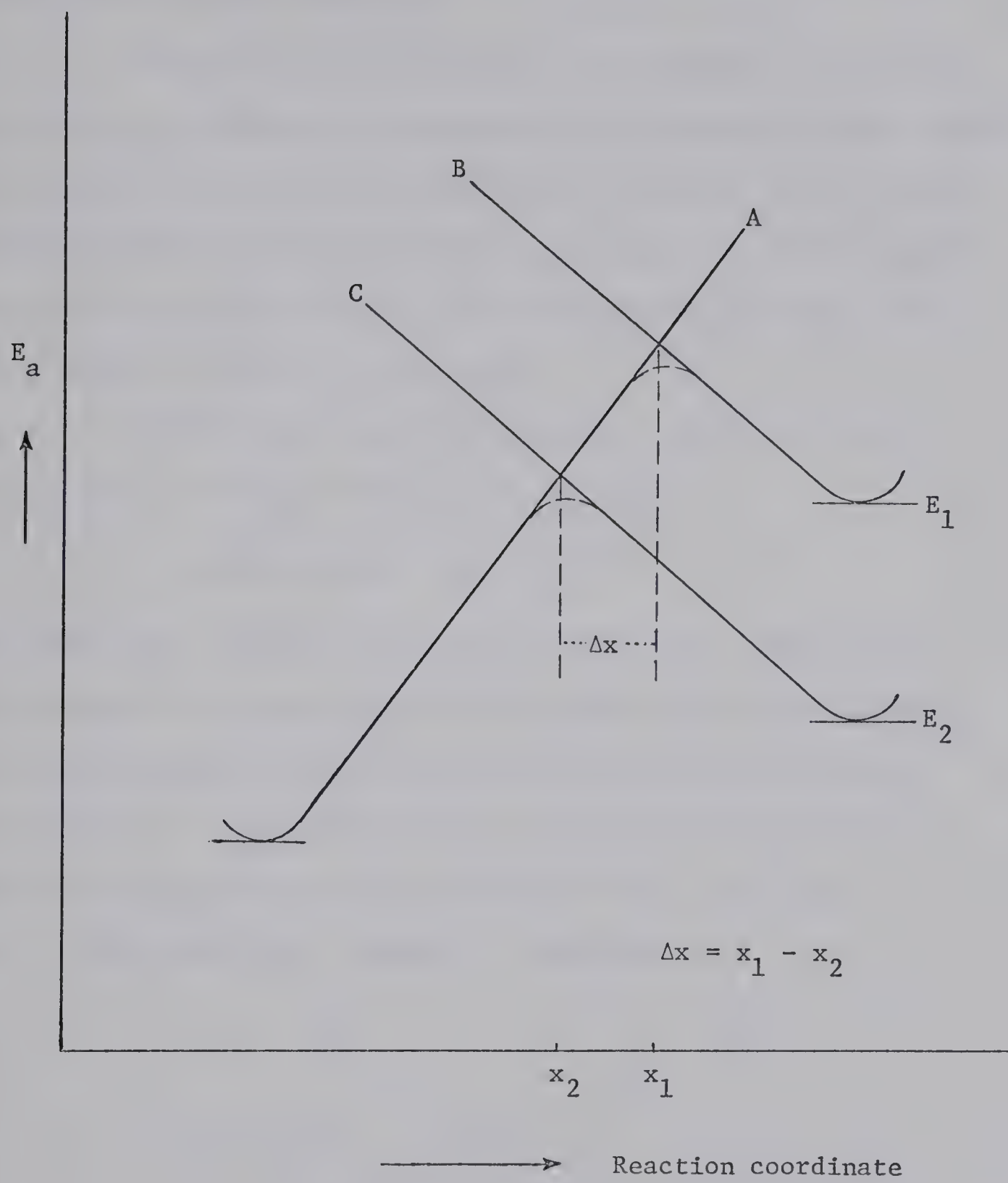
be expected to be better than 4 to 5% for the  $k_H/k_D$  ratio (see Chapter II, the kinetic studies section). The magnitude of the isotope effects may be rationalized in the following manner. In an unimolecular reaction of the following type:



the energy diagram for such a reaction (Figure 21) can be represented by two Morse curves A and B, for the reactant and the alkyl radical respectively, and a transition state located at  $X_1$  along the reaction coordinate. Then, if we increase the stability of the formed radical (i.e., decreasing its energy state from  $E_1$  to  $E_2$ ) for such a reaction, then the approximate Morse curve for such a radical would be that indicated by C, which leads to a transition state located at  $X_2$  along the reaction coordinate. It may be seen, as a consequence of this change that, beside lowering  $E_a$ , the transition state for the new reaction is displaced by  $\Delta X$  along the reaction coordinate (i.e., the molecules reach the transition state sooner). If we accept this as the case in our system, then, during the thermolysis of our allylic azo compounds, the molecules reach the transition state with less progress along the reaction coordinate. This means that the amount of C-N bond stretching, and the degree of change in hybridization has decreased on going from alkyl to allyl system. This is essentially an application of the Hammond postulate (64).



Figure 21







### Polanyi Plot for Azo Compounds

The possibility of observing a good Polanyi plot for the thermolysis of azoalkanes is enhanced by the observation that induced decomposition in azo-bis-3-propene (54) is insignificant. When the activation energy of a well-studied azo compound is plotted against the bond dissociation energy of the corresponding R-H bond, then a fit as shown in Figure 22 is obtained.

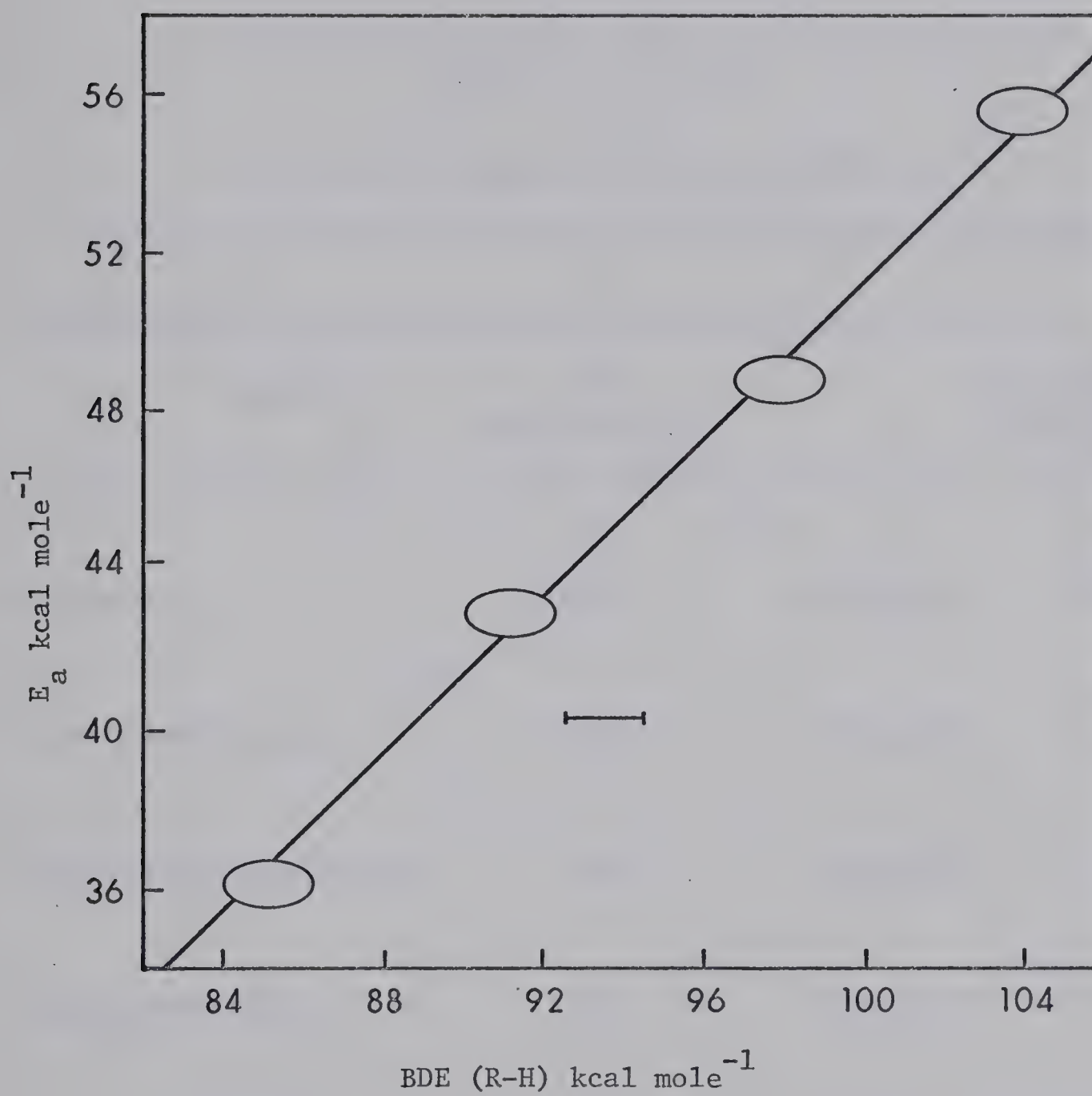
A least squares analysis using the data in Table XXII gives a best fit straight line of the equation

$$E_a = 0.996 \text{ BDE(R-H)} - 48.4$$

The data gives a correlation coefficient of 0.998. Consequently there appears the possibility that the activation energy obtained from the thermolysis of an azo compound, wherein chain induced decomposition is suppressed, can be correlated with the bond dissociation energy of the corresponding R-H bond. This matter is under further study by K. Takagi at this time.



Figure 22



Polanyi plot for the thermolysis of azo compounds



T A B L E X X I I

Activation energies of some azo alkanes  
and bond dissociation energies of the corresponding R-H bonds

Compound	$E_a$ (kcal mole <sup>-1</sup> )	BDE(R-H) (kcal)
$\text{CH}_3\text{-N=N-CH}_3$	55.5	$\text{D}(\text{CH}_3\text{-H}) = 104.0$
$\text{CH}_3\text{-CH}_2\text{-N=N-CH}_2\text{CH}_3$	48.5	$\text{D}(\text{C}_2\text{H}_5\text{-H}) = 98.0$
$\text{CH}_2\text{=CH-CH}_2\text{-N=N-CH}_2\text{-CH=CH}_2$	36.06	$\text{D}(\text{C}_3\text{H}_5\text{-H}) = 85.0$
$(\text{CH}_3)_3\text{C-N=N-C}(\text{CH}_3)_3$	42.8	$\text{D}(\text{t-C}_4\text{H}_9\text{-H}) = 91.0$
$(\text{CH}_3)_2\text{CH-N=N-CH}(\text{CH}_3)_2$	40.9	$\text{D}(\text{i-C}_3\text{H}_7\text{-H}) = 93.5$





## C O N C L U S I O N S

(1) The decrease in activation energy,  $19.4 \text{ kcal mole}^{-1}$ , on going from azomethane to azo-bis-3-propene (54) is consistent with the cleavage of both carbon-nitrogen bonds in the rate-determining transition state. The recently observed value of the allyl resonance energy  $9.6 \text{ kcal mole}^{-1}$  (94) is such that both allyl groups must be involved.

(2) The mechanistic proof for the simultaneous cleavage of both carbon-nitrogen bonds sought after by the study of secondary deuterium kinetic isotope effects was not obtained because of the low values observed in the allylic system. These unusually small values may be rationalized in terms of the Hammond postulate (64).

(3) The quality of the Polanyi plot obtained from the thermolysis of azoalkanes is such that further studies of these compounds are encouraged.



## E X P E R I M E N T A L

All boiling points are uncorrected.

The purification of the azo compounds were carried out on the same column and Autoprep stated in Chapter I. The ultra-violet spectra were obtained on a JASCO ORD/UV-5 spectrophotometer. Deuterium analysis, product analysis, nuclear magnetic resonance spectra, infrared spectra, and mass spectra were obtained using the same instruments indicated in Chapter I.

Microanalyses were performed by the Microanalytical Laboratory of the Department of Chemistry, University of Alberta (Edmonton).

(A) Preparation

Diethyl N,N'-diallylbicarbamate (57). Into a 500 ml Morton Flask fitted with a condenser, dropping funnel, nitrogen inlet, and high speed mechanical stirrer was placed 57.2% sodium hydride (4.32 g, 0.18 mole) and dry 1,2-dimethoxyethane (160 ml) (distilled from lithium aluminum hydride immediately before use). The reaction mixture was then stirred for 10 minutes under a nitrogen atmosphere. The reaction flask was kept at room temperature while diethyl hydrazodicarboxylate (59) (15.84 g, 0.09 mole) was added in portions to the well stirred mixture. After the addition was completed the stirring was continued for an additional three hours, then a mixture of allyl benzenesulfonate (35.64 g, 0.18 mole) in dry 1,2-dimethoxyethane (40 ml) was added dropwise



to the solution of the dianion (60). The reaction mixture was then moderately stirred under nitrogen at 20°C for an additional fifteen hours. It was then treated cautiously with excess water, and the diallyl compound 57 was extracted with a total of 500 ml of benzene. Most of the benzene was removed on a rotatory evaporator, and the product was purified by distillation which gave 19.2 g (83% yield) bp 92-93° (0.5 Torr). The nmr spectrum is displayed in Figure 12.

(a) N,N'-Diallylhydrazine (58). The hydrolysis of the diethyl-N,N'-diallylbicarbamate (57) was accomplished using the method described by Cohen et al. (96). In a typical run, a solution of the diallyl compound 57 (16.6 g, 0.065 mole) and potassium hydroxide (14.6 g, 0.26 mole) in a mixture of methanol (60 ml) and water (15 ml) was refluxed under nitrogen atmosphere for three hours. Precipitated potassium carbonate was filtered off, an additional amount of potassium hydroxide (~3.5 g) was added and the mixture was refluxed for one hour then cooled and concentrated in vacuo at which time more potassium carbonate precipitated. The residue was extracted well with ether. The washings were dried over anhydrous sodium sulfate. Ether was then removed by fractional distillation using a Vigreux column. The product was distilled collecting 3.0 g (41% yield) bp 75-76° (42 Torr). The product was sufficiently susceptible to oxygen that a good microanalysis could not be obtained.

(b) Azo-bis-3-propene (54). To a well stirred slurry of red mercuric oxide (25 g, 0.115 mole) and sodium sulfate (25 g) in





dry ether (140 ml) at 0°C, was added dropwise a solution of N,N'-diallylhydrazine (58) (3.0 g, 0.0265 mole) in ether (30 ml). The mixture was stirred for eight hours, the ether solution was then filtered, concentrated and the azo compound 54 separated by preparative gas chromatography using a column temperature of 90°C and 60 ml per minute carrier gas flow rate. The yield was 1.5 g (51%)  $n_D^{20} = 1.5784$ . The infrared and nmr spectra are shown in Figures 13 and 14 respectively. The uv spectrum has a  $\lambda_{\text{max}}$  at 358 nm ( $\epsilon = 24$  in methanol).

Anal. Calcd. for  $C_6H_{10}N_2$ : C, 65.40; H, 9.17; N, 25.43

Found: C, 65.43; H, 9.17; N, 25.26

Allyl- $\alpha,\alpha$ -d<sub>2</sub> alcohol was prepared from the reduction of acrylyl chloride with lithium aluminum deuteride using the method of Schultz et al.(86). The nmr analysis showed that the compound is greater than 99% deuterated in the desired position.

Allyl- $\alpha,\alpha$ -d<sub>2</sub> benzenesulfonate was prepared by the addition of allyl- $\alpha,\alpha$ -d<sub>2</sub> alcohol to a mixture of benzene sulfonylchloride and 2,4,6-collidine at -4°C using the procedure described by Bergstrom et al.(87).

N-Allyl-N,N'-dicarboethoxyhydrazine (62) was prepared in the same manner as for the aforementioned diallyl compound 57, except that 57% sodium hydride (2.77 g, 0.115 mole) was added to a solution of diethyl hydrazodicarboxylate (20.33 g, 0.115 mole + 10% in excess) in 1,2-dimethoxyethane (160 ml). Allyl benzenesulfonate (22.77 g, 0.115 mole) was then added to the monoanion (61) solution.



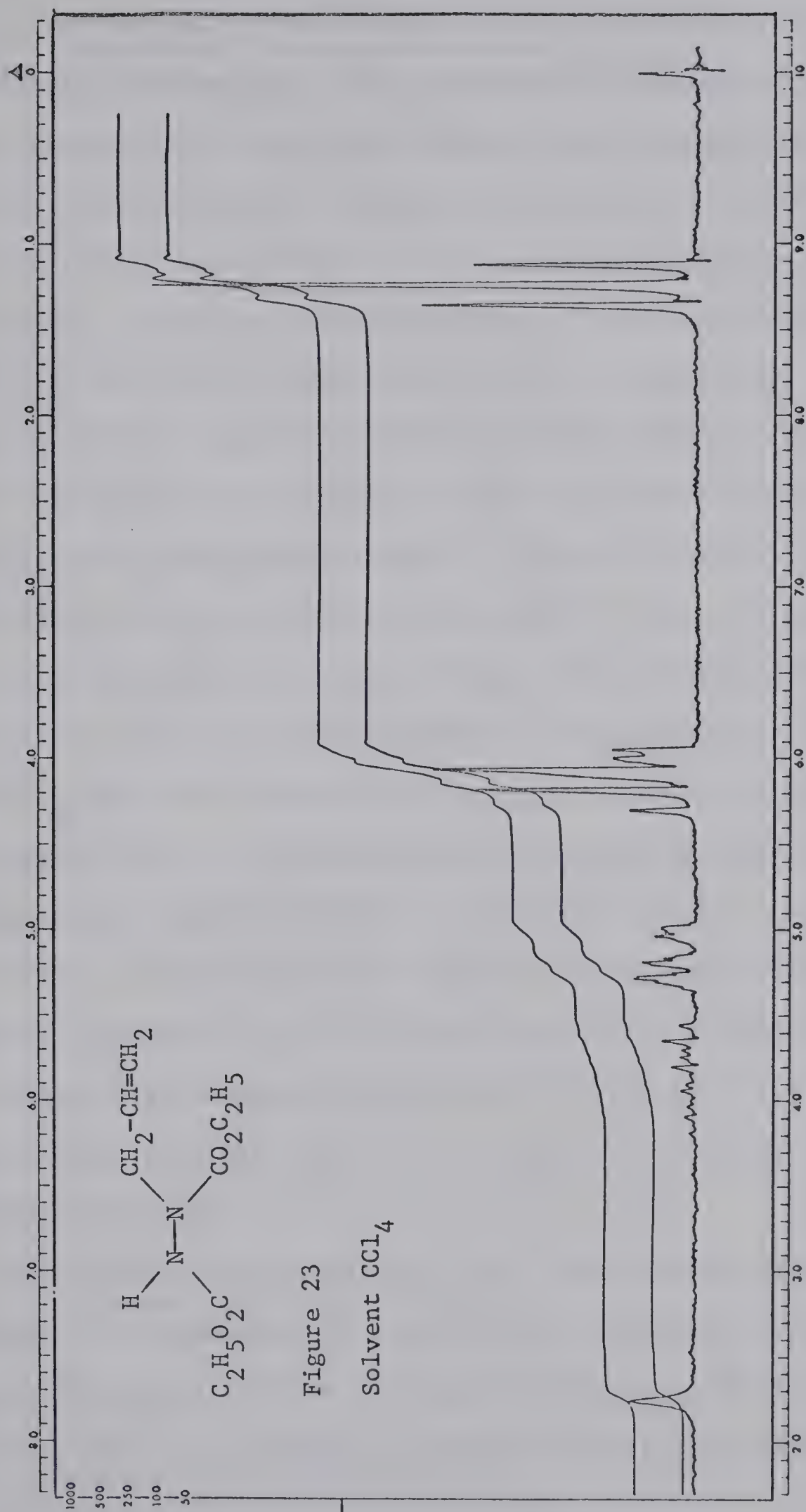


Purification and separation by distillation was carried out using a spinning band fractionating column, the yield was 16.5 g (59%) bp 99-101° (0.5 Torr). The nmr spectrum (Figure 23) displayed a singlet at 2.24 $\tau$  (N-H), multiplet at ~4.14 $\tau$  (methine), multiplet at ~4.88 $\tau$  (vinylidine), overlapping doublet and quartet at ~5.88 $\tau$  (allyl and methylenes), and a triplet at 8.75 $\tau$  (methyls) in the ratio of 0.91:1.00:2.03:6.05:6.06, calcd. 1:1:2:6:6.

Diethyl N-allyl-N'-(allyl- $\alpha,\alpha$ -d<sub>2</sub>)-bicarbamate (64) was prepared in the same manner as the aforementioned undeuterated diallyl compound 57, except that a solution of the monoallyl compound 62 (14.0 g, 0.0648 mole) in dry 1,2-dimethoxyethane (30 ml) was added to 57% sodium hydride (1.6 g, 0.065 mole) in 1,2-dimethoxyethane (150 ml). The dideuterioallyl benzenesulfonate (13.5 g, 0.675 mole) in 1,2-dimethoxyethane (20 ml) was then added to the solution of the monoanion (63). Distillation gave 15.1 g of product (90% yield) bp 92-93° (0.5 Torr).

(c) 3-Propenyl-azo-3'-propene-3',3'-d<sub>2</sub> (55). The preparation of 55 was accomplished from the hydrolytic decarboxylation of the diallyl compound 64 (15.1 g, 0.0585 mole) then subsequent oxidation of the resulted hydrazine using the same procedure used for the preparation of the aforementioned natural azo compound 54. The yield was 1.4 g (51%). The nmr spectrum (Figure 15) showed that it is over 98% deuterated in the allylic position of one of the allyl groups, mass spectral analysis (10 ev) showed a molecular ion which has a mass of 112.







Diethyl N,N'-(diallyl- $\alpha,\alpha,\alpha',\alpha'$ -d<sub>4</sub>)-bicarbamate (67)

was initially synthesized in the same manner as the undeuterated diallyl compound 57, except that dideuterioallyl benzenesulfonate was used. The nmr analysis revealed that about 16-17% of the total deuteriums were scrambled to the vinylidine positions of the molecule. This was further justified on the basis of the nmr analysis of the corresponding tetradeuterioazo compound 56. Since the dideuterioazo compound 55 had been produced without scrambling it was felt that the rearrangements must be occurring during the first allylation step (possibly due to the greater nucleophilicity of the dianion (60) giving an SN'<sub>2</sub> reaction ). Thus, a second method was used in hope that such a possibility of deuterium scrambling via the SN'<sub>2</sub> process would be minimized. The tetradeuteriodiallyl compound 67 was then prepared using the same method described for the preparation of the dideuteriodiallyl compound 64, except that dideuterioallyl benzenesulfonate was used in both steps. Starting with 20.33 g (0.115 mole) of the diethyl hydrazodicarboxylate (59) there was collected 15.2 g (51% yield based on the dicarboxylate 59) of the diallyl compound 67, bp 92-93°C (0.5 Torr). The nmr analysis indicated that 13.9% of the total deuterium is at the vinylidine position.

(d) Azo-bis-3-propene-3,3-d<sub>2</sub> (56). The preparation of 56 was achieved by the hydrolysis of the tetradeuteriodiallyl compound (67) (15.2 g, 0.058 mole) and the subsequent oxidation of the resulted hydrazine using the same procedure as described for the preparation of the







undeuterated azo compound 54. The yield was 1.42 g (51%). The nmr spectrum (Figure 16) shows that the deuterium content at the vinylidene position is 13.9% of the total deuterium present in the molecule, mass spectral analysis (10 ev) showed a molecular ion which has a mass of 114.

#### (B) Kinetic Measurements

The rates of thermolysis of the azo compounds 54, 55, and 56 were carried out in the same reactor used for the 1-pyrazoline kinetic studies (see Chapter I, experimental section, p. 81), a schematic diagram of the apparatus is shown in Figure 9. Samples were injected into the reactor as neat liquids. In a typical run a sample of 65  $\mu$ l was injected into the reactor by means of a Hamilton hypodermic syringe using a 6" needle. This amount of the sample corresponds to an initial pressure of 90 Torr. The thermolysis was carried out for more than nine half-lives, at this stage the pressure inside the reactor doubled to 180 Torr. The  $E_{\infty}$  was taken at this pressure. The reactor was then pumped out and those materials trapped on the vacuum line were taken for further identification and proportions. The rate constant was obtained by taking 12-15 points at regular intervals and over the first two half-lives, then plotting  $\log E_{\infty} - E_t$  vs.  $t$ , the slope of the line gave  $\frac{k}{2.303 RT}$  (Figure 17).



(C) Control Experiments

( i) Azo-bis-3-propene-3,3- $\text{d}_2$  (56) (70 mg, 614 mmole) was heated in the reactor at  $142^\circ\text{C}$  to 40% decomposition. The reactor was then pumped out and those materials which were trapped on the vacuum line were separated on an Autoprep using a 20% Ucon-insoluble on Fluoropack column at  $80^\circ\text{C}$  and 60 ml per minute carrier gas flow rate. The deuterated azo compound was then transferred to an nmr tube containing carbon tetrachloride and tetramethylsilane for analysis. The analysis indicated that 17.1% of the total deuteriums are at the vinylidene position.

(ii) 3-Propenyl-azo-3'-propene-3',3'- $\text{d}_2$  (55) (~5 mg, ~44.6 mmole) was distilled under vacuum into a break seal of 13 ml capacity. The tube was then removed from the vacuum rack and heated in an oven at  $142 \pm 0.5^\circ$  for 32 minutes (calculated 40% reaction). The content was then transferred into a vacuum line connected directly to the ionization chamber of a mass spectrometer for analysis. The analyses were carried out at 70, 10, and 9 ev. No fragmentation was observed at 9 ev and only the molecular ions were detected.

(D) Product Analysis

( i) Product analysis studies were carried out on samples trapped directly from the reaction at the end of each



kinetic run. Each sample was then analyzed on a gas chromatograph for product compositions.

(ii) Exact product compositions were obtained using the bulb crusher method as described in Chapter I.

(iii) Identification of the products was achieved by the comparison of their retention times with those of an authentic sample on the following; 10 ft. dimethylsulfolane on chromosorb W, 20 ft. mineral oil on firebrick in tandem with a 20 ft. 10% n-butylmaleate column. The relative retention times are recorded in Table XXIII. The products of the thermolysis for 54, 55, and 56 were trapped at the end of each kinetic run, and then distilled under vacuum into nmr tubes containing carbon tetrachloride and tetramethylsilane, the tubes were then removed from the vacuum rack and submitted for nmr spectra (Figures 18, 19, and 20 respectively). The mass spectral analyses were done on samples trapped directly from the reactor. In a typical experiment, products of the thermolysis at the end of the kinetic run were trapped in a vacuum line, the sample was then distilled under vacuum into a break seal which then was removed from the vacuum line which is connected to the ionization chamber of a mass spectrometer.





T A B L E X X I I I

Relative retention data for the  
thermolysis products of azo-bis-3-propene (54)

Column	Column temp. (C°)	Helium flow rate(ml min <sup>-1</sup> )	Compound	Relative re- tention time (N <sub>2</sub> = 1.000)
10', dimethylsulfolane on chromosorb W	25	40	Propylene 1,5-hexadiene	1.42 5.56
20', mineral oil on firebrick	30	50	Propylene 1,5-hexadiene	1.13 22.60
20', mineral oil on firebrick in tandem with a 20', 10% n- butylmaleate	25	50	Propylene 1,5-hexadiene	1.75 23.25





## R E F E R E N C E S

1. T. S. Chambers and G. B. Kistiakowsky, J. Am. Chem. Soc., 56, 399 (1934).
2. (a) B. S. Rabinovitch, E. W. Schlag, and K. B. Wiberg, J. Chem. Phys., 28, 504 (1958);  
(b) E. W. Schlag and B. S. Rabinovitch, J. Am. Chem. Soc., 82, 5996 (1960);  
(c) B. S. Rabinovitch, D. W. Setser, and F. W. Schneider, Can. J. Chem., 39, 2609 (1961);  
(d) D. W. Setser and B. S. Rabinovitch, J. Am. Chem. Soc., 86, 564 (1964).
3. (a) S. W. Benson, J. Chem. Phys., 34, 521 (1961);  
(b) S. W. Benson and P. S. Nangia, *ibid.*, 38, 18 (1963).
4. M. C. Flowers and H. M. Frey, Proc. Roy. Soc., (London) A 257, 122 (1960).
5. M. C. Flowers and H. M. Frey, J. Chem. Soc., 2758 (1960).
6. D. W. Setser and B. S. Rabinovitch, Can. J. Chem., 40, 1425 (1962).
7. W. B. DeMore and S. W. Benson, Adv. Photochem., II, 237, 249, 255-258 (1964).
8. B. S. Rabinovitch, E. Tschuikow, and E. W. Schlag, J. Am. Chem. Soc., 81, 1081 (1959).
9. R. J. Crawford and A. Mishra, J. Am. Chem. Soc., 87, 3768 (1965).



10. A. Mishra, Ph.D. Thesis, University of Alberta, 1965.
11. R. J. Crawford, A. Mishra, and R. J. Dummel, J. Am. Chem. Soc., 88, 3959 (1966).
12. R. J. Crawford and A. Mishra, *ibid.*, 88, 3963 (1966).
13. R. J. Crawford and D. M. Cameron, Can. J. Chem., 45, 691 (1967).
14. K. W. Egger, D. M. Golden, and S. W. Benson, J. Am. Chem. Soc., 86, 5420 (1964).
15. (a) S. Seltzer, *ibid.*, 83, 2625 (1961);  
(b) S. Seltzer, *ibid.*, 85, 14 (1963);  
(c) S. Seltzer and F. T. Dunne, *ibid.*, 87, 2628 (1965).
16. R. J. Crawford and L. H. Ali, *ibid.*, 89, 3908 (1967).
17. D. E. McGreer and W-S. Wu, Can. J. Chem., 45, 461 (1967).
18. R. J. Crawford and G. L. Erickson, J. Am. Chem. Soc., 89, 3907 (1967).
19. T. V. Van Auken and K. L. Rinehart, *ibid.*, 84, 3736 (1962).
20. (a) D. E. McGreer, R. S. McDaniel, and M. G. Vinje, Can. J. Chem., 43, 1389 (1965);  
(b) D. E. McGreer, N. W. K. Chiu, and M. G. Vinje, *ibid.*, 43, 1398 (1965);  
(c) D. E. McGreer, N. W. K. Chiu, M. G. Vinje, and K. C. Wong, *ibid.*, 43, 1407 (1965).
21. J. Hamelin and R. Carrié, Bull Soc. Chim. de France, 1968 2162-2167; *idem.*, *ibid.*, 2513-2519; *idem.*, *ibid.*, 2521-2525.
22. R. Hoffmann, J. Am. Chem. Soc., 90, 1475 (1968).



23. For a complete summary, see E. A. Halevi in "Progress in Physical Organic Chemistry", Vol. 1, Interscience Publishers, Inc., New York, N. Y., 1963, p.109.
24. J. Bigeleisen, J. Chem. Phys., 17, 675 (1949).
25. M. Wolfsberg and M. J. Stern, Pure Appl. Chem., 8, 225, idem., ibid., 325 (1964).
26. J.H. Schachtschneider and R. J. Snyder, Spectro Chim. Acta., 19, 117 (1963).
27. K. Mislow, S. Borčić, and V. Prelog, Helv. Chim. Acta., 40, 2477 (1957).
28. (a) A. Streitwieser, Jr., R. H. Jagon, R. C. Fahey, and S. Suzuki, J. Am. Chem. Soc., 80, 2326 (1958);  
(b) A. Streitwieser, Jr., and G. Alan Dafforn, Tetrahedron Letters, No. 16, 1263 (1969).
29. R. R. Johnson and E. S. Lewis, Proc. Chem. Soc., 52 (1958).
30. E.S.Lewis, R. R. Johnson, and G. M. Coppinger, J. Am. Chem. Soc., 81, 3140 (1959).
31. (a) W. H. Saunders, Jr., S. Ašperger, and D. H. Edison, J. Am. Chem. Soc., 80, 2421 (1958);  
(b) W. H. Saunders, Jr., and R. Glaser, ibid., 82, 3586 (1960).
32. (a) S. Borčić, M. Nikoletic, and D. E. Sunko, Chem. and Ind. (London), 527 (1960).  
(b) S. Borčić, M. Nikoletic, and D. E. Sunko, J. Am. Chem. Soc., 84, 1615 (1962).





33. V. J. Shiner, Jr., W. E. Buddenbaum, B. L. Murr, and G. Lamaty, J. Am. Chem. Soc., 90, 418 (1968).
34. L. S. Bartell, Tetrahedron Letters, No. 6, 13 (1960); J. Am. Chem. Soc., 83, 3567 (1961).
35. (a) E. S. Lewis and C. E. Boozer, J. Am. Chem. Soc., 74 6306 (1952);  
(b) E. S. Lewis and C. E. Boozer, *ibid.*, 76, 791 (1954);  
(c) E. S. Lewis, Tetrahedron, 5, 143 (1959).
36. (a) V. J. Shiner, Jr., J. Am. Chem. Soc., 75, 2925 (1953);  
(b) V. J. Shiner, Jr., *ibid.*, 76, 1603 (1954);  
(c) V. J. Shiner, Jr., Tetrahedron, 5, 243 (1959);  
(d) V. J. Shiner, Jr., J. Am. Chem. Soc., 83, 240 (1961);  
(e) V. J. Shiner, Jr., B. L. Murr, and G. Heinemann, *ibid.*, 85, 2413 (1963).
37. (a) H. C. Brown and G. J. McDonald, J. Am. Chem. Soc., 88, 2514 (1966);  
(b) H. C. Brown, M-E. Azzaro, J. G. Koelling, and G. J. McDonald, *ibid.*, 88, 2520 (1966);
38. G. J. Karabatsos, G. S. Sonnicksen, C. G. Papaioannou, S. E. Scheppele, and R. L. Shone, J. Am. Chem. Soc., 89, 463 (1967).
39. See (a) Ref. 28a, p.2329 and note 24;  
(b) Ref. 15a, especially note 28.
40. S. G. Cohen and C. H. Wang, J. Am. Chem. Soc., 77, 3628 (1955).



41. C. G. Overberger and A. V. DiGiulio, ibid., 81, 2154 (1959)  
and references therein.
42. (a) E. S. Scheppele and S. Seltzer, ibid., 90, 358 (1968);  
(b) A. A. Zavitsas and S. Seltzer, ibid., 86, 1265 (1964).
43. T. W. Koenig and W. D. Brewer, Tetrahedron Letters, No. 32, 2773  
(1965).
44. C. E. Boozer, B. W. Ponder, J. C. Trisler, and C. E. Wightman,  
J. Am. Chem. Soc., 78, 1506 (1956).
45. S. Seltzer and E. J. Hamilton, Jr., J. Am. Chem. Soc., 88,  
3775 (1966).
46. S. Rummel, H. Hubner, and P. Krumbiegel, Z. Chem., 7, 351 (1967).
47. T. W. Koenig and R. Wolf, J. Am. Chem. Soc., 89, 2948 (1967).
48. D. B. Denny and N. Tunkel, Chem., Ind. (London), 1383 (1959).
49. S. Seltzer, J. Am. Chem. Soc., 83, 1861 (1961).
50. W. A. Pryor, R. W. Henderson, R. A. Patsiga, and N. Carroll,  
J. Am. Chem. Soc., 88, 1199 (1966).
51. S. Evani, Ph.D. Thesis, University of Alberta, 1967.
52. J. E. Baldwin, and J. A. Kapecki, J. Am. Chem. Soc., 91, 3106  
(1969).
53. M. Matsuoka and M. Szwarc, ibid., 83, 1260 (1961).
54. M. Feld, A. P. Stefani, and M. Szwarc, ibid., 84, 4451 (1962).
55. M. Takahasi and R. J. Cvetanovic, Can. J. Chem., 40, 1037  
(1962).
56. L. C. Leitch and A. T. Morse, Can. J. Chem., 30, 924 (1952).
57. M. S. Kharasch and F. R. Mayo, J. Am. Chem. Soc., 55, 2468  
(1933).



58. G. G. Smith and F. D. Bagley, *Rev. Sci. Instr.*, 32, 703 (1961).
59. A. N. Frost and R. L. Pearson, "Kinetic and Mechanism", John Wiley and Sons, Inc., New York, 1961, 2nd edition, pp.99-100.
60. L. P. Hammett, "Introduction to Physical Chemistry", McGraw Hill Book Co., New York, 1952, p.410.
61. S. W. Benson, "The Foundations of Chemical Kinetics", McGraw Hill Book Co., New York, 1960, pp.91-94.
62. E. M. Hodnett and P. S. Juneja, *J. Org. Chem.*, 33, 1233 (1968).
63. (a) C. G. Swain, E. C. Stivers, J. F. Reuwer, and L. J. Schaad, *J. Am. Chem. Soc.*, 80, 5885 (1958);  
(b) J. Bigeleisen, "Tritium in the Physical and Biological Sciences", Vol. 1, International Atomic Energy Agency, Vienna, 1962, p.161.
64. G. S. Hammond, *J. Am. Chem. Soc.*, 77, 334 (1955).
65. K. B. Wiberg, *Physical Organic Chemistry*, J. Wiley and Sons, Inc., New York, 1964 p.360.
66. See Ref. 23, p.168.
67. A. W. Baker and R. C. Lord, *J. Chem. Phys.*, 23, 1636 (1955).
68. R. C. Lord and P. Venkateswarlu, *J. Opt. Soc. Am.*, 43, 1079 (1958).
69. D. Cameron, Ph.D. Thesis, University of Alberta, 1967.
70. H. Zollinger, "Azo and Diazo Chemistry, Aliphatic and Aromatic Compounds", Interscience Publishers, New York, 1961, Chapters 9 and 12.
71. A. F. Trotman-Dickenson, *Gas Kinetics*, Butterworths, London, 1955, p.70.





72. (a) J. A. Leermakers, J. Am. Chem. Soc., 55, 3499 (1933);  
(b) D. H. Volman, P. A. Leighton, F. E. Blacet, and R. K. Brinton, J. Chem. Phys., 18, 203 (1950).
73. M. C. Lin and K. J. Laidler, Can. J. Chem., 44, 2927 (1966).
74. (a) C. G. Overberger and M. B. Berenbaum, J. Am. Chem. Soc., 73, 2618 (1951);  
(b) Idem, ibid., 73, 4883 (1951).
75. (a) W. Forst and O. K. Rice, Can. J. Chem., 41, 562 (1963);  
(b) C. Steel and A. F. Trotman-Dickenson, J. Chem. Soc., 975, (1959).
76. H.C. Ramsperger, J. Am. Chem. Soc., 51, 2134 (1929), and references therein.
77. (a) O. K. Rice and H. C. Ramsperger, J. Am. Chem. Soc., 49, 1617 (1927); idem., ibid., 50, 617 (1928);  
(b) R. A. Marcus and O. K. Rice, J. Phys. Colloid. Chem., 55, 894 (1951).
78. (a) H. S. Sandhu, J. Phys. Chem., 72, 1857 (1968).  
(b) W. D. Clarke, Ph.D. Dissertation, University of Oregon, Eugene, Oregon, 1959.
79. J. B. Levy and B. K. W. Copeland, J. Am. Chem. Soc., 82, 5314 (1960).
80. S. G. Cohen and C. H. Wang, J. Am. Chem. Soc., 77, 2457 (1955).
81. (a) G. Williams and A. C. Lawrence, Prog. Roy. Soc. (London) A156, 455 (1936);  
(b) C. G. Overberger, M. T. O'Shaughnessy, and H. Shalit,





- J. Am. Chem. Soc., 71, 2661 (1959);
- (c) K. Ziegler, W. Deparade and W. Meyer, Ann., 567, 141 (1950).
82. M. G. Evans and M. Polanyi, Trans Faraday Soc., 34, 11 (1938).
83. (a) A. F. Trotman-Dickenson, Chem. Ind. (London), 379 (1965);
- (b) G. C. Fettis and A. F. Trotman-Dickenson, J. Chem. Soc., 3037 (1961);
- (c) G. C. Fettis and A. F. Trotman-Dickenson, J. Am. Chem. Soc., 81, 5260 (1959);
- (d) J. Grzeckowiak, J. A. Kerr, and A. F. Trotman-Dickenson, Chem. Comm., 109 (1965).
84. J. A. Kerr, Chem. Rev., 66, 465 (1966).
85. A. Zweig and A. K. Hoffmann, J. Am. Chem. Soc., 85, 2736 (1963).
86. R. D. Schultz and F. W. Millard, J. Org. Chem., 24, 297 (1959).
87. C. G. Bergstrom and S. Siegel, J. Am. Chem. Soc., 74, 254 (1952).
88. F. Daniels, et al, "Experimental Physical Chemistry", McGraw Hill Book Company Inc., Fifth Edition, (1956), p.339.
89. J. L. Franklin and F. H. Field, J. Am. Chem. Soc., 75, 2819 (1953).
90. M. Szwarc and A. H. Schon, J. Chem. Phys., 18, 237 (1950).
91. A. S. Gordon, S. R. Smith, and J. R. McNesby, J. Am. Chem. Soc., 81, 5059 (1959).
92. S. W. Benson, A. N. Bose, and P. Nangia, ibid., 85, 1388 (1963).



93. R. J. Ellis and H. M. Frey, J. Chem. Soc., 5578 (1964).
94. D. M. Golden, N. A. Gac, and S. W. Benson, J. Am. Chem. Soc., 91, 2136 (1969).
95. V. Belanić-Lipovac, S. Borčić, and D. E. Sunko, Croat. Chem. Acta, 37, 61 (1965).
96. S. G. Cohen and R. Zand, and C. Steel, J. Am. Chem. Soc., 83, 2895 (1961).
97. W. E. Doering and V. Toscano, Unpublished results cited in Table X, H. E. O'Neal and S. W. Benson, J. Phys. Chem., 71, 2903 (1967).









**B29930**